Universidade Estadual de Londrina

RAFAEL MASASHI FUKUDA

OTIMIZAÇÃO CONVEXA E HEURÍSTICA EM DETECTORES MIMO-OFDM E MIMO EM LARGA ESCALA:

DESEMPENHO E COMPLEXIDADE

Londrina
2019

RAFAEL MASASHI FUKUDA

OTIMIZAÇÃO CONVEXA E HEURÍSTICA EM DETECTORES MIMO-OFDM E MIMO EM LARGA ESCALA:

DESEMPENHO E COMPLEXIDADE

Dissertação apresentada ao Programa de Pós-Graduação em Engenharia Elétrica da Universidade Estadual de Londrina para obtenção do Título de Mestre em Engenharia Elétrica.

Área de concentração: Sistemas Eletrônicos
Especialidade: Sistemas de Telecomunicações

Orientador: Prof. Dr. Taufik Abrão

Londrina
2019

Ficha Catalográftca

Fukuda, Rafael Masashi
Otimização Convexa e Heurística em Detectores MIMO-OFDM e MIMO em Larga Escala: Desempenho e Complexidade . Londrina, PR, 2019. 95 p.

Dissertação (Mestrado) – Universidade Estadual de Londrina, PR. Departamento de Engenharia Elétrica .

1. Sistemas de Telecomunicações. 2. Sistemas MIMO-OFDM. 3. Sistemas *Massive* MIMO 4. Sistemas MIMO de Larga Escala 5. Detectores. 6. Heurística 7. Otimização Convexa I. Universidade Estadual de Londrina. Departamento de Engenharia Elétrica. Departamento de Engenharia Elétrica . II. Título.

RAFAEL MASASHI FUKUDA

OTIMIZAÇÃO CONVEXA E HEURÍSTICA EM DETECTORES MIMO-OFDM E MIMO EM LARGA ESCALA:

DESEMPENHO E COMPLEXIDADE

Dissertação apresentada ao Programa de Pós-Graduação em Engenharia Elétrica da Universidade Estadual de Londrina para obtenção do Título de Mestre em Engenharia Elétrica.

Área de concentração: Sistemas Eletrônicos
Especialidade: Sistemas de Telecomunicações

BANCA EXAMINADORA

Orientador: Prof. Dr. Taufik Abrão
Universidade Estadual de Londrina - UEL

Prof. Dr. José Carlos Marinello Filho
Universidade Estadual de Londrina - UEL

Prof. Dr. Paulo Rogério Scalassara
Universidade Tecnológica Federal do Paraná – UTFPR

Londrina, 1 de maio de 2019.

We are not provided with wisdom, we must discover it for ourselves,
after a journey through the wilderness which no one else can make for us,
which no one can spare us.
Marcel Proust

Agradecimentos

Aos meus pais e demais familiares por todos os incentivos e apoio oferecidos.

Aos professores que tive durante a vida e cujos ensinamentos contribuíram para a minha formação. Um agradecimento especial ao professor orientador Taufik pela dedicação e empenho colocados durante o desenvolvimento deste trabalho.

À empresa HS Technology por possibilitar que parte do meu tempo fosse dedicado ao desenvolvimento desta Dissertação.

Ao departamento de Engenharia Elétrica, UEL e ao programa de Mestrado por auxiliar em mais esta etapa de formação. E, apesar de não ter recebido bolsa, segue o agradecimento à CAPES por auxiliar na manutenção do programa de Mestrado: "o presente trabalho foi realizado com apoio da Coordenação de Aperfeiçoamento de Pessoal de Nível Superior - Brasil (CAPES) - Código de Financiamento 001".

Aos colegas do laboratório de Telecom & SP pelo convívio e reuniões técnicas que contribuíram para o desenvolvimento do trabalho.

E a todos que contribuíram de forma direta ou indireta para a conclusão desta etapa.

Resumo

A detecção é uma etapa importante durante a recuperação da informação transmitida no lado do receptor. Porém, a solução ótima *Maximum-Likelihood* (ML) verifica todas as combinações possíveis (solução por força bruta) para encontrar o vetor solução resultando em alta complexidade computacional sendo pouco adequada para aplicações práticas. Nessa dissertação de Mestrado, duas abordagens são consideradas buscando melhorar o compromisso entre complexidade e desempenho: os algoritmos heurísticos e a otimização convexa. O primeiro trabalho é focado na aplicação de duas técnicas heurísticas evolutivas chamadas *Particle Swarm Optimization* (PSO) e *Differential Evolution* (DE) na detecção em sistemas *Multiple Input Multiple Output* combinados com *Orthogonal Frequency Dvision Multiplexing* (MIMO-OFDM) em cenários com correlação espacial entre as antenas, sendo a performance dos detectores e a complexidade computacional são caracterizadas. O segundo trabalho é uma extensão do primeiro e aborda a utilização de detectores híbridos que são uma combinação entre detectores lineares com os algoritmos heurísticos. Com os detectores híbridos, a convergência dos algoritmos é acelerada e, consequentemente, a complexidade computacional é reduzida substancialmente, enquanto mantém performance similar aos detectores heurísticos puros utilizando o PSO e DE. No terceiro trabalho, o *framework* de otimização convexa é considerado no contexto de sistemas *Massive* MIMO (M-MIMO) com grande número de antenas. O trabalho é dividido em duas partes principais. Na primeira, foram considerados detectores formulados como *Linear Programming* (LP) e *Quadratic Programming* (QP) e *Semidefinite Programming* (SDP) analisados em cenários realistas considerando erro na estimativa do canal, correlação espacial, carregamento do sistema e diferentes ordens de modulação. Na segunda parte, a utilização de algoritmos projetados é proposta para resolver o detector formulado como QP, a complexidade computacional dos algoritmos é caracterizada em termos de *Floating Point Operations* (FLOPs), e a influência de características específicas do sistema M-MIMO, particularmente o *channel hardening*), na redução do número de iterações dos algoritmos projetados é ilustrada através de simulações numéricas.

Palavras-chave: 1. Sistemas de Telecomunicações; 2. Sistemas MIMO-OFDM; 3. Sistemas *Massive* MIMO; 4. Sistemas MIMO de Larga Escala; 5. Detectores; 6. Heurística; 7. Otimização Convexa.

Abstract

The detection task is a crucial and demanding step in order to correctly recover the transmitted information on the receiver side in the presence of interference from the other antennas. However, the Maximum-Likelihood (ML) detector, which is the optimal solution, checks all the possible combinations (brute-force solution) in order to find the best solution vector and due to its high computational complexity, it is unsuitable for practical applications. In this Dissertation, two different approaches are considered aiming to improve the performance complexity trade-off: heuristic algorithms and convex optimization. The first work investigates the application of two different evolutionary heuristics namely Particle Swarm Optimization (PSO) and Differential Evolution (DE) in detection considering a Multiple Input Multiple Output Orthogonal Frequency Division Multiplexing system (MIMO-OFDM) operating under spatial correlation between antennas. The performance of the algorithm and its computational complexity are characterized. The second work extends the first considering hybrid detectors, which is a combination of linear and heuristic detectors aiming to reduce the number of iterations, hence reducing the computational complexity, while providing similar performance compared with PSO and DE detectors. In the third work, the convex optimization framework is considered in a Massive MIMO (M-MIMO) scenario with large number of antennas. The work is divided in two main parts. In the first part, detectors are formulated as Linear Programming (LP), Quadratic Programming (QP) and Semidefinite Programming (SDP) are evaluated numerically in realistic scenarios considering error in the channel estimate, spatial correlation, system loading and different modulation orders. In the second part, projected algorithms are considered to solve the detector formulated as a QP, the computational complexity further characterized in terms of FloatingPoint Operation (FLOPs) and the influence of specific characteristics of the M-MIMO system, particularly the channel hardening, in the reduction of the number of iterations in the projected algorithms are illustrated through numerical simulations.

Keywords: 1. Telecommunication Systems; 2. MIMO-OFDM; 3. *Massive* MIMO; 4. Large Scale MIMO Systems; 5. Detectors; 6. Heuristics; 7. Convex Optimization.

Sumário

Lista de Figuras

Lista de Tabelas

Abreviações e Siglas

BER *Bit Error Rate*

BS *Base Station*

CP *cyclic prefix*

CSI *Channel State Information*

DE *Differential Evolution*

DFT *discrete Fourier transform*

DSPG *Diagonally Scaled Projected Gradient*

EPA *Equal Power Allocation*

FLOP *Floating Point Operations*

IDFT *inverse discrete Fourier transform*

LP *Linear Programming*

LS-MIMO *Large-Scale Multiple-Input Multiple Output*

M-MIMO *Massive Multiple-Input Multiple Output*

MCS *Monte Carlo Simulations*

MF *Matched Filter*

MIMO-OFDM *Multiple-Input Multiple Output Orthogonal Frequency Division Multiplexing*

ML *Maximum Likelihood*

MMSE *Minimum Mean Square Error*

NLOS *Non Line of Sight*

OFDM *Orthogonal Frequency Division Multiplexing*

PG *Projected Gradient*

PNNA *Projected Newton with Neumann Approximation*

PN *Projected Newton*

PSO *Particle Swarm Optimization*

QAM *Quadrature and Amplitude Modulation*

QP *Quadratic Programming*

SDP *Semidefinite Programming*

ULA *Uniform Linear Array*

URA *Uniform Rectangular Array*

ZF *Zero Forcing*

Lista de Símbolos

N_t	Número de antenas do transmissor
N_r	Número de antenas do receptor
N	Número de subportadoras
c_1	Fator cognitivo
c_2	Fator social
w	Fator de inércia
F_{mut}	Fator de mutação
F_{cr}	Fator de *crossover*
$\boldsymbol{\iota}$	Vetor de indivíduos
$\boldsymbol{\nu}$	Vetor de mutação
$\boldsymbol{\psi}$	Vetor de *crossover*
N_{dim}	Dimensionalidade do problema
N_{pop}	Tamanho da população
N_{ind}	Número de indivíduos
ρ	Fator de correlação espacial
τ	Parâmetro de qualidade da estimação de canal
$\mathcal{I}$	Número de iterações das heurísticas
$\mathcal{I}_{\text{hyb}}$	Número de iterações dos detectores híbridos
$\mathbf{H}$	Matriz de canal
$\underline{\mathbf{H}}$	Representação da matriz de canal em números reais
K	Número de usuários
M	Número de antenas da estação rádio-base
$\sigma_{\text{TM}}, \beta_{\text{TM}}$	Parâmetros da busca em linha
N_{iter}	Número de iterações até o critério de parada ser atingido
m_{iter}	Número de execuções da busca em linha
τ_{RMS}	*Delay spread*
$(\Delta B)_c$	Banda de coerência do canal

Notação Matemática

$(.)^+$	$\max(., 0)$
$\otimes$	Produto de Kronecker
$\succeq$	Matriz semidefinida positiva

1 Introdução

Sistemas de telecomunicações estão presentes no dia-a-dia durante a utilização de telefones celulares e computadores conectados com a internet, *stream* de vídeos, e muitas outras aplicações. Em telecomunicações, exitem três tópicos recorrentes que continuam através das épocas (MARZETTA et al., 2016): há um crescente aumento na demanda de taxas de transferência de dados; o espectro de frequências é limitado e se torna cada vez mais escasso e, por consequência, há uma necessidade em se desenvolver esquemas de comunicação cada vez mais eficientes espectral e energeticamente.

Para se atingir maiores eficiências espectrais e/ou maior confiabilidade na recepção dos sinais, pode-se lançar mão de esquemas de transmissão *Multiple Input Multiple Output* (MIMO). Os sistemas MIMO chamaram a atenção na década de 90 em trabalhos como em (FOSCHINI, 1996; TELATAR, 1999), os quais demonstraram as vantagens em se utilizar sistemas com múltiplas antenas e a viabilidade de se alcançar altas taxas de eficiência espectral. Os sistemas MIMO podem ser classificados em modo multiplexagem (aumento da eficiência espectral) e modo diversidade (melhoria na confiabilidade do sinal detectado). No modo multiplexagem, informações diferentes são enviadas pelas várias antenas do transmissor resultando em uma maior taxa da transmissão de dados.

Ao enviar um sinal de transmissão através de um meio não guiado, o mesmo fica sujeito à interferência, distorções e atenuações causadas pelo canal de comunicação. Particularmente para o efeito da seletividade em frequência, a *Orthogonal Frequency Division Multiplexing* (OFDM) pode ser utilizada. Quando devidamente projetado, o sistema OFDM com um número de subportadoras grande o suficiente para atingir a condição de *flat-fading*, a seletividade em frequência pode ser combatida; um exemplo ilustrando o efeito do *Power Delay Profile* (PDP) pode ser observado na Fig. 1.1. Especificamente, o modelo exponencial IEEE 802.11 foi considerado (CHO et al., 2010) chamado de *ideal* na figura da esquerda, enquanto os pontos *simulação* foram gerados multiplicando o PDP por amostras de canal *fading* aleatórias. Através da resposta em frequência, observa-se que se

o número de subportadoras for aumentado, a atenuação em cada uma delas se tornaria praticamente plana (*flat fading*).

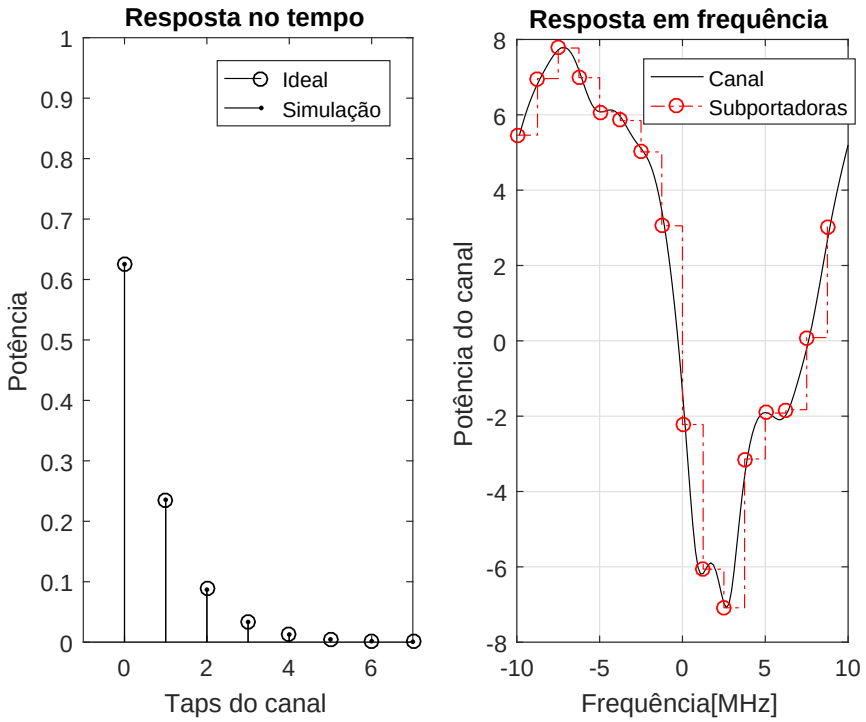

Figura 1.1: Ilustração do PDP no domínio do tempo e da frequência. Parâmetros considerados foram $\tau_{rms} = 51$ ns, $BW = 20$ MHz, $N = 16$ subportadoras.

Um diagrama de blocos do sistema OFDM é apresentado na Fig. 1.2. Foi considerado um esquema OFDM clássico em banda-base descrito na literatura, por exemplo, em (GOLDSMITH, 2005). No transmissor, representado pela Fig. 1.2(a), o modulador OFDM utiliza uma modulação digital, aqui considerada QAM e realiza a conversão paralelo para serial (bloco P/S); a *Inverse Discrete Fourier Transform* (IDFT) é aplicada e o *cyclic prefix* (CP) é adicionado; o sinal passa pela conversão serial-paralelo (bloco S/P), e o sinal finalmente é transmitido. No receptor da Fig. 1.2(b), o sinal recebido passa por demodulador OFDM, composto de conversor serial-paralelo, seguido de *Discrete Fourier Transform* (DFT). O CP é descartado, o sinal é serializado, e posteriormente demapeado pela respectiva modulação digital. O OFDM pode ser combinado com as múltiplas antenas resultando no sistema MIMO-OFDM, mantendo as características dos dois sistemas; o sistema MIMO-OFDM foi considerado nos dois primeiros trabalhos.

Quando o número de antenas do sistema MIMO atinge a ordem de dezenas, centenas ou mesmo unidades de milhares, o sistema é denominado *massive* MIMO (M-MIMO) ou *Large Scale* MIMO (LS-MIMO) (CHOCKALINGAM; RAJAN, 2014), termos utilizados de maneira intercambiável ao longo desta Dissertação. Essa topologia é promissora e um dos candidatos para a quinta geração (5G) de telefonia

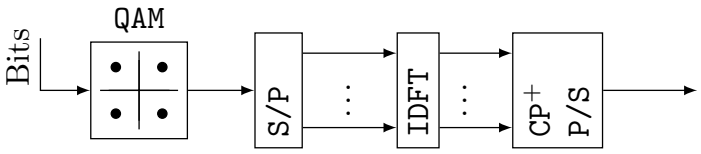

(a) Transmissor OFDM.

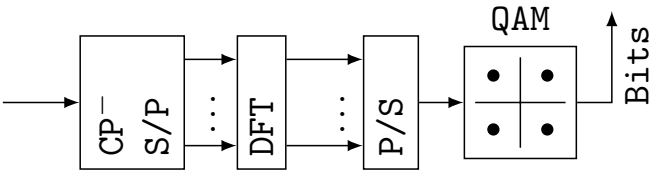

(b) Receptor OFDM.

Figura 1.2: Diagrama de blocos de um transmissor e receptor OFDM.

móvel (GUPTA; JHA, 2015; Shafi et al., 2017). O uso de grande número de antenas pode trazer melhorias de eficiência energética e espectral, os efeitos de *fading* e o ruído térmico tendem a desaparecer, a interferência entre usuários dentro de uma célula é reduzida (MARZETTA, 2010), dentre outras vantagens.

Nessas condições, novos desafios construtivos surgem e alguns fenômenos começam a prevalecer no sistema, sendo esta uma área de pesquisa recente com muitos cenários a serem estudados; assim, o sistema M-MIMO foi considerado no terceiro trabalho. Ademais, o uso de algumas técnicas que são interessantes para avaliação de sistemas MIMO tradicionais com poucas antenas tornam-se inviáveis, como o detector de máxima verossimilhança (*Maximum Likelihood* - ML), uma vez que o detector ML realiza uma busca exaustiva a partir da combinação de todos os símbolos possíveis transmitidos, considerando todas as antenas de transmissão e de recepção. Estratégias para superar estas limitações foram propostas no terceiro trabalho: o problema da detecção é relaxado e o *framework* de otimização convexa é considerado. Essa área apresenta uma sólida teoria e ampla literatura disponível, por exemplo, (BOYD; VANDENBERGHE, 2004; ANTONIOU; LU, 2007), e alguns algoritmos são propostos e aplicados em problemas de larga escala com grande número de variáveis, como em (BERTSEKAS, 1981; SCHMIDT; KIM; SRA, 2011; KIM; SRA; DHILLON, 2010).

O trabalho é organizado como segue. O capítulo 2 traz detalhes sobre o sistema MIMO-OFDM considerado. A seção 2.1 aborda o primeiro trabalho no qual algoritmos heurísticos evolucionários *Particle Swarm Optimization* (PSO) e *Differential Evolution* (DE) são aplicados ao problema da detecção em sistemas MIMO-OFDM em cenários com correlação espacial entre as antenas. A calibração

dos parâmetros de entrada (FILHO; SOUZA; ABRAO, 2012) das técnicas heurísticas evolucionárias consideradas neste trabalho (PSO e DE) foram realizadas; a performance dos detectores é avaliada em termos de *Bit-Error-Rate* (BER) e a complexidade em quantidade de *Floating Point Operations* (FLOPs), definidos como sendo equivalente a uma soma, subtração, multiplicação ou divisão (GOLUB; LOAN, 2013). A complexidade computacional dos algoritmos heurísticos evolucionários aplicados ao problema de detecção dependem principalmente da quantidade de iterações/gerações e do número de partículas/indivíduos utilizados nos algoritmos PSO/DE.

A seção 2.2 detalha o segundo trabalho, onde detectores híbridos combinando detectores lineares e algoritmos heurísticos são propostos visando reduzir o número de iterações/gerações. Foram avaliadas via simulação Monte-Carlo as combinações de detectores lineares *Matched Filter* (MF) e *Minimum Mean Square Error* (MMSE) com as heurísticas PSO e DE no segundo estágio de detecção. A calibração de parâmetros de entrada do estágio heurístico foi executada novamente para cada um dos detectores híbridos. Através das simulações Monte Carlo, o número de iterações/gerações dos detectores híbridos foi reduzido substancialmente em comparação às estratégias heurísticas puras e, consequentemente, a complexidade computacional é diminuída, mantendo desempenhos em termos de BER semelhantes aos detectores heurísticos. Em outras palavras, o compromisso desempenho-complexidade foi melhorado substancialmente.

O capítulo 3 descreve uma terceira configuração de detecção, o qual considera um cenário *uplink* em sistemas M-MIMO, com terminais móveis dos usuários com uma única antena. O trabalho é dividido em duas partes. Na primeira, a performance de detectores formulados a partir de *Linear Programming* (LP) utilizando norma $\ell 1$ (LP$\ell 1$) e norma infinito (LP$\ell\infty$), *Quadratic Programming* (QP) e *Semidefinite Programming* (SDP) é avaliada em um cenário realista degradado por correlação espacial, erro na estimativa do canal, diferentes carregamentos do sistema (incremento na relação número de usuários e número de antenas) e a performance para diferentes ordens de modulação QAM (*Quadrature and Amplitude Modulation*) são obtidas através de simulações Monte Carlo utilizando *solvers* (*linprog, lsqlin*, CVX configurado com SDPT3). Na segunda parte, a aplicação de algoritmos específicos (algoritmos projetados) para a formulação QP foram propostos e caracterizados, sendo que o QP foi escolhido por apresentar um menor número de variáveis desconhecidas (complexidade menor) e bom desempenho. Uma das características dos algoritmos projetados é que sua convergência depende do condicionamento do Hessiano e, para o detector em M-MIMO formu-

lado como QP, o Hessiano é idêntico a *Gram matrix*. Apesar de $\mathbf{H}$ ser uma matriz com elementos aleatórios, em cenários M-MIMO com grande número de antenas, o comportamento dos autovalores de $\mathbf{H}^T\mathbf{H}$ tende a ser determinístico e seguir a lei de Marcenko-Pastur, dada através de (CHOCKALINGAM; RAJAN, 2014)

$$f_\lambda(\lambda) = \left(1 - \frac{1}{\frac{K}{M}}\right)^+ \delta(\lambda) + \frac{\sqrt{(\lambda - a)^+(b - \lambda)^+}}{2\pi\frac{K}{M}\lambda}, \tag{1.1}$$

com $a = (1-\sqrt{\frac{K}{M}})^2, b = (1+\sqrt{\frac{K}{M}})^2, \delta(\lambda)$ denotando a função delta de Kronecker, e a função $(.)^+ = \max(., 0), K$ denotando o número de usuários e M o número de antenas da estação rádio-base. A função pode ser visualizada na Fig. 1.3, onde $f_\lambda(\lambda)$ é avaliada para os diferentes carregamentos do sistema $\frac{K}{M}$ considerados. O *condition number* é calculado como a divisão entre o máximo e o mínimo autovalor. Conforme o carregamento diminui, a *Gram matrix* se torna bem condicionada pois os autovalores mínimos $\lambda_{\min}$ vão se afastando cada vez mais de zero (CHOCKALINGAM; RAJAN, 2014).

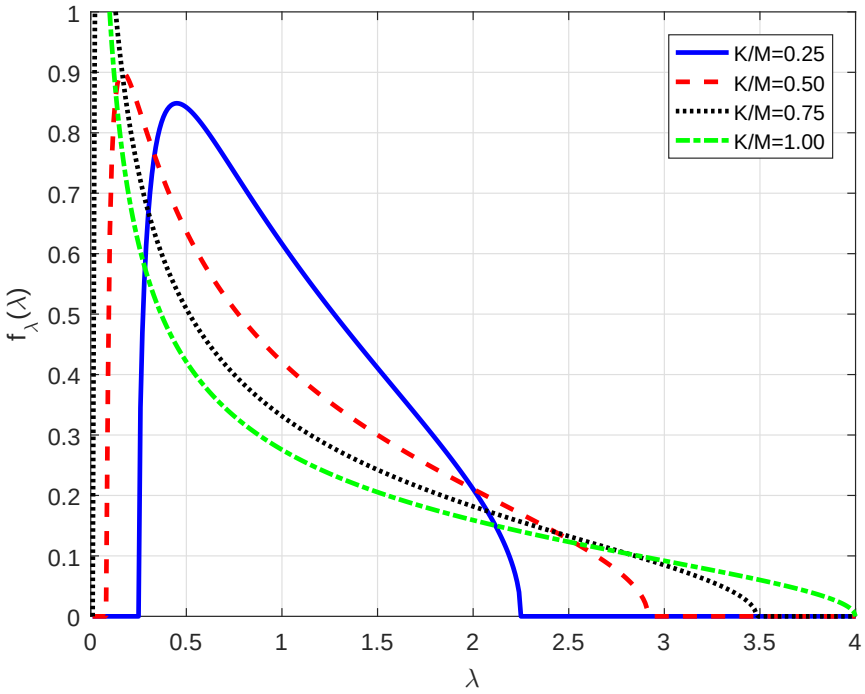

Figura 1.3: Comportamento dos autovalores da *Gram matrix* de acordo com a lei de Marcenko-Pastur.

Por fim, no capítulo 4 as conclusões e observações são apresentadas, e no Apêndice A, os trabalhos desenvolvidos durante o Mestrado são incluídos.

2 Detecção em Sistemas MIMO-OFDM

A modelagem do sistema considerado no primeiro e no segundo trabalho é apresentada aqui. O diagrama de blocos do sistema MIMO-OFDM ponto-a-ponto operando em modo multiplexagem é apresentado na Fig. 2.1. No transmissor, o *stream* de bits é multiplexado entre as N_t antenas do transmissor e recebido pelas N_r antenas do receptor, passando por blocos de transmissor e receptor do sistema OFDM clássico descritos na seção 1; após o bloco de recepção OFDM estão localizados os detectores, que são o foco deste trabalho.

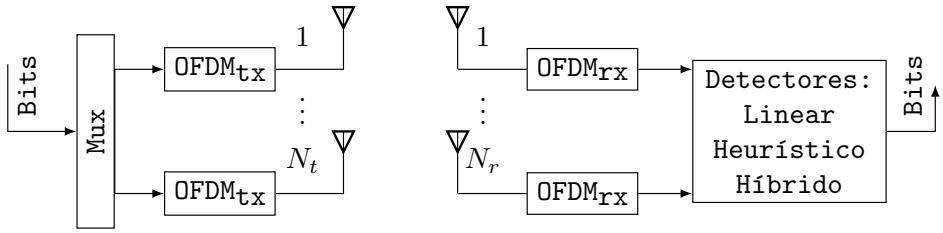

Figura 2.1: Diagrama de blocos do sistema MIMO-OFDM.

O sistema MIMO-OFDM pode ser representado matematicamente por (GORE, 2003)

$$\mathbf{y}[n] = \mathbf{H}[n]\mathbf{x}[n] + \mathbf{z}[n], \tag{2.1}$$

sendo $\mathbf{y}[n], \mathbf{H}[n], \mathbf{x}[n], \mathbf{z}[n]$ o sinal recebido, a matriz de canal, os símbolos transmitidos e o ruído aditivo para cada subportadora, respectivamente, e $n = 0, \ldots, N-1$ o índice das N subportadoras.

Buscando alcançar altos níveis de eficiência, o canal MIMO geralmente é considerado em um ambiente com alto espalhamento (isotrópico) e modelado seguindo uma distribuição Rayleigh independente (MARZETTA et al., 2016), porém, isso pode não ocorrer na prática. Como *rule-of-thumb*, o canal fading independente é assumido quando a distância de separação entre as antenas é maior que a metade do comprimento de onda (HAMPTON, 2014). Quando essa distância não é respeitada, por exemplo, por limitações de espaço do hardware, ocorre a

correlação espacial. O canal correlacionado utilizando o modelo de Kronecker é representado por

$$\mathbf{H}[n] = \sqrt{\mathbf{R}_r}\mathbf{G}[n]\sqrt{\mathbf{R}_t^H}, \tag{2.2}$$

sendo $\mathbf{R}_r, \mathbf{R}_t$ as matrizes de correlação do receptor e do transmissor, respectivamente, e $\mathbf{G}[n]$ é uma matriz com elementos independentes e identicamente distribuídos (iid).

As duas configurações ULA e URA diferem na construção da matriz de correlação. Para a ULA, a matriz de correlação é dada da forma (ZELST; HAMMERSCHMIDT, 2002)

$$\mathbf{R}_t = \mathbf{R}_r = \begin{bmatrix} 1 & \rho & \rho^4 & \dots & \rho^{(N_t-1)^2} \\ \rho & 1 & & & \vdots \\ \rho^4 & \rho & 1 & & \rho^4 \\ \vdots & \vdots & \vdots & \ddots & \rho \\ \rho^{(N_t-1)^2} & \dots & \rho^4 & \rho & 1 \end{bmatrix}, \tag{2.3}$$

sendo $\rho \in [0, 1]$ o índice de correlação entre as antenas, e, assumiu-se $N_t = N_r$ por simplicidade.

Para a URA, considerando um arranjo de antenas de tal forma a $N_r = N_x N_y$, onde N_x e N_y representam a quantidade de antenas nas direções do eixo-x e do eixo-y da região planar, respectivamente. Assumindo que a correlação do eixo-x denotado por $\mathbf{R}_x$ não depende do eixo-y e vice-versa para a matriz de correlação do eixo-y $\mathbf{R}_y$, a matriz de correlação é expressa por (LEVIN; LOYKA, 2010)

$$\mathbf{R}_t = \mathbf{R}_r = \mathbf{R}_x \otimes \mathbf{R}_y. \tag{2.4}$$

As matrizes de correlação do receptor e do transmissor são o resultado do produto de Kronecker entre as matrizes de correlação ULA para o eixo-x e eixo-y.

No primeiro trabalho são considerados os detectores lineares e heurísticos, com *Uniform Linear Array* (ULA) e *Uniform Rectangular Array* (URA) para a correlação espacial nas antenas do transmissor e receptor. No segundo trabalho, os detectores lineares, heurísticos e híbridos são comparados em um cenário com antenas em um arranjo ULA.

2.1 Detectores MIMO-OFDM Heurísticos Evolucionários

No primeiro trabalho, o problema da detecção é abordado utilizando algoritmos heurísticos evolucionários PSO e DE. Apesar de terem sido abordados em outros trabalhos como em (KHAN; NAEEM; SHAH, 2007; SEYMAN; TASPINAR, 2014; TRIMECHE et al., 2013), a calibração dos parâmetros para uma seleção mais adequada dos parâmetros de entrada (FILHO; SOUZA; ABRAO, 2012) bem como a caracterização considerando diferentes arranjos de antenas (ULA e URA) caracterizam contribuições deste trabalho.

As heurísticas PSO e DE foram escolhidas por sua simplicidade. O PSO é baseado no comportamento social de pássaros em bando (KENNEDY; EBERHART, 1995), apresentando parâmetros de entrada c_1, c_2, w chamados de fatores cognitivos, sociais e de inércia, respectivamente; cada partícula é associada a uma posição, e as posições são atualizadas em cada iteração. Os fatores cognitivos estão associados às posições pessoais (*personal best*); valores altos indicam que as partículas têm mais independência para explorar novas áreas da região de busca, enquanto fatores sociais estão associados à melhor posição do enxame (*global best*), e valores altos priorizam a busca ao redor da melhor posição global do enxame; o w pode ser uma constante, ou uma função linear ou não-linear dependente do número de iterações, cumprindo o papel de balancear a busca global e local (SHI; EBERHART, 1998); a estratégia adotada neste trabalho foi a não-linear decrescente da forma $0.99w$, com o algoritmo priorizando a busca global (em áreas maiores do espaço de busca) no início e com o passar das iterações, o peso tende para a busca local ao redor do *global best*.

A heurística DE é baseada em uma população de indivíduos $\boldsymbol{\iota}$ que evoluem a partir de operações de mutação, *crossover* e seleção, produzindo novos indivíduos com o passar das gerações do algoritmo (STORN; PRICE, 1997). Durante a mutação, os vetores de mutação são gerados combinando a diversidade da população de indivíduos ponderada pelo fator de mutação F_{mut}, assim, visando aumentar a diversidade dos vetores, os vetores de mutação $\boldsymbol{\nu}$ são amalgamados aos indivíduos $\boldsymbol{\iota}$ durante a operação de *crossover* gerando os vetores de *crossover* $\boldsymbol{\psi}$. Na etapa de seleção, a próxima geração é definida avaliando $\boldsymbol{\psi}$ e $\boldsymbol{\iota}$ através da *fitness function* selecionando aqueles que proporcionam o menor valor (problema é de minimização). A *fitness function* é baseada na distância Euclidiana (KHAN; NAEEM; SHAH, 2007; SEYMAN; TASPINAR, 2014; TRIMECHE et al., 2013) e utilizada para a avaliação da qualidade das soluções geradas em cada iteração/geração dos

algoritmos PSO/DE.[1]

2.1.1 Resultados Numéricos

Os parâmetros utilizados durante as simulações numéricas MCS são apresentados na tabela 2.1. Durante as simulações, considerou-se o conhecimento perfeito do canal e a alocação igualitária de potência entre as antenas (*equal power allocation, EPA*), sem linha de visada (*non-line of sight*, NLOS).

Tabela 2.1: Parâmetros das simulações com o sistema MIMO-OFDM e as heurísticas puras.

Parâmetro	**Valor**
OFDM	
Largura de banda BW	20MHz
Ordem da modulação	4-QAM
Delay spread, τ_{RMS}	51ns
# Subportadoras N	64
$(\Delta B)_c$	3.125MHz
Planicidade $\frac{(\Delta B)_c}{BW/N}$	10
MIMO	
# Antenas, $N_t \times N_r$	4×4
Detectores MIMO-OFDM	ML, ZF, MMSE, PSO e DE
Índice de correlação espacial	$\rho \in [0;\ 0.5;\ 0.9]$
Arranjo das antenas	Linear (ULA); Retangular (URA)
Detectores Heurísticos	
Espaço de busca	[-1; 1]
Dimensionalidade N_{dim}	$2N_t$
População e indivíduos	$N_{\text{pop}} = N_{\text{ind}} = 5N_{\text{dim}} = 40$
Iterações e gerações	$N_{\text{iter}} = N_{\text{gen}} = 100$
Detector PSO	
Cognitive factor c_1	4
Social factor $c_2(\rho)$	1 (0) 0.5 (0.5) 1 (0.9)
Inertia $w(\rho)$	1.5 (0) 1.5 (0.5) 3.5 (0.9)
Detector DE	
Fator de *crossover* $F_{\text{cr}}(\rho)$	0.6 (0) 0.6 (0.5) 0.8 (0.9)
Fator de mutação $F_{\text{mut}}(\rho)$	0.6 (0) 0.8 (0.5) 1.8 (0.9)

A escolha dos parâmetros de entrada dos algoritmos heurísticos podem influenciar os resultados de desempenho do sistema estudado, se escolhidos de ma-

[1] Apesar do algoritmo DE apresentar etapas com nomenclatura semelhante ao *Genetic Algorithm* (GA), eles são algoritmos distintos. O GA (GOLDBERG, 1989) utiliza uma terminologia mais próxima da teoria de Darwin; cada indivíduo possui genes. As etapas do GA incluem a reprodução onde, de forma parecida com a seleção natural, os indivíduos melhor avaliados pela *fitness function* tem mais chances de serem escolhidos para passar seus genes para a próxima geração. Durante a etapa de *crossover*, dois parentes têm uma certa quantidade (escolhida aleatoriamente) de genes trocados entre si. A operação de mutação provoca alterações aleatórias nos genes de alguns indivíduos.

neira incorreta (BONYADI; MICHALEWICZ, 2017; CLERC; KENNEDY, 2002; TRELEA, 2003). Aqui, os parâmetros de entrada foram determinados através de simulações Monte Carlo, conforme ilustrado nas Figs. 2.2 e 2.3, onde o desempenho do sistema MIMO-OFDM é dado em termos de BER, parâmetros de entrada dos algoritmos PSO e DE aplicados na detecção em sistemas MIMO-OFDM ponto-a-ponto, com quantidade suficiente de subportadoras para atingir a condição de *flat-fading*.

O procedimento de calibração de parâmetros de entrada adotado para os algoritmos heurísticos evolutivos é similar ao apresentado em (FILHO; SOUZA; ABRAO, 2012). Um parâmetro por vez é alterado e aquele que proporciona o melhor desempenho (menor BER) é escolhido, repetindo o procedimento para os demais parâmetros, conforme ilustrado na Fig. 2.2(a). Na Fig. 2.2(b), o comportamento com o passar das iterações do PSO é ilustrado, sendo possível notar que a quantidade de iterações é maior para níveis de E_b/N_0 maiores, ficando em torno de 50 iterações na condição $E_b/N_0 = 15$ dB para atingir a convergência, a partir do qual o aumento do número de iterações não provoca melhoria de desempenho significativo.

De maneira similar, os parâmetros de entrada do algoritmo DE aplicado ao problema de detecção MIMO-OFDM foram calibrados, conforme ilustrado na Fig. 2.3(a); para este algoritmo evolucionário, os parâmetros de entrada analisados são os fatores de mutação F_{mut} e de *crossover* F_{cr}. A convergência do DE é mostrada na Fig. 2.3(b); observou-se um comportamento semelhante ao PSO, necessitando de mais iterações quando se aumenta E_b/N_0, e cerca de 50 iterações para atingir convergência completa na condição $E_b/N_0 = 15$ dB.

Após a calibração dos parâmetros, o desempenho do sistema foi simulado, para os diferentes níveis de correlação espacial entre as antenas do transmissor e do receptor, conforme apresentado na Fig. 2.4. É possível observar que a correlação espacial deteriora a performance dos detectores, incluindo o ML. Os detectores utilizando as heurísticas DE e PSO apresentam melhor desempenho se comparados aos detectores lineares para os três cenários de correlação espacial. Para o índice de correlação mais alto, $\rho = 0.9$, o detector *Zero Forcing* (ZF) oferece desempenho proibitivamente deteriorado, mesmo aumentando E_b/N_0, enquanto os detectores heurísticos apresentam performance próxima do MMSE até cerca de 12 dB, ultrapassando o desempenho do detector linear MMSE com o aumento de E_b/N_0 nas regiões de média e elevada SNR. Comparando a performance dos dois arranjos uniformes de antenas, ULA e URA, o URA apresentou performance levemente melhor do que o ULA para alta E_b/N_0 e média correlação

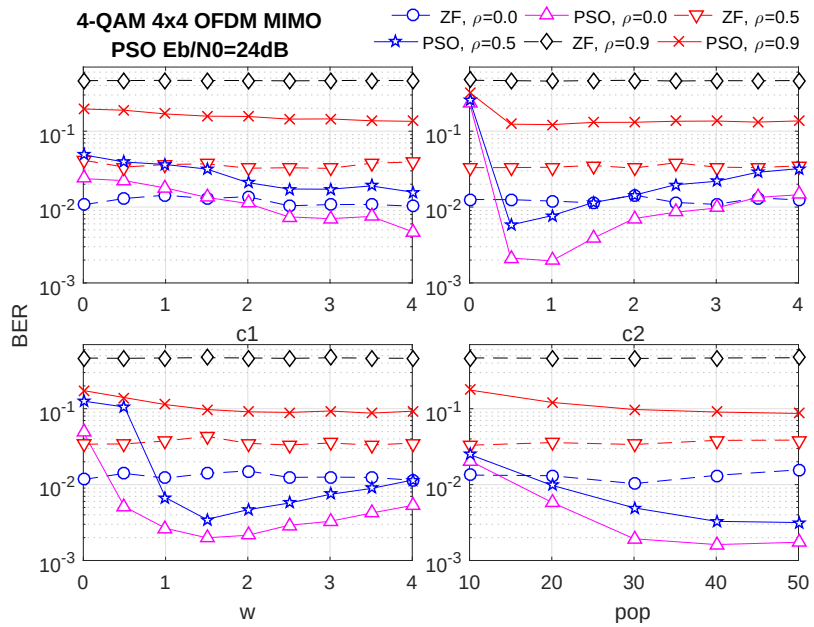

(a) Calibração dos parâmetros do PSO.

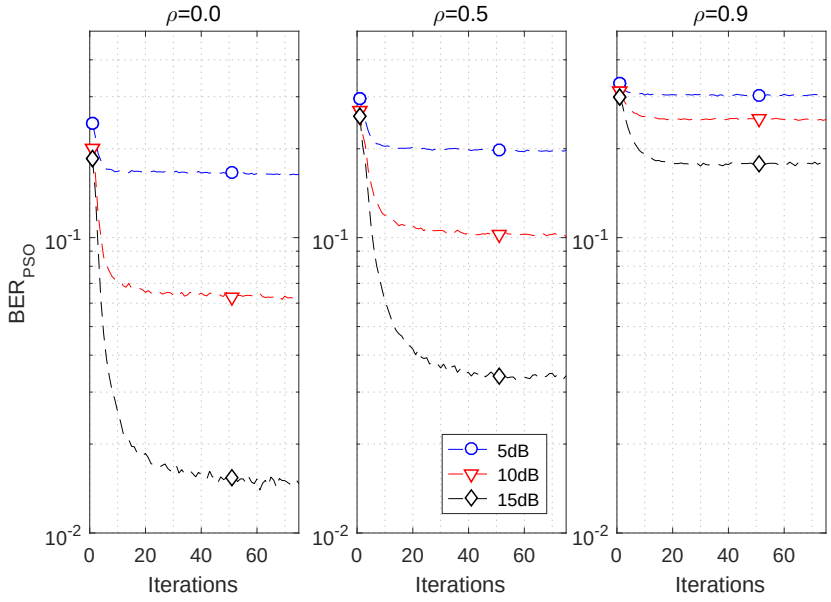

(b) Convergência do PSO.

Figura 2.2: Calibração dos parâmetros de entrada do algoritmo PSO aplicado na detecção em sistemas MIMO-OFDM.

espacial $\rho = 0.5$. Observa-se que a correlação na configuração URA é um pouco mais agressiva pois a quantidade de antenas próximas umas das outras é maior, e apesar disso a performance foi parecida com a ULA.

A complexidade computacional relativa é apresentada na Fig. 2.5. A complexidade computacional do detector ML depende da dimensionalidade do problema, i.e., cresce exponencialmente com a quantidade de antenas do transmissor e polinomialmente com a ordem da modulação QAM. A figura da esquerda mostra a redução da complexidade computacional em relação ao detector ML. Observa-se que os detectores MIMO-OFDM lineares apresentam a maior redução (são

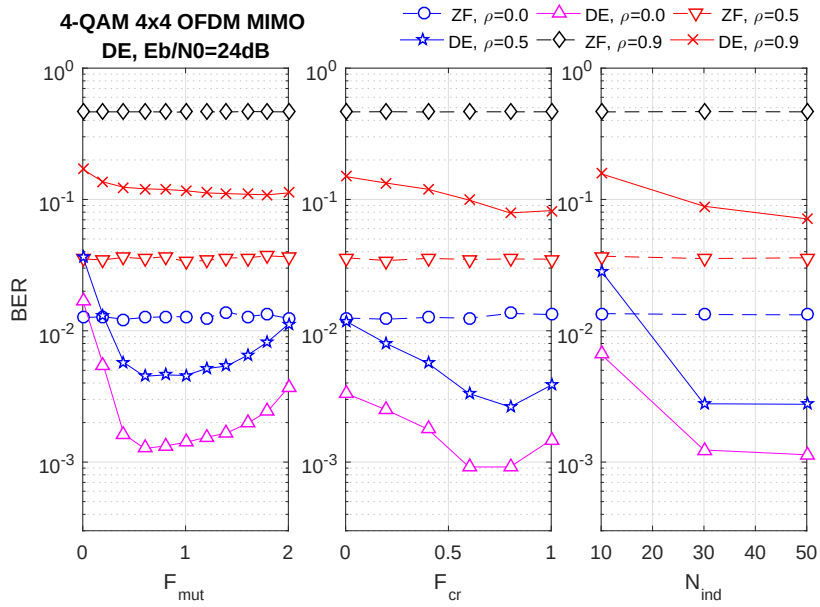

(a) Calibração dos parâmetros do DE.

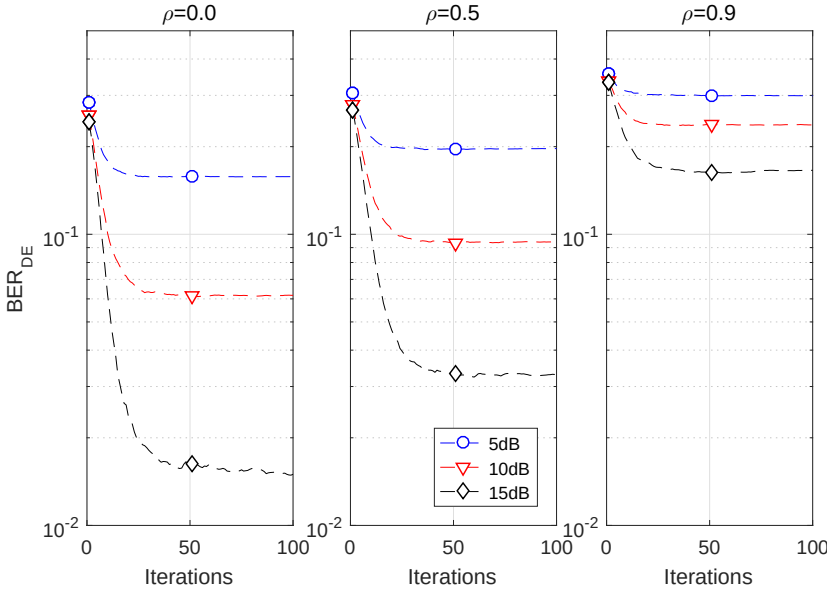

(b) Convergência do DE.

Figura 2.3: Calibração dos parâmetros de entrada do algoritmo DE aplicado na detecção em sistemas MIMO-OFDM.

menos complexos), seguidos do detector utilizando PSO e depois o DE. Na figura da direita, é mostrado o aumento da complexidade em relação ao detector ZF. Observa-se que a complexidade computacional relativa do MMSE é bastante próxima da complexidade do ZF. Os detectores heurísticos PSO, seguido do DE apresentam aumento da complexidade em relação ao ZF, e o detector ML apresenta um aumento bastante rápido e proibitivo com o aumento do número de antenas do sistema. Finalmente, pode-se concluir que as duas estratégias heurísticas analisadas são promissoras em termos de complexidade computacional no contexto *massive* MIMO ($N_t >= 64$), dado que a complexidade relativa decresce

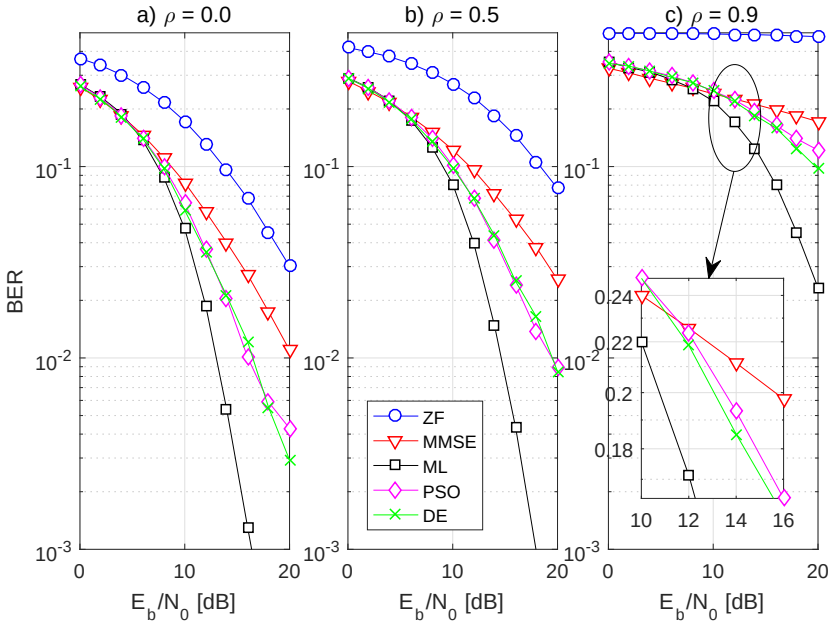

(a) Arranjo de antenas ULA.

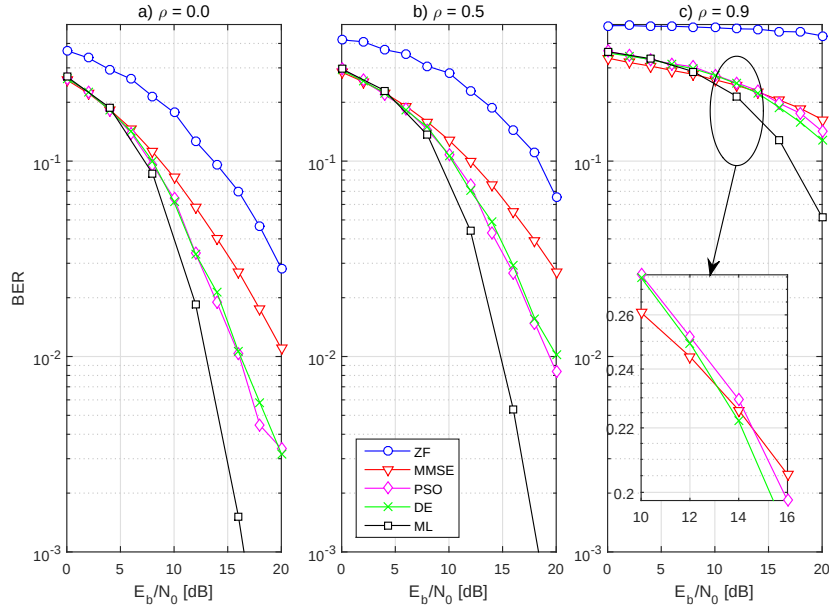

(b) Arranjo de antenas URA.

Figura 2.4: Performance dos detectores em um sistema MIMO-OFDM para os arranjos de antenas ULA e URA.

com o aumento do número de antenas na BS, porém é necessário investigar em termos de desempenho para uma efetiva implementação neste contexto.

2.1.2 Conclusões Parciais: Detectores MIMO-OFDM Heurísticos Puros

O foco do primeiro trabalho foi a aplicação das heurísticas PSO e DE como detectores em sistemas MIMO-OFDM com correlação espacial. De maneira geral, o aumento da correlação provoca a degradação do desempenho dos detectores;

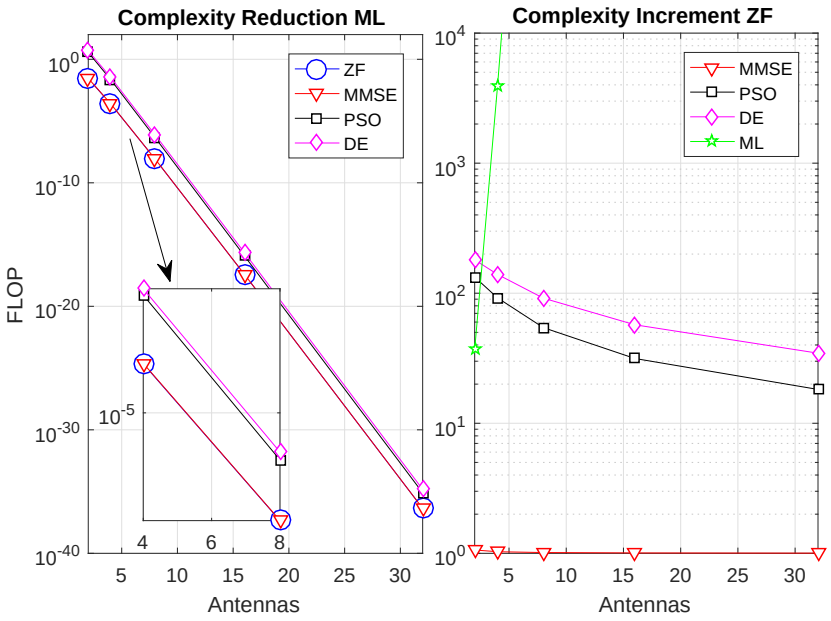

Figura 2.5: Complexidade computacional relativa para os detectores em sistema MIMO-OFDM em cenário ponto-a-ponto, considerando 4-QAM e $\mathcal{I} = 50$ iterações tanto para o DE quanto para o PSO.

foram observadas diferenças marginais de performance entre a configuração ULA e URA. Além disso, foram exploradas questões como a escolha dos parâmetros de entrada do PSO e DE; a quantidade de iterações é bastante semelhante (foi utilizado o valor $\mathcal{I} = 50$ para gerar a Fig. 2.5), porém há uma diferença de complexidade devido à etapa de seleção do DE, sendo necessário aplicar a *fitness function* tanto para o vetor de *crossover* quanto para os indivíduos, enquanto o PSO avalia apenas as partículas, as quais possuem a mesma dimensão N_{dim} dos vetores de indivíduos. Ambos os detectores MIMO-OFDM heurísticos apresentaram desempenho superior aos detectores lineares; dentre os heurísticos evolucionários, o PSO apresentou um melhor compromisso entre complexidade e desempenho pois é capaz de atingir desempenho semelhante ao DE com menor complexidade.

2.2 Detectores Híbridos

A complexidade computacional dos detectores heurísticos utilizando PSO e DE estudados no primeiro trabalho depende diretamente da quantidade de iterações $\mathcal{I}$ necessárias para cada uma das heurísticas. Com isso em mente, no segundo trabalho dessa Dissertação de Mestrado, detectores híbridos combinando detectores lineares e heurísticos são propostos visando reduzir a quantidade de iterações; ou, de modo equivalente, melhorar ainda mais o compromisso desempenho-complexidade. Os detectores híbridos são comparados em termos de performance (BER) e complexidade (número de FLOPs) aos lineares e aos heurísticos conside-

rando um sistema MIMO-OFDM ponto-a-ponto operando em modo multiplexagem com correlação espacial e antenas em configuração ULA.

Nas heurísticas DE e PSO aplicadas na detecção, a população e as posições iniciais foram geradas aleatoriamente (KENNEDY; EBERHART, 1995; STORN; PRICE, 1997) seguindo uma distribuição uniforme dentro da região de busca que, por sua vez, depende da constelação da modulação digital; durante as simulações numéricas, a modulação 4-QAM foi considerada, e portanto o espaço de busca foi limitado ao intervalo $[-1; 1]$.

Para os detectores híbridos, é realizada a combinação dos detectores lineares e os heurísticos de modo que um detector linear é estabelecido no primeiro estágio, seguido por um detector heurístico evolutivo no segundo estágio de detecção. Assim, no segundo estágio, a população e as posições iniciais são geradas ao adicionar números aleatórios com distribuição gaussiana $\mathcal{N}(0, 1)$ nas soluções produzidas pelos detectores lineares. Conforme ilustrado na seção a seguir, através de simulações numéricas MCS, a utilização de um ponto inicial razoavelmente próximo da solução (que são os símbolos transmitidos) fez com que a quantidade de iterações dos algoritmos híbridos fosse reduzida se comparada com as soluções heurísticas e, consequentemente, apresente uma complexidade computacional menor.

Dessa forma, duas diferentes estratégias para a escolha da população e das posições iniciais consideradas neste trabalho são:

- nos detectores com heurística, a utilização de inicialização aleatória seguindo uma distribuição uniforme dentro da região de busca;
- detectores híbridos que utilizam informações de detectores lineares para a geração da população e das posições iniciais. As combinações de detectores lineares e heurísticos avaliadas foram PSO-MF, PSO-MMSE, DE-MF e DE-MMSE.

2.2.1 Resultados Numéricos

Simulações numéricas MCS foram realizadas tendo em vista comparar o desempenho e complexidade de detectores lineares, heurísticos e híbridos em sistemas MIMO-OFDM ponto-a-ponto operando em modo multiplexagem em cenários com diferentes níveis de correlação espacial com antenas em arranjo ULA. Além disso, assumiu-se conhecimento perfeito do canal e alocação de potência igualitária. Os parâmetros considerados são apresentados na tabela 2.2. Os detectores foram

analisados observando o compromisso entre desempenho (avaliado em BER) e complexidade computacional (avaliado em termos de FLOPs).

Tabela 2.2: Parâmetros das simulações com o sistema MIMO-OFDM comparando os detectores híbridos.

Parâmetro	**Valor**
OFDM	
Largura de banda BW	20MHz
Ordem da modulação	4-QAM
Delay spread, τ_{RMS}	51ns
# Subportadoras N	64
MIMO	
# Antenas, $N_t \times N_r$	4×4
Detectores MIMO-OFDM	ML, ZF, MMSE, PSO, PSO-MF, PSO-MMSE, DE, DE-MF, DE-MMSE
Índice de correlação espacial	$\rho \in [0;\ 0.5;\ 0.9]$
Detectores Heurísticos e Híbridos	
Espaço de busca	[-1; 1]
Dimensionalidade N_{dim}	$2N_t$
População e indivíduos	$N_{\text{pop}} = N_{\text{ind}} = 5N_{\text{dim}} = 40$
Detector PSO	
Cognitive factor c_1	4
Social factor $c_2(\rho)$	1 (0) 0.5 (0.5) 1 (0.9)
Inertia $w(\rho)$	1.5 (0) 1.5 (0.5) 3.5 (0.9)
Detector PSO-MF	
c_1^{MF}	4
$c_2^{\text{MF}}(\rho)$	0.5 (0) 0.5 (0.5) 1 (0.9)
$w^{\text{MF}}(\rho)$	1.5 (0) 2 (0.5) 2.5 (0.9)
Detector PSO-MMSE	
$c_1^{\text{MMSE}}(\rho)$	3.5(0) 4(0.5) 4(0.9)
$c_2^{\text{MMSE}}(\rho)$	0.5 (0) 0.5 (0.5) 0.5 (0.9)
$w^{\text{MMSE}}(\rho)$	2 (0) 3 (0.5) 3 (0.9)
Detector DE	
Fator de *crossover* $F_{\text{cr}}(\rho)$	0.6 (0) 0.6 (0.5) 0.8 (0.9)
Fator de mutação $F_{\text{mut}}(\rho)$	0.6 (0) 0.8 (0.5) 1.8 (0.9)
Detector DE-MF	
$F_{\text{mut}}^{\text{MF}}(\rho)$	2 (0) 2 (0.5) 2 (0.9)
$F_{\text{cr}}^{\text{MF}}(\rho)$	0.8 (0) 0.7 (0.5) 0.9 (0.9)
Detector DE-MMSE	
$F_{\text{mut}}^{\text{MMSE}}(\rho)$	1.7 (0) 2 (0.5) 2 (0.9)
$F_{\text{cr}}^{\text{MMSE}}(\rho)$	0.6 (0) 0.7 (0.5) 0.8 (0.9)

A calibração dos parâmetros de entrada pode influenciar no desempenho dos detectores; assim, o procedimento descrito no primeiro trabalho para as heurísticas evolutivas, ilustradas em Fig. 2.2(a) e Fig. 2.3(a), foi aplicado para os detectores híbridos, conforme ilustrado na Fig. 2.6 e Fig. 2.7.

Através das figuras, é possível notar que existem determinados valores ou

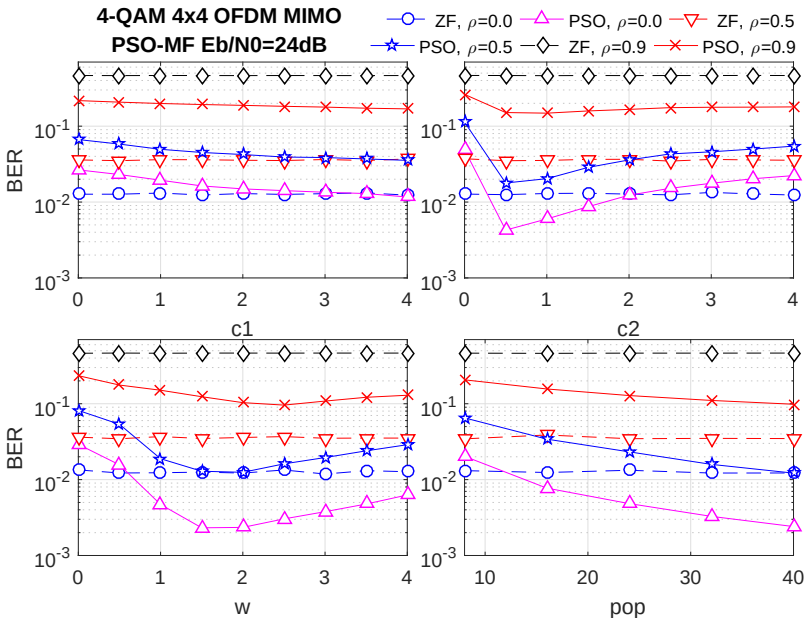

(a) Calibração do PSO-MF.

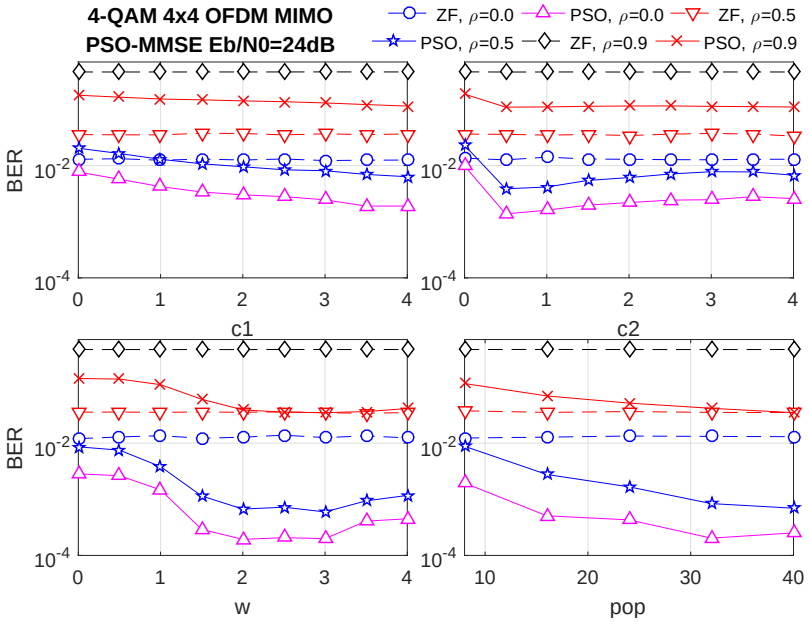

(b) Calibração do PSO-MMSE.

Figura 2.6: Calibração dos parâmetros de entrada dos detectores híbridos PSO-MF, PSO-MMSE.

faixa de valores de parâmetros que são mais adequados (apresentam menor BER) do que outros, e que tais parâmetros podem ser diferente entre os detectores heurísticos e detectores híbridos (por exemplo, observando o fator F_{mut} do DE com o do DE-MF), e inclusive diferentes dependendo do nível de correlação espacial. Os gráficos comparando a convergência dos detectores com heurística e os híbridos são apresentados na Fig. 2.8(a) e 2.8(b). Tais figuras ilustram o comportamento dos algoritmos com o passar das iterações. É possível notar que os detectores híbridos PSO-MF, PSO-MMSE, DE-MF e DE-MMSE necessitam de uma quantidade menor de iterações ($\mathcal{I}_{\text{hyb}} \approx 15$) para atingir um desempenho de

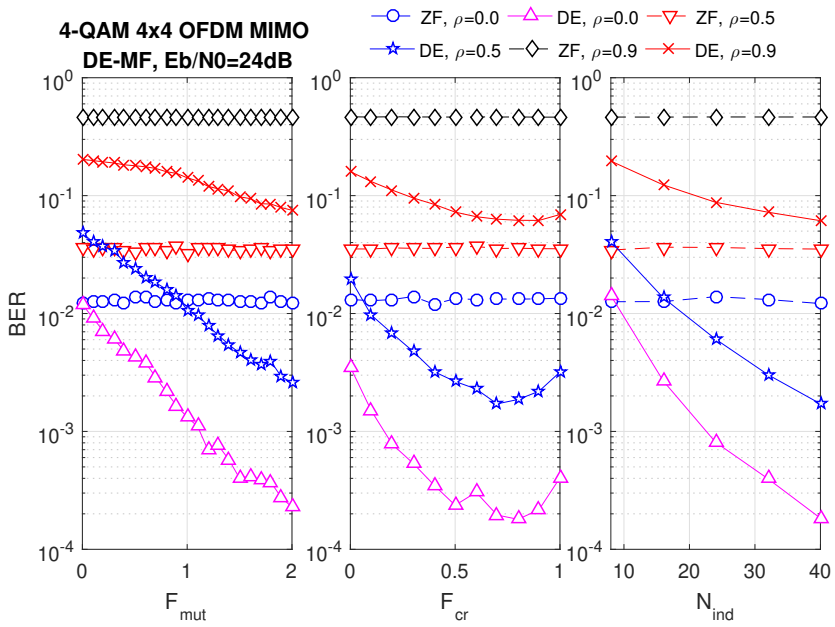

(a) Calibração do DE-MF.

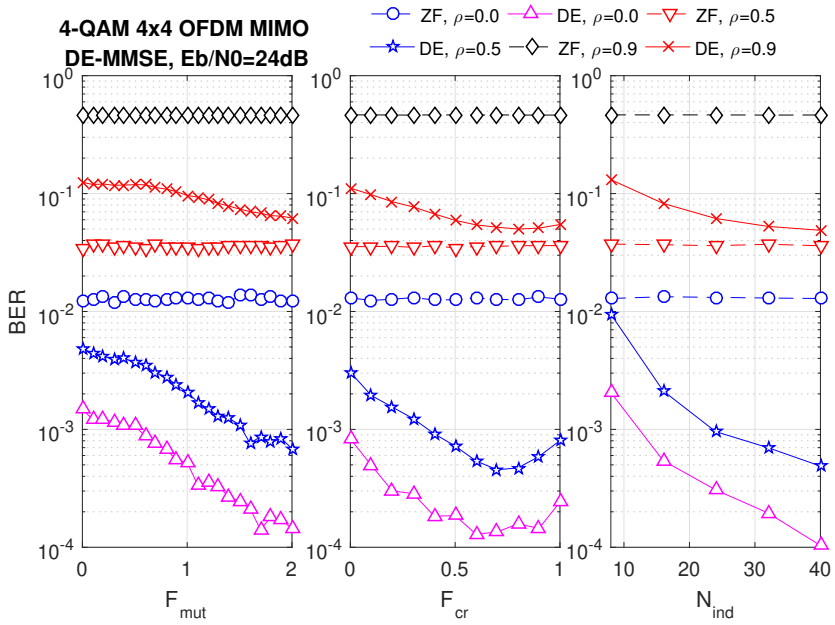

(b) Calibração do DE-MMSE.

Figura 2.7: Calibração dos parâmetros de entrada dos detectores híbridos DE-MF, DE-MMSE.

BER reduzido, enquanto os detectores heurísticos necessitam de cerca de $\mathcal{I} \approx 50$ iterações, conforme observado também no primeiro trabalho.

Após a calibração dos parâmetros de entrada dos detectores, o desempenho dos detectores híbridos foi simulado. A Fig. 2.9 mostra a performance dos detectores lineares MF e MMSE, da heurística PSO e dos detectores híbridos, PSO-MF e PSO-MMSE com quantidade diferente de iterações. Para o PSO-MF, nota-se que $\mathcal{I}_{\text{hyb}} = 15$ é suficiente para atingir performance similar ao detector com PSO e $\rho = 0$; para o PSO-MMSE, a melhoria em performance é mais expressiva, e

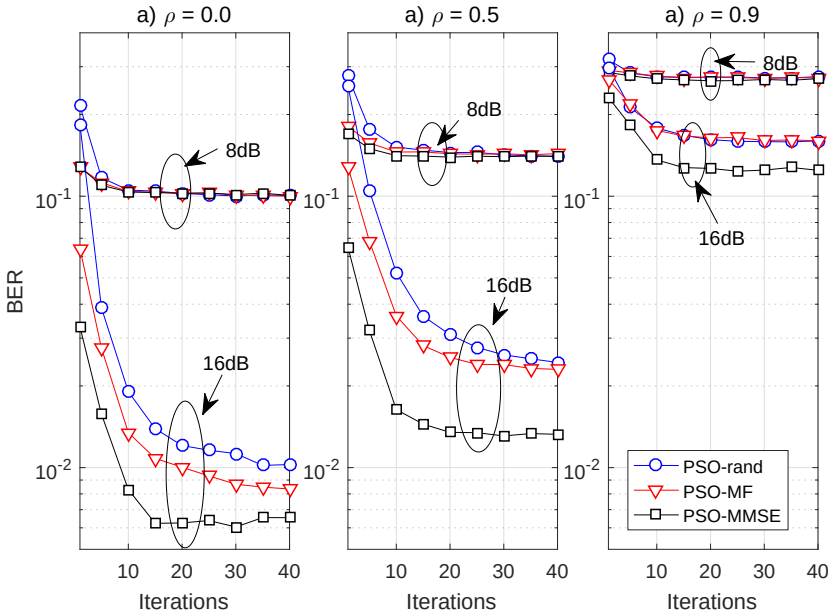

(a) Convergência dos detectores.

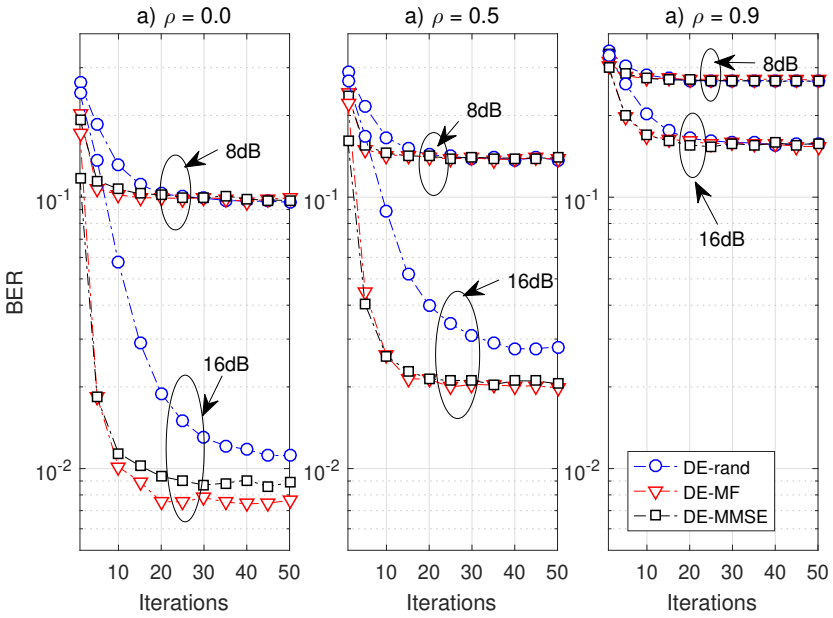

(b) Convergência dos detectores.

Figura 2.8: Convergência dos detectores híbridos PSO-MF, PSO-MMSE.

mesmo com $\mathcal{I} = 10$ é suficiente para atingir uma performance superior ao PSO. Já a Fig. 2.10 mostra a performance dos detectores híbridos DE-MF e DE-MMSE. A performance dos detectores híbridos apresentam desempenho superior ao DE, e foi observada pouca diferença de performance entre o DE-MF e o DE-MMSE para $\mathcal{I}_{\text{hyb}}$ acima de 10 iterações.

A Fig. 2.11 sumariza o desempenho dos detectores analisados. Nela, é possível observar que o detector MIMO-OFDM híbrido PSO-MMSE apresenta performance mais próxima ao ML. De fato, os detectores híbridos apresentam performance melhor do que os detectores heurísticos PSO e DE para $\rho = 0$ e $\rho = 0.5$,

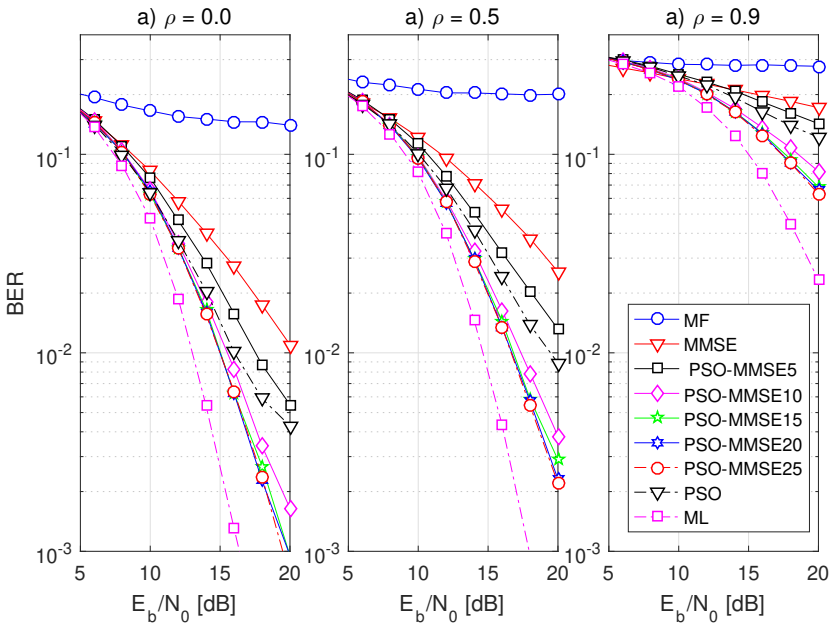

(a) Performance do detector PSO-MMSE.

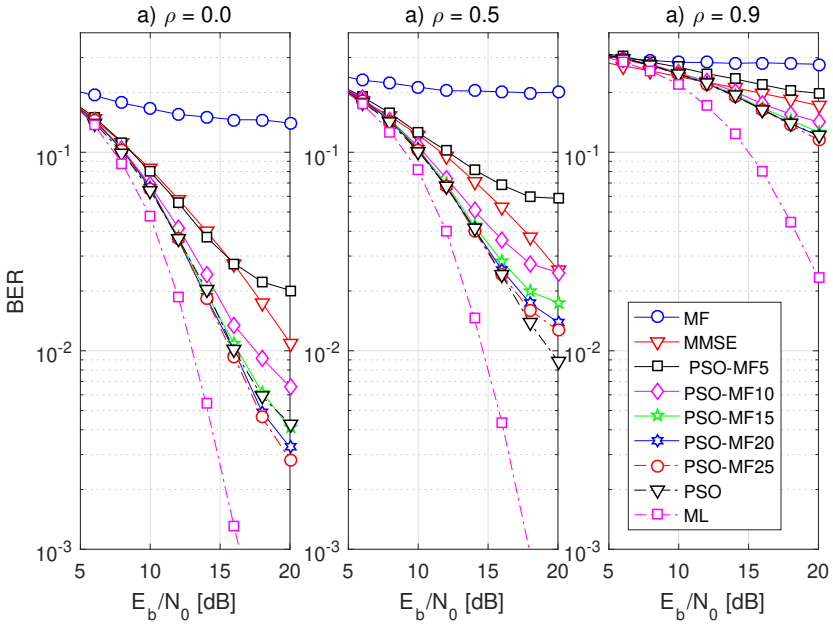

(b) Performance do detector híbrido PSO-MF.

Figura 2.9: Desempenho dos detectores híbridos PSO-MMSE e PSO-MF com parâmetros de entrada calibrados em sistema MIMO-OFDM com correlação.

enquanto o DE-MF e DE-MMSE apresentam performance similar para $\rho = 0.9$, e o PSO-MF apresenta uma performance próxima porém levemente pior que os detectores heurísticos.

Já a complexidade computacional dos detectores estudados é apresentada na Fig. 2.12. Como esperado, o ML apresenta a maior complexidade computacional, enquanto o MF apresenta a menor complexidade, seguido do MMSE. Os detectores híbridos apresentam complexidade computacional menor do que as heurísticas PSO e DE.

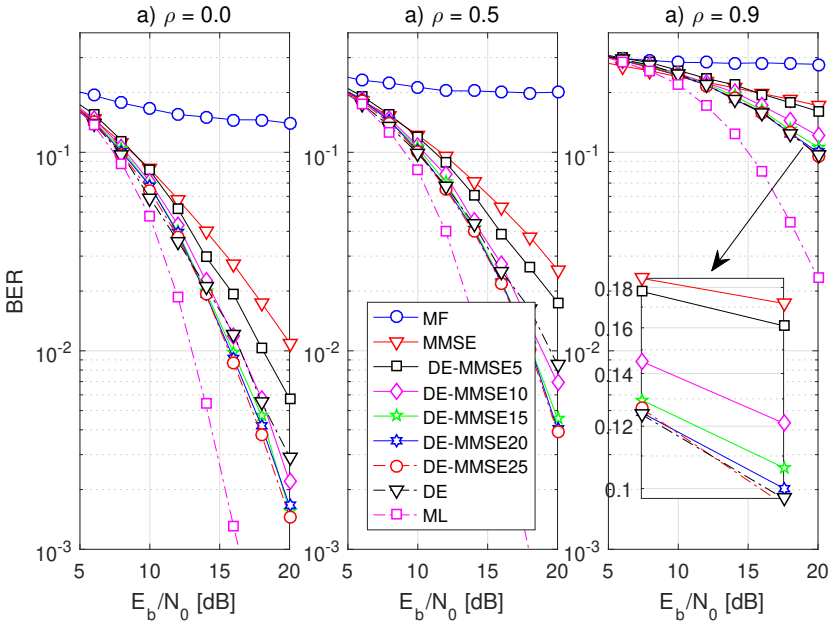

(a) Desempenho do detector DE-MMSE.

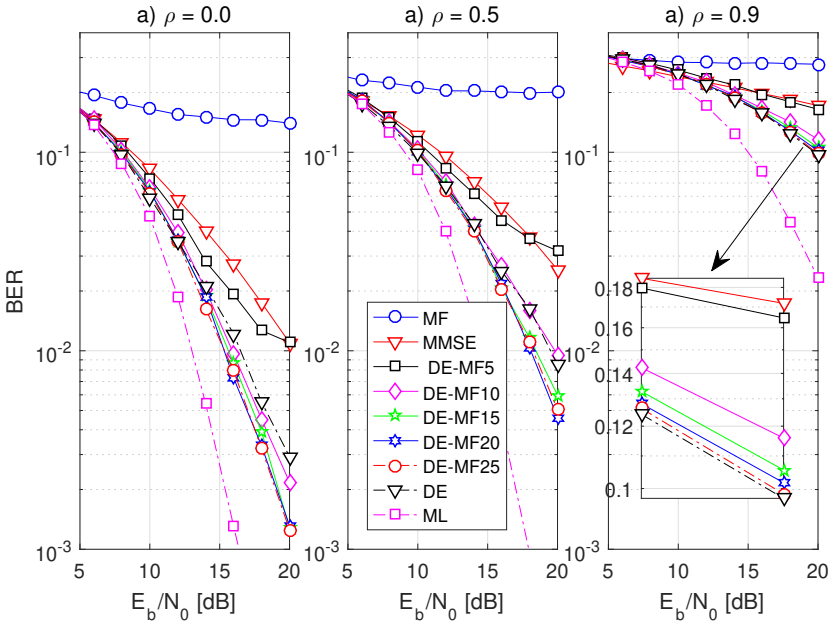

(b) Performance do detector híbrido DE-MF.

Figura 2.10: Performance dos detectores híbridos DE-MMSE e DE-MF com parâmetros de entrada calibrados em sistema MIMO-OFDM com correlação.

2.2.2 Conclusões Parciais: Detectores MIMO-OFDM Híbridos

Nesse segundo trabalho, detectores híbridos que combinam detectores lineares e heurísticos são estudados. Através de simulações numéricas MCS, a quantidade de iterações para que os detectores híbridos atingissem a convergência foi menor que as heurísticas evolutivas puras e, consequentemente, apresentaram complexidade computacional menor. As combinações de detectores lineares e heurísticos avaliadas foram PSO-MF, PSO-MMSE, DE-MF e DE-MMSE. O

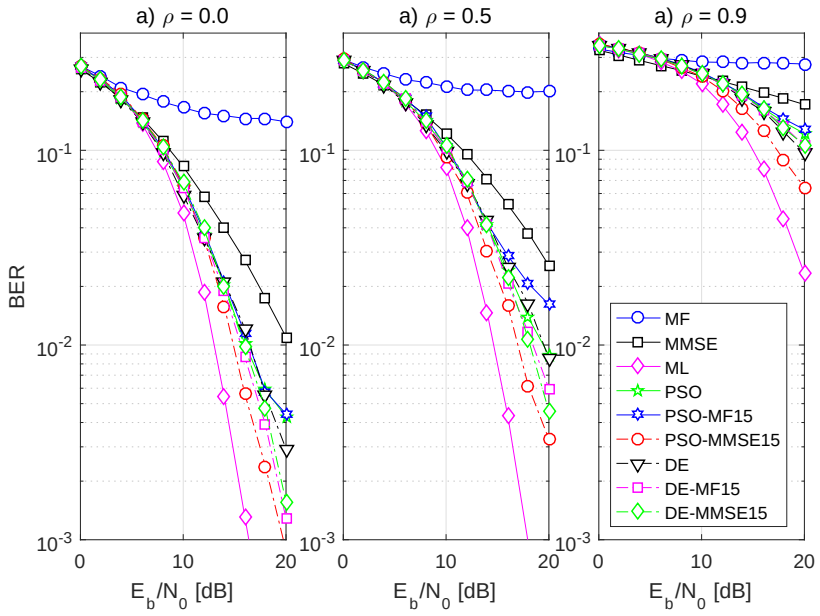

Figura 2.11: Desempenho em BER de diferentes detectores em um sistema 4-QAM MIMO-OFDM com correlação espacial.

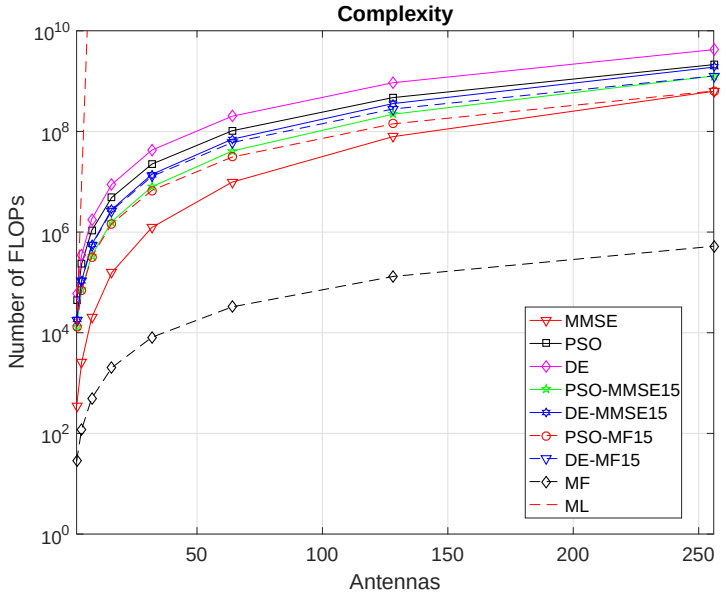

Figura 2.12: MIMO-OFDM Complexity considering an increasing number of antennas for linear, heuristic and hybrid detectors in a point-to-point scenario; $N_t = N_r, N_{\text{dim}} = 2N_t, N_{\text{pop}} = N_{\text{ind}} = 5 \cdot N_{\text{dim}}, \mathcal{I} = 50, \mathcal{I}_{\text{hyb}} = 15$.

PSO-MMSE apresentou a melhor performance durante as simulações; o DE-MF e DE-MMSE apresentaram desempenho parecido, enquanto o PSO-MF apresentou performance próxima porém pior em termos de BER. Dessa forma, os detectores MIMO-OFDM híbridos analisados foram capazes de melhorar o compromisso desempenho complexidade, proporcionando performance melhor ou muito próxima dos detectores com heurísticas evolutivas puras PSO e DE, apresentando uma complexidade computacional menor.

3 Detecção em Sistemas MIMO de Larga Escala

Em sistemas LS-MIMO, alguns efeitos começam a aparecer, como o *channel hardening*, onde a *Gram matrix* $\mathbf{H}^T\mathbf{H}$ se torna bem condicionada. Alguns detectores propostos na literatura buscam reduzir a complexidade computacional aproximando a inversa da matriz, por exemplo, com as séries de Neumann (WU et al., 2014), porém com a performance degradada com o aumento do número de usuários (TANG et al., 2016; MANDLOI; BHATIA, 2017) . Outra característica importante é que detectores lineares apresentam desempenho quase ótimo (RUSEK et al., 2013) quando o número de antenas M da *Base Station* (BS) é muito maior que o número de usuários K, porém a utilização de K muito pequeno pode limitar a capacidade do sistema (CHOCKALINGAM; RAJAN, 2014).

No terceiro trabalho desta Dissertação, o problema da detecção é relaxado e o *framework* de otimização convexa é considerado. Esta metodologia de otimização convexa apresenta uma sólida teoria e ampla literatura disponível, por exemplo, (BOYD; VANDENBERGHE, 2004; ANTONIOU; LU, 2007), e alguns algoritmos são propostos e aplicados em problemas de larga escala com grande número de variáveis, como em (BERTSEKAS, 1981; SCHMIDT; KIM; SRA, 2011; KIM; SRA; DHILLON, 2010).

O terceiro trabalho é dividido em duas partes. Na primeira, o problema da detecção M-MIMO é apresentado como diferentes problemas de otimização, especificamente o LP com a norma ℓ_1 (LPℓ1) (CUI; HO; TELLAMBURA, 2006), o LP utilizando norma infinita ℓ_∞ (LP$\ell\infty$), a formulação QP (ELGHARIANI; ZOLTOWSKI, 2016) e SDP, um detector bem definido na literatura (SIDIROPOULOS; LUO, 2006; NEGRAO; MUSSI; ABRAO, 2016). A performance dos detectores é caracterizada através de simulações numéricas MCS em cenários realistas compostos de erro na estimativa do canal, correlação espacial, carregamento do sistema e ordem de modulação, buscando apresentar uma extensiva análise explorando diferentes aspectos do sistema. Na segunda parte, os algoritmos projetados foram aplicados à

formulação QP; adicionalmente uma análise de complexidade computacional em termos de FLOPs é desenvolvida, evidenciando que diferentes carregamentos do sistema alteram a taxa de convergência dos algoritmos considerados neste estudo.

3.1 Detectores com Otimização Convexa

Nesta seção são mostrados a modelagem matemática do sistema LS-MIMO e também os detalhes da formulação dos detectores com otimização convexa. Considerando a representação em valores reais de um sistema LS-MIMO *uplink* onde cada usuário possui apenas uma antena, o sistema pode ser representado por

$$\mathbf{y} = \mathbf{H}\mathbf{x} + \mathbf{z}, \tag{3.1}$$

sendo $\mathbf{y}$ e $\mathbf{z} \in \mathbb{R}^{2M}, \mathbf{x} \in \mathbb{R}^{2K}$ e $\mathbf{H} \in \mathbb{R}^{2M \times 2K}$ o sinal recebido, ruído aditivo com variância σ_z^2, os símbolos transmitidos e a matriz do canal, respectivamente. Os valores K e M denotam o número de usuários e o número de antenas da BS.

No cenário realista considerado, a correlação espacial em configuração ULA foi considerada através do modelo de Kronecker (HAMPTON, 2014), construída da forma

$$\mathbf{H} = \sqrt{\mathbf{R}_M}\underline{\mathbf{H}}\sqrt{\mathbf{R}_K}, \tag{3.2}$$

sendo $\underline{\mathbf{H}}, \mathbf{R}_M$ e $\mathbf{R}_K$ a matriz com os coeficientes relacionados ao *small-scaling fading* independentes e identicamente distribuídos (iid), e as matrizes de correlação da BS e dos usuários.

A matriz de correlação espacial das antenas da BS $\mathbf{R}_M$ é a mesma da relação (2.3), e assumiu-se que $\mathbf{R}_K = \mathbf{I}$ pois os usuários são autônomos e não dependem uns dos outros.

Além disso, o erro na estimativa do canal também foi considerado, representado por

$$\widetilde{\mathbf{H}} = \sqrt{1-\tau^2}\mathbf{H} + \tau\mathbf{N}, \tag{3.3}$$

cada elemento da matriz $\mathbf{N}$ segue uma distribuição $\mathcal{N}(0,1)$ e $\tau \in [0,1]$ é o parâmetro de qualidade da estimativa do canal, onde $\tau = 0$ representa o conhecimento perfeito e $\tau = 0.1$ erro de 10%.

3.1.1 *Quadratic Programming*

Para recuperar a informação, o detector ML pode ser escrito como o problema de otimização

$$\begin{aligned} \min_{\mathbf{x}} \quad & \|\mathbf{y} - \mathbf{H}\mathbf{x}\|_p^2 \\ \text{s.t.} \quad & \mathbf{x} \in \mathcal{B}, \end{aligned} \tag{3.4}$$

onde os símbolos $\mathcal{B}$ são relacionados à modulação digital, por exemplo, para 16-QAM, $\mathcal{B} = \{-3; -1; 1; 3\}$, e p representa a norma. Note que o problema é denominado *Integer Programming*, pois $\mathbf{x}$ assume apenas valores inteiros.

Um procedimento usual visto em alguns trabalhos como (CUI; HO; TELLAMBURA, 2006; SIDIROPOULOS; LUO, 2006; Zhang; Lu; Gulliver, 2007) é relaxar o problema transformando a restrição inteira em uma restrição de caixa (*box constraint*). Utilizando $p = 2$, o *Quadratic Programming* (QP) pode ser escrito como

$$\begin{aligned} \min_{\mathbf{x}} \quad & \mathbf{x}^T\mathbf{H}^T\mathbf{H}\mathbf{x} - 2\mathbf{y}^T\mathbf{H}\mathbf{x} \\ \text{s.t.} \quad & \mathbf{b}_1 \leq \mathbf{x} \leq \mathbf{b}_2, \end{aligned} \tag{3.5}$$

onde o termo $\mathbf{y}^T\mathbf{y}$ foi omitido pois não altera o ponto ótimo, $\mathbf{b}_1 = -\mathbf{3}, \mathbf{b}_2 = \mathbf{3}$ para o caso da 16-QAM. Observa-se que o Hessiano da função objetivo da formulação QP resulta na *Gram matrix* $\mathbf{H}^T\mathbf{H}$, que assume um papel importante na convergência dos algoritmos projetados.

3.1.2 *Linear Programming*

Considerando o problema de otimização (3.4), agora sem o quadrado na função objetivo

$$\begin{aligned} \min_{\mathbf{x}} \quad & \|\mathbf{y} - \mathbf{H}\mathbf{x}\|_p \\ \text{s.t.} \quad & \mathbf{b}_1 \leq \mathbf{x} \leq \mathbf{b}_2, \end{aligned} \tag{3.6}$$

é possível obter diferentes detectores considerando diferentes normas p. Especificamente:

- **LP com norma $\boldsymbol{\ell_1}$** (LPℓ1): o problema da detecção (3.6) pode ser expresso como um *linear programming* (CUI; HO; TELLAMBURA, 2006)

$$\begin{aligned} \min_{\mathbf{x}, \mathbf{t}} \quad & \mathbf{1}^T\mathbf{t} \\ \text{s.t.} \quad & -\mathbf{t} \leq \mathbf{y} - \mathbf{H}\mathbf{x} \leq \mathbf{t}, \\ & \mathbf{b}_1 \leq \mathbf{x} \leq \mathbf{b}_2, \end{aligned} \tag{3.7}$$

- **LP com norma ℓ_∞** (LP$\ell\infty$): seguindo um procedimento similar ao da norma $\ell 1$, o problema de minimização da norma $\ell\infty$ pode ser convertido para um LP, procedimento chamado de *Chebyshev approximation* (BOYD; VANDENBERGHE, 2004). Aplicando ao problema detecção em sistemas M-MIMO, o seguinte detector é obtido:

$$\begin{aligned} \min_{\mathbf{x},t} \quad & t \\ \text{s.t.} \quad & -\mathbf{1}t \leq \mathbf{y} - \mathbf{H}\mathbf{x} \leq \mathbf{1}t, \\ & \mathbf{b}_1 \leq \mathbf{x} \leq \mathbf{b}_2. \end{aligned} \tag{3.8}$$

3.1.3 *Semidefinite Programming*

O detector utilizando a SDP é bem definido na literatura e conhecido por apresentar bom desempenho. Reorganizando os termos, a função objetivo do problema (3.5) pode ser expressa como

$$\mathbf{x}^T\mathbf{H}^T\mathbf{H}\mathbf{x} - 2\mathbf{y}^T\mathbf{H}\mathbf{x} = \begin{bmatrix}\mathbf{x} & 1\end{bmatrix}\begin{bmatrix}\mathbf{H}^T\mathbf{H} & -\mathbf{H}^T\mathbf{y} \\ -\mathbf{y}^T\mathbf{H} & 0\end{bmatrix}\begin{bmatrix}\mathbf{x} \\ 1\end{bmatrix} = \mathbf{x}_{\text{SDP}}\mathbf{L}\mathbf{x}_{\text{SDP}}.$$

Para a formulação SDP, é importante reconhecer que (LUO et al., 2010)

$$\mathbf{x}_{\text{SDP}}\mathbf{L}\mathbf{x}_{\text{SDP}} = \text{Trace}(\mathbf{x}_{\text{SDP}}\mathbf{L}\mathbf{x}_{\text{SDP}}) = \text{Trace}(\mathbf{L}\mathbf{x}_{\text{SDP}}\mathbf{x}_{\text{SDP}}^T) = \text{Trace}(\mathbf{L}\mathbf{X}),$$

onde a matriz $\mathbf{X}$ deve possuir rank um e ser uma matriz semidefinida positiva, condição denotada por $\mathbf{X} \succeq 0$. Relaxando a restrição de rank, o detector com SDP pode ser formulado como (SIDIROPOULOS; LUO, 2006)

$$\begin{aligned} \min_{\mathbf{X}} \quad & \text{trace}(\mathbf{L}\mathbf{X}) \\ \text{s.t.} \quad & \mathbf{X} \succeq 0, \\ & \mathbf{X}(N_{sdp}, N_{sdp}) = 1, \\ & b_1^{\mathcal{B}^2} \leq \mathbf{X}(i,i) \leq b_2^{\mathcal{B}^2}, \end{aligned} \tag{3.9}$$

onde a matriz $\mathbf{X}$ $N_{sdp} \times N_{sdp}$ é a variável desconhecida a ser otimizada, $N_{sdp} = 2K + 1$, o indexador $i = 1, \ldots, N_{sdp} - 1$ e os escalares $b_1^{\mathcal{B}^2}$ e $b_2^{\mathcal{B}^2}$ representam os limites superior e inferior do conjunto $\mathcal{B}^2$. Os limitantes das restrições de desigualdade podem ser interpretados da seguinte forma: ao invés da variável $\mathbf{x}$ que originalmente dependia da constelação $\mathcal{B}$, a variável de otimização da formulação SDP é uma matriz $\mathbf{X}$ relacionada ao quadrado de $\mathbf{x}$ e, consequentemente, depende do quadrado da constelação $\mathcal{B}^2$. Por exemplo, para uma 16-QAM, o conjunto se

torna $\mathcal{B}^2 = \{1, 9\}$, $b_1^{\mathcal{B}^2} = 1$ e $b_2^{\mathcal{B}^2} = 9$.

O método para a extração do vetor solução da matriz $\mathbf{X}$ foi a aproximação por rank-1 (LUO et al., 2010),

$$\mathbf{x}_{\text{SDP}}^{\star} = \mathbf{v}_1 \sqrt{\lambda}_1, \tag{3.10}$$

onde λ_1 denota o maior autovalor e $\mathbf{v}_1$ o seu respectivo autovetor.

3.2 Algoritmos Projetados

Os algoritmos implementados em *solvers* visam resolver uma vasta gama de problemas (*general-purpose*), porém, podem ser custosos computacionalmente (KIM; SRA; DHILLON, 2010). O algoritmo *two-metric projection* (TMP) foi concebido considerando uma estrutura particular de problema de otimização, propondo resolver problemas com restrições simples (*simple constraints*), por exemplo, restrições em que a variável desconhecida é não-negativa, e restrições de caixa (*box constraints*). Dependendo da matriz de direção $\mathbf{D}_n$ escolhida, o TMP pode se tornar diferentes algoritmos. Os algoritmos considerados neste trabalho foram:

1. $\mathbf{D}_n = \mathbf{I}$, resultando no *Projected Gradient* (PG) (SCHMIDT; KIM; SRA, 2011);
2. $\mathbf{D}_n = (\nabla^2 f(\mathbf{x}))^{-1} = (\mathbf{H}^T\mathbf{H})^{-1}$, com a direção sendo a inversa do Hessiano, resultando no algoritmo *Projected Newton* (PN) (BERTSEKAS, 1981);
3. $\mathbf{D}_n = \dfrac{1}{\text{diag}(\nabla^2 f(\mathbf{x}))}$, utilização da inversa da diagonal do Hessiano, chamado de *Diagonally Scaled Projected Gradient* (DSPG);
4. Aproximação da inversa do Hessiano utilizando séries de Neumann, chamado de *Projected Newton with Neumman Approximation (PNNA)*.

O algoritmo PN é descrito em detalhes em (BERTSEKAS, 1981) e também no Apêndice A.3. É possível notar que o PN, algoritmo que resolve problemas com restrições, especificamente, com *simple constraints*, apresenta grandes semelhanças com a sua versão que resolve problemas sem restrições, o método de Newton (*Newton's Method*, NM). Ambos são algoritmos iterativos, a direção é dada pelo inverso do Hessiano, e executam uma busca em linha para definir um passo (*step size*) para a próxima iteração. Os algoritmos param quando encontram um ponto crítico. Numericamente, foi considerado um certo ε_n calculado a partir do parâmetro de entrada ε, cujo valor foi ajustado através de simulações numéricas,

junto com os parâmetros de busca em linha β_{TM} e σ_{TM}, conforme ilustrado na próxima seção.

3.3 Resultados Numéricos

Os resultados numéricos são divididos em duas partes. Na primeira, o desempenho dos detectores formulados no *framework* de otimização convexa LPℓ1, LP$\ell\infty$, QP e SDP são avaliados em termos de BER. Na segunda, os algoritmos projetados são aplicados e caracterizados através de números de iterações N_{iter} e número de execuções de busca em linha m_{iter} para encontrar a solução do QP.

3.3.1 Avaliação de Desempenho

Na primeira parte, simulações MCS foram realizadas para caracterizar a performance dos detectores para LS-MIMO dentro do *framework* de otimização convexa avaliados em diferentes condições de operação, conforme sintetizado na tabela 3.1.

Tabela 3.1: Parâmetros utilizados para as simulações em sistema M-MIMO.

Parâmetro	**Valor**
Número de antenas na BS, M	128
Número de usuários, K	128
Ordem de modulação	16-QAM
Detectores LS-MIMO	ZF, MMSE, LP ℓ_1, LP ℓ_∞, QP, SDP
LP, QP e SDP *solvers*	*linprog, lsqlin*, CVX (SDPT3)
Condições do canal ρ e τ	0
Cenários	
Qualidade da estimação de canal, τ	[0; 0.05; 0.10]
Correlação de antena, ρ	[0; 0.5; 0.9]
Número de usuários, K	[128; 96; 64; 32]
Ordem de modulação	[4; 16; 64] QAM

Na Fig. 3.1, erros na estimativa do canal de 5% e 10% são considerados. O desempenho é comprometido para todos os detectores, enquanto um comportamento similar ao observado no cenário com estimativa perfeita do canal: o SDP apresenta o melhor desempenho, seguido do QP, LP$\ell\infty$, LPℓ1, e os lineares MMSE e ZF.

A Fig. 3.2 mostra o impacto da correlação espacial entre as antenas. No geral, a performance foi deteriorada para média correlação $\rho = 0.5$. Para o ambiente com alta correlação espacial $\rho = 0.9$, a performance é severamente comprometida,

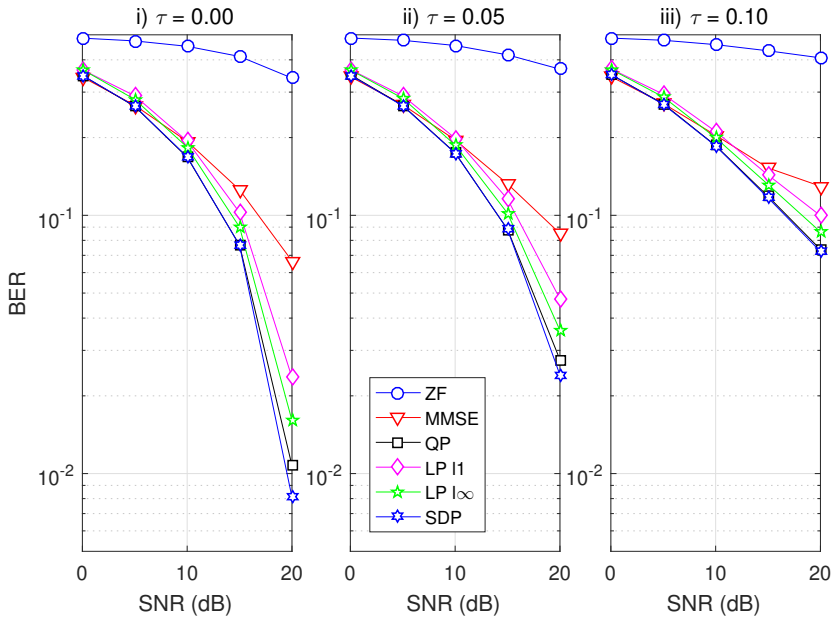

Figura 3.1: Desempenho com erro na estimativa do canal.

apresentando BER próxima e acima de 0.3 em ambiente com SNR de 20 dB para todos os detectores estudados.

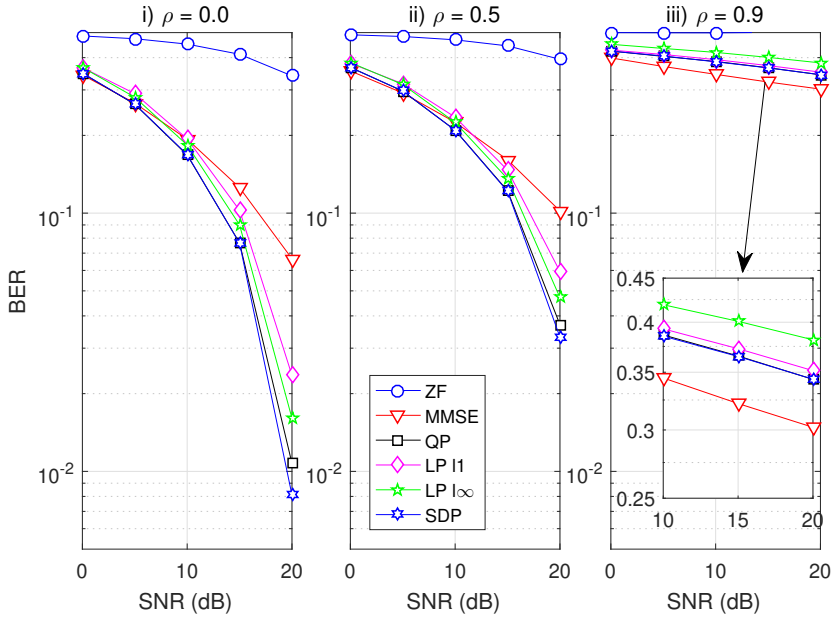

Figura 3.2: Desempenho com correlação espacial.

Para a Fig. 3.3, o carregamento do sistema $\frac{K}{M}$ foi alterado mudando o número de usuários do sistema enquanto o número de antenas da BS é mantido constante. Neste cenário, os detectores lineares apresentam comportamento quase ótimo (RUSEK et al., 2013), ficando bastante próximo do desempenho dos detectores QP e SDP. Os detectores com LP apresentaram alteração de comportamento em relação aos cenários anteriores, pois LPℓ1 apresentou desempenho melhor em relação ao LP$\ell\infty$ com a redução do carregamento do sistema.

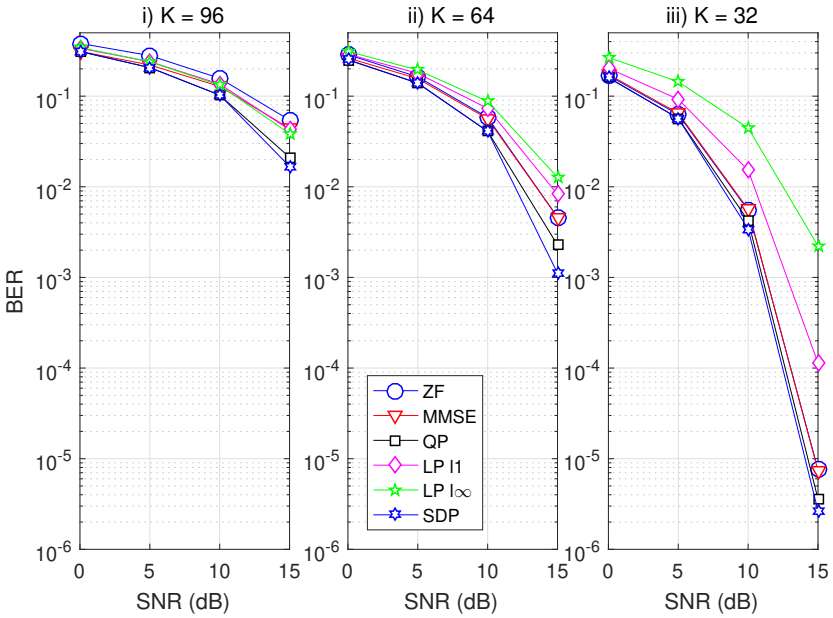

Figura 3.3: Desempenho variando carregamento do sistema.

Na Fig. 3.4, a mudança na ordem da modulação QAM é explorada numericamente. Para o cenário com baixa ordem de modulação 4-QAM, a melhora do desempenho do SDP em relação ao QP e demais detectores é mais evidente; além disso, o desempenho dos detectores com LP$\ell 1$ e LP$\ell\infty$ ficam bastante próximos, comportamento diferente do observado para modulações de alta ordem 16-QAM e 64-QAM, onde o desempenho do LP$\ell\infty$ é superior ao LP$\ell 1$.

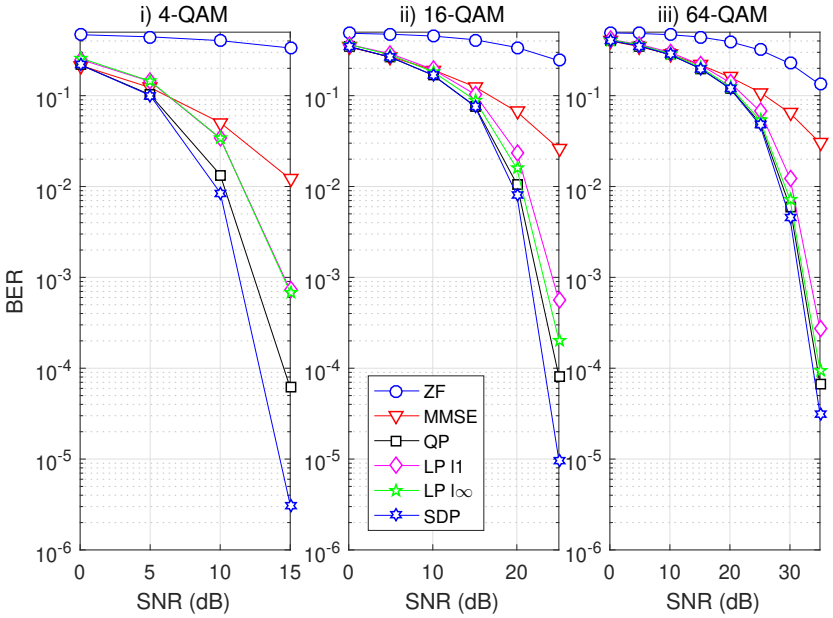

Figura 3.4: Desempenho com diferentes ordens de modulação QAM.

A partir dos gráficos apresentados nesta seção, nota-se que o SDP apresenta a melhor performance (com exceção do cenário com alta correlação $\rho = 0.9$, onde a performance de todos os detectores é severamente prejudicada) nas configurações consideradas, e a melhora da performance em relação ao QP é mais evidente

para modulação 4-QAM. O detector QP apresentou performance satisfatória com resultados superiores aos detectores M-MIMO lineares ZF e MMSE e os detectores LP$\ell 1$ e LP$\ell\infty$ nos diferentes cenários estudados. Dessa forma, a formulação QP foi avaliada utilizando os algoritmos projetados que exploram a estrutura do problema de otimização, e caracterizado numericamente na próxima seção.

3.3.2 Caracterização dos Algoritmos Projetados

Na segunda parte do terceiro trabalho, os algoritmos projetados são caracterizados de duas formas, observação do comportamento com o aumento do número de usuários e número de antenas constante, e no segundo cenário, o comportamento quando o carregamento é constante e a dimensionalidade do problema é aumentada. Os parâmetros considerados durante as simulações são apresentados na tabela 3.2. Algumas referências sugerem valores para os parâmetros da busca em linha como $\beta_{\text{TM}} = 0.5$ e $\sigma_{\text{TM}} = 10^{-4}$ (BERTSEKAS, 1981), porém não apresentam justificativa para esta escolha; aqui, tais parâmetros são obtidos através de simulações numéricas utilizando a mesma a metodologia sistemática para a escolha dos parâmetros de entrada descrita no primeiro e no segundo trabalho.

Tabela 3.2: Parâmetros da simulação para os algoritmos projetados.

Parâmetro	**Valores**
M	128
K	128
SNR	15 dB
Detectores	QP, MMSE
Algoritmos para QP	PN, PNNA, DSPG, PG
Intervalos	
γ	$\in [0; 1.5]$
β_{TM}	$\in [0.1; 0.9]$
σ_{TM}	$\in [0.1; 0.4]$
ε	$\in [0.5; 0.0001]$
Cenários	
Usuários K	[128; 96; 64; 32]
Carregamento constante $\frac{K}{M} = \frac{1}{4}$	$M = [128; 256]$

A Fig. 3.5 ilustra o comportamento para os diferentes parâmetros de busca em linha β_{TM} e σ_{TM}; a variável ε está associada ao critério de parada dos algoritmos projetados (anexo 3, equação 25) e sua influência foi observada apenas para o PN, ressaltando que a quantidade de iterações $N_{\max} = 5$ é pequena e não é suficiente para que os algoritmos atinjam a performance MMSE.

A influência de ε é melhor representada na Fig. 3.6, onde a performance dos

algoritmos projetados para cenários com diferente número de usuários é mostrada, junto com as curvas do detector MMSE e as informações de N_{iter} que representam a quantidade de iterações necessárias para o critério de parada ser atingido. Na Fig. 3.6(a), nota-se que valores de $\varepsilon = 0.5$ causam a parada prematura dos algoritmos DSPG, PNNA e PG pois o desempenho ainda melhoraria se os algoritmos rodassem por mais iterações. Na Fig. 3.6(b), o segundo *round* de simulações para escolha de ε é ilustrado, onde alguns dos valores são reduzidos para $\varepsilon = 0.1$ (parâmetros calibrados presentes na tabela 3.3), e os valores de N_{iter} são mais adequados, pois a performance em BER praticamente não se alteraria, mesmo se os algoritmos projetados fossem executados por mais iterações. Nota-se que, com a redução do carregamento do sistema, há uma redução do número de iterações N_{iter}, que está diretamente associado a complexidade computacional dos algoritmos projetados.

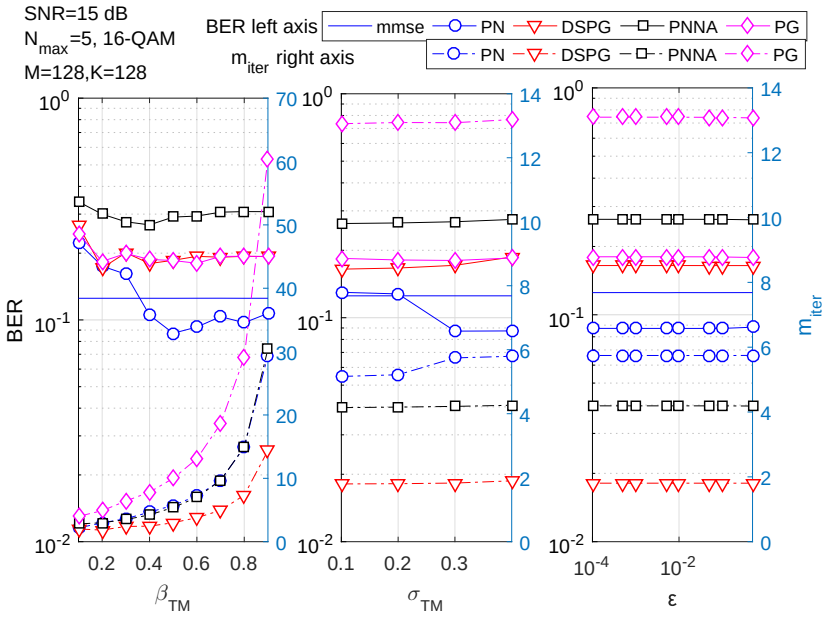

(a) Calibração para $K = 128$.

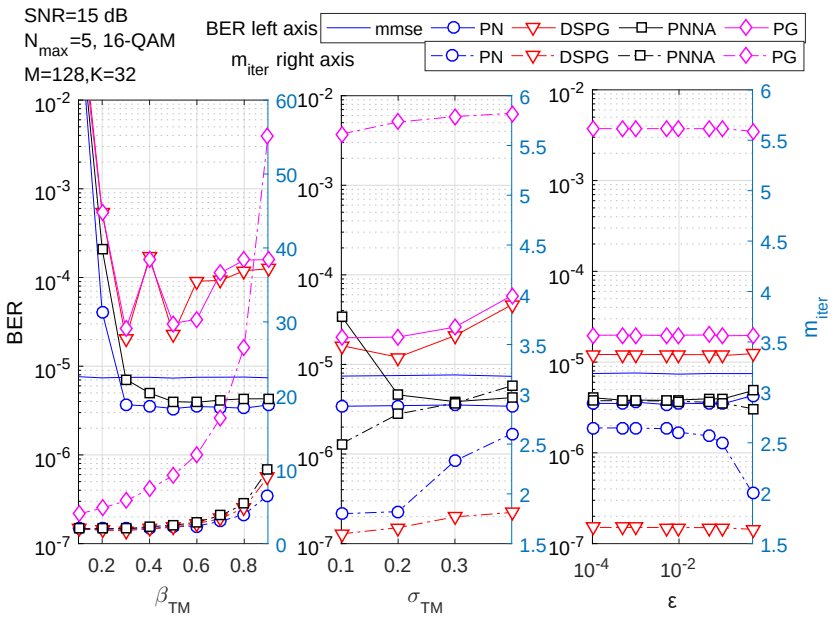

(b) Calibração para $K = 32$.

Figura 3.5: Calibração dos parâmetros $\beta_{\text{tm}}, \sigma_{\text{tm}}$ e ε.

Tabela 3.3: Parâmetros de entrada dos algoritmos projetados ajustados, considerando o cenário com carregamento variável. A ordem dos detectores é [PN; DSPG; PNNA; PG].

Parâmetro	K=128	K=96	K=64	K=32
γ	[1; 0; 0; 0]	[0; 0; 0; 0]	[0; 0; 0; 0]	[0; 0; 0; 0]
β_{TM}	[0.5; 0.2; 0.4; 0.6]	[0.5; 0.4; 0.2; 0.2]	[0.5; 0.6; 0.3; 0.4]	[0.5; 0.3; 0.6; 0.3]
σ_{TM}	[0.3; 0.1; 0.1; 0.3]	[0.3; 0.4; 0.2; 0.1]	[0.3; 0.3; 0.1; 0.2]	[0.4; 0.2; 0.3; 0.1]
ε, round 1	[0.5; 0.5; 0.5; 0.5]	[0.5; 0.5; 0.5; 0.5]	[0.5; 0.5; 0.5; 0.5]	[0.5; 0.5; 0.5; 0.5]
ε, round 2	[0.5; 0.1; 0.1; 0.1]	[0.5; 0.1; 0.1; 0.1]	[0.1; 0.1; 0.1; 0.1]	[0.1; 0.1; 0.1; 0.1]
N_{iter}	[15; 29; 51; 37]	[6; 20; 23; 19]	[5; 15; 13; 12]	[3; 7; 6; 8]
m_{iter}	[6.49; 1.72; 4.01; 12.67]	[4.09; 2.11; 2.51; 4.63]	[2.89; 2.82; 2.40; 7.23]	[2.61; 1.70; 2.94; 5.64]

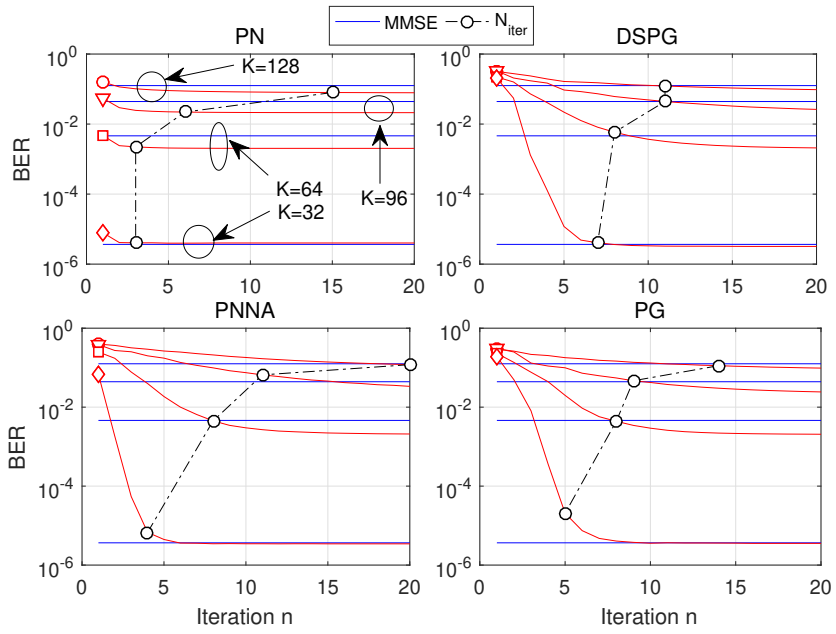

(a) Convergência considerando valores de ε do *round* 1.

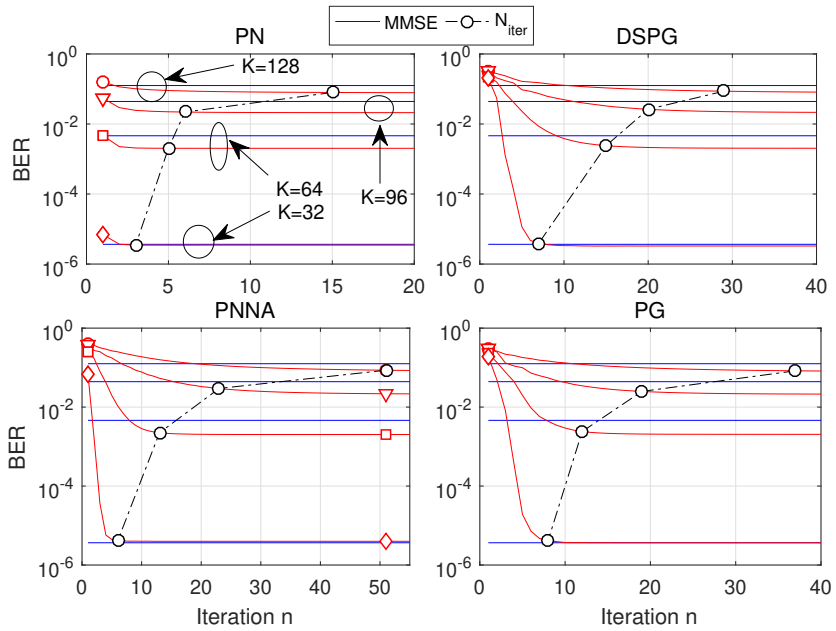

(b) Convergência considerando valores de ε do *round* 2.

Figura 3.6: Convergência dos algoritmos projetados variando o carregamento do sistema, considerando $M = 128$ e $SNR = 15$ dB.

Na Fig. 3.7, o comportamento dos algoritmos projetados é caracterizado analisando a situação onde o número de variáveis desconhecidas (usuários K) é aumentado mantendo o carregamento do sistema em $\frac{K}{M} = \frac{1}{4}$. A escolha dos parâmetros $\beta_{\text{TM}}, \sigma_{\text{TM}}$ e ε foi definida novamente através de simulações numéricas ilustradas pela Fig. 3.7(a). A convergência dos algoritmos projetados é apresentada na Fig. 3.7(b); nota-se que quando K é aumentado mantendo o carregamento do sistema constante, o número de iterações para atingir a convergência N_{iter} permanece praticamente inalterado.

Tabela 3.4: Parâmetros ajustados dos algoritmos projetados para o cenário com carregamento constante. A ordem é [PN; DSPG; PNNA; PG].

Parameter	$M = 256, K = 64$
γ	[0; 0; 0; 0]
β_{TM}	[0,5; 0,5; 0,5; 0,5]
σ_{TM}	[0,3; 0,2; 0,2; 0,2]
ε	[0.1; 0.1; 0.1; 0.1]
N_{iter}	[4; 8; 6; 8]
m_{iter}	[2.29; 2.11; 2.50; 10.11]

3.4 Complexidade computacional

Na primeira parte do terceiro trabalho, o desempenho foi avaliado em BER para diferentes detectores formulados utilizando otimização convexa e, durante as implementações, foi empregado o uso de *solvers linprog* e *lsqlin* do Matlab (MATLAB, a, b), e o SDP3 (TÜTÜNCÜ; TOH; TODD, 2003) selecionado através do CVX (GRANT; BOYD, 2014). Nota-se que tanto o QP quanto o LP podem ser resolvidos utilizando algoritmos de pontos interiores (ANTONIOU; LU, 2007; NOCEDAL; WRIGHT, 2006); tais algoritmos resolvem um sistema linear de equações em cada iteração, consequentemente, a complexidade computacional é cúbica (ELGHARIANI; ZOLTOWSKI, 2016; LAU et al., 2009), a mesma dos detectores lineares. Já para o SDP, algumas implementações específicas de algoritmos de pontos interiores sugerem uma complexidade computacional da ordem de $\mathcal{O}(K^{3.5})$ (MA et al., 2008; LUO et al., 2010). As informações sobre os detectores utilizando otimização convexa, o tamanho do problema e a complexidade são sintetizadas na tabela 3.5. Confrontando com o desempenho em BER obtido na seção anterior, nota-se que o SDP apresentou um bom desempenho porém com um custo computacional por iteração elevado; já o QP apresentou o segundo melhor desempenho entre os detectores estudados e a menor quantidade de variáveis desconhecidas em sua formulação.

Tabela 3.5: Tamanho do problema em termos do número de variáveis desconhecidas e as respectivas complexidades para os detectores em LS-MIMO.

Detector	**# Variáveis**	**Restrições**	**Complexidade**
QP (3.5)	$2K$	$4K$	$\mathcal{O}(N_{\mathrm{iter}}K^3)$
LPℓ1 (3.7)	$2K + 2M$	$4M + 4K$	$\mathcal{O}[N_{\mathrm{iter}}(K + M)^3]$
LP$\ell\infty$ (3.8)	$2K + 1$	$4M + 4K$	$\mathcal{O}[N_{\mathrm{iter}}(K + 1)^3]$
SDP (3.9)	$(2K + 1)^2$	$4K + 1$	$\mathcal{O}(N_{\mathrm{iter}}K^{3.5})$

Para a segunda parte, a complexidade computacional dos algoritmos projeta-

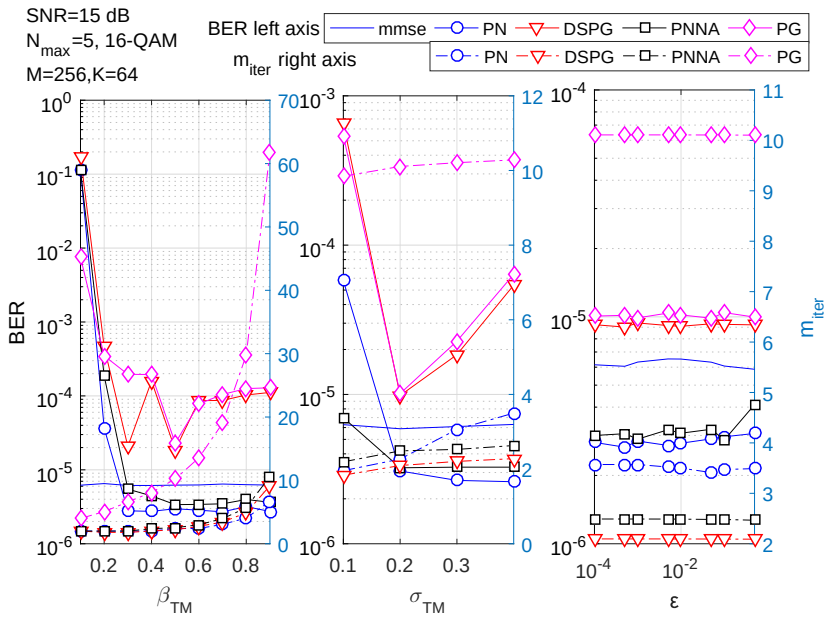

(a) Calibração dos parâmetros para $M = 256$, carregamento do sistema $\frac{1}{4}$, $SNR = 15$ dB.

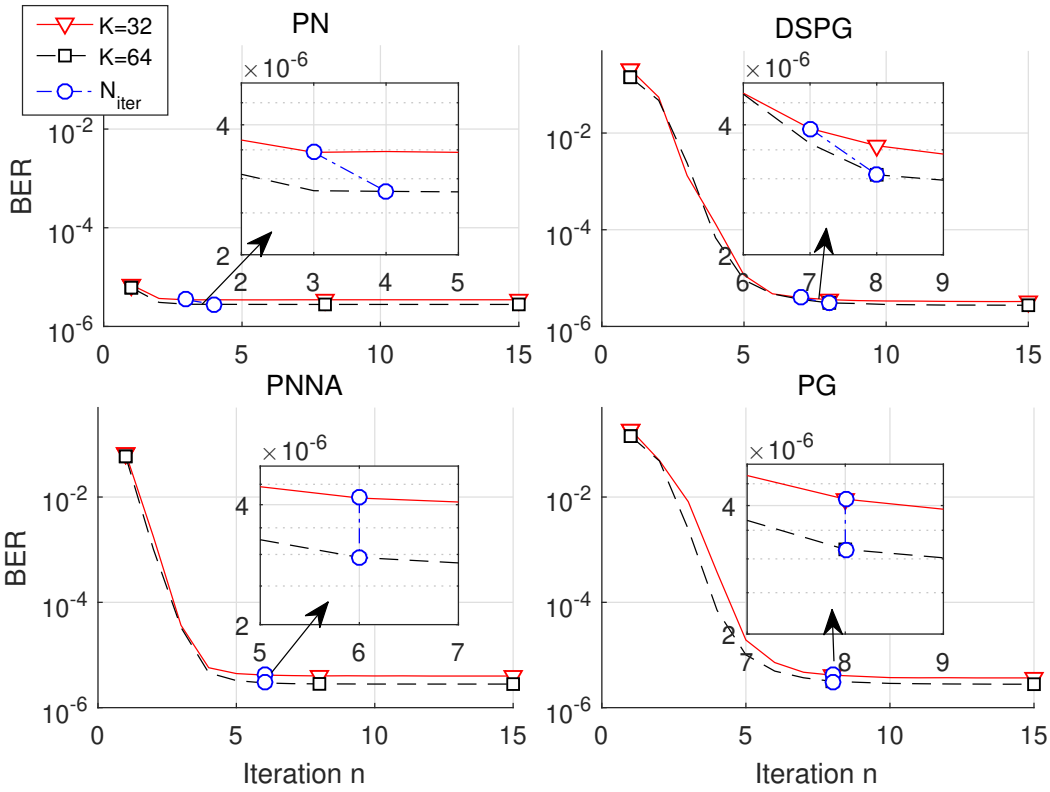

(b) Convergência para $K = 32, M = 128$ e para $K = 64, M = 256$, carregamento do sistema $\frac{1}{4}$, $SNR = 15$ dB.

Figura 3.7: Comportamento dos algoritmos projetados quando a dimensionalidade do problema é aumentada.

dos é apresentada na Fig. 3.8. Na figura da esquerda, nota-se que a complexidade computacional em número de FLOPs dos algoritmos projetados é maior que a do detector linear MMSE para os diferentes números de usuários e $M = 128$. Ou seja, a performance dos algoritmos projetados supera a do MMSE (Fig. 3.6(b)),

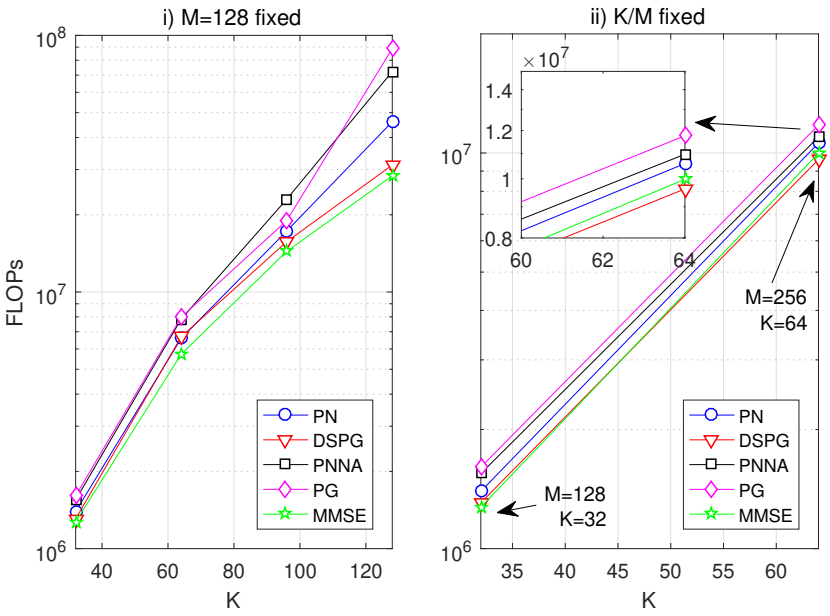

Figura 3.8: Número de FLOPs para os detectores M-MIMO utilizando os algoritmos projetados variando K, e na condição K/M constante.

ao custo de uma complexidade computacional maior, sendo o DSPG algoritmo que apresenta a complexidade computacional mais próxima do MMSE. A figura da direita mostra a complexidade computacional mantendo o carregamento do sistema em $\frac{1}{4}$. Diferente da complexidade cúbica reportada na literatura para os algoritmos de pontos interiores (ELGHARIANI; ZOLTOWSKI, 2016), os algoritmos projetados apresentam complexidade da ordem de $\mathcal{O}(N_{\text{iter}} m_{iter} K^2)$, dependendo diretamente do número de iterações N_{iter} até o critério de parada e do número de execuções da busca em linha m_{iter}. Quando o número de usuários é aumentado mas o carregamento é mantido constante, a quantidade de iterações N_{iter} praticamente não se altera, conforme observado durante simulações numéricas e mostrado na Fig. 3.7. Através das simulações, observou-se que para $K = 64, M = 256$, a complexidade computacional do DSPG começa a se tornar menor que a do MMSE, conforme ilustrado na figura da direita. Dessa forma, recomanda-se a utilização dos algoritmos projetados, particularmente o DSPG, quando a condição $N_{\text{iter}} m_{\text{iter}} < K$ puder ser satisfeita (por exemplo, $K = 64, M = 256$) em que se obtem uma performance levemente melhor com menor complexidade computacional comparado ao MMSE, ou em situações em que a melhora de desempenho justifique o pequeno aumento de complexidade computacional (por exemplo, $K = 128, M = 128$).

3.5 Conclusões Parciais: Detectores LS-MIMO

No terceiro trabalho, o problema da detecção em sistemas M-MIMO é estudado utilizando algoritmos de otimização convexa. Na primeira parte, as formulações LP$\ell 1$, LP$\ell\infty$, SDP e QP são simuladas em um cenário realista composto de erro na estimativa do canal, correlação espacial, alterações no carregamento do sistema, e altas ordens de modulação QAM.

Foram consideradas duas situações para a caracterização dos algoritmos projetados.

- A primeira situação detalhou o comportamento dos algoritmos projetados variando o carregamento do sistema $\frac{K}{M}$ alterando o número de usuários; para carregamento baixo, *gram matrix* bem condicionada (Fig. 1.3). Foram monitorados o número de iterações até o critério de parada N_{iter} e o número de vezes em que a busca em linha foi computada m_{iter}. Com a redução do carregamento, o número de iterações N_{iter} é reduzido para todos os algoritmos projetados.

- Após a implementação e o levantamento das expressões de complexidade, os detectores lineares MIMO de larga escala dependem de K^3, enquanto os projetados dependem de $N_{iter}m_{iter}K^2$. Dessa forma, foram realizadas simulações aumentando-se o número de K de forma a observar se a condição $N_{\text{iter}}m_{\text{iter}} < K$ ocorre ou não. Através das simulações, mantendo um carregamento baixo $\frac{1}{4}$ e o cenário $K = 64, M = 256$, o algoritmo DSPG foi capaz de apresentar número de FLOPs menor que o detector linear MMSE.

4 Conclusões

A detecção do sinal é uma etapa fundamental para os sistemas de telecomunicações, porém fundamentalmente o problema permanece *NP-hard*, e a solução ótima ML apresenta alta complexidade computacional em quase todos os cenários de interesse, sendo pouco adequada para aplicações práticas. Neste trabalho, foram estudadas a utilização de algoritmos heurísticos evolutivos e a aplicação de técnicas/procedimentos de otimização convexa no problema da detecção de dois sistemas diferentes denominados de MIMO-OFDM e LS-MIMO.

O foco do primeiro trabalho foi a aplicação das heurísticas PSO e DE como detectores em sistemas MIMO-OFDM com correlação espacial. De maneira geral, o aumento da correlação provoca a degradação em performance dos detectores; foram observadas diferenças marginais de performance entre a configuração ULA e URA em um sistema com 4×4 antenas. Além disso, foram exploradas questões como a escolha dos parâmetros de entrada do PSO e DE, visando uma comparação justa entre as heurísticas. Ambos os detectores heurísticos apresentaram desempenho melhor que os detectores lineares; entre os heurísticos, o PSO apresentou um melhor compromisso entre complexidade e desempenho, pois é capaz de atingir desempenho semelhante ao DE com menor complexidade.

No segundo trabalho, detectores híbridos, compostos de uma combinação entre detectores lineares no primeiro estágio e heurísticos evolucionários no segundo estágio, são estudados. Através de simulações numéricas, os detectores híbridos apresentaram uma complexidade computacional menor. As combinações de detectores lineares e heurísticos avaliadas foram PSO-MF, PSO-MMSE, DE-MF e DE-MMSE. O PSO-MMSE apresentou a o melhor desempenho avaliado por meio de simulações computacionais MCS. O DE-MF e DE-MMSE apresentaram desempenho similares, enquanto o PSO-MF apresentou performance próxima porém um pouco pior em termos de BER para a condição de alta SNR. Os detectores híbridos são capazes de melhorar o compromisso entre desempenho e complexidade, proporcionando performance melhor ou bastante próxima dos detectores com as heurísticas PSO e DE e apresentando uma complexidade computacional

menor.

No terceiro trabalho, o problema da detecção em sistemas M-MIMO foi estudado utilizando algoritmos de otimização convexa. Na primeira parte, as formulações LPℓ1, LP$\ell\infty$, SDP e QP foram simuladas em um cenário realista composto de erro na estimativa do canal, correlação espacial, alterações no carregamento do sistema, e altas ordens de modulação QAM. Na segunda parte, os algoritmos projetados foram aplicados na formulação QP. Para esta classe de algoritmos de detecção, a complexidade computacional depende do número de iterações N_{iter} e do número de execuções da busca em linha m_{iter}. A utilização dos algoritmos projetados é recomendada em cenários onde $N_{\text{iter}}m_{\text{iter}} < K$ para que a complexidade computacional seja menor que a complexidade dos detectores lineares. Através de simulações numéricas, constatou-se que a complexidade do DSPG é menor já para cenários $M = 256, K = 64$, configuração em que o número de FLOPs para o DSPG já se mostrou menor que o MMSE.

4.1 Trabalhos Futuros

Algumas propostas de trabalhos futuros incluem:

- Em (CUI; HO; TELLAMBURA, 2006), a detecção em conjunto com a decodificação são estudados para o detector com LPℓ1, e em (ELGHARIANI; ZOLTOWSKI, 2016) a performance do QP também com codificação. Uma possível proposta seria a investigação e comparação do funcionamento dos detectores avaliados (LPℓ1, LP$\ell\infty$, QP e SDP) utilizando estratégias de codificação.

- Investigar a influência da escolha do ponto inicial; ao invés de iniciar os algoritmos no meio da região *feasible*, utilizar, por exemplo, o detector linear MF e verificar a taxa de convergência dos algoritmos projetados.

- Em (ELGHARIANI; ZOLTOWSKI, 2016) o QP é comparado com as heurísticas *Local Ascent Search* e *Reactive Tabu Search* em cenário M-MIMO, porém apenas a ordem de complexidade é analizada e foram considerados algoritmos de pontos interiores. Uma possível investigação seria aprofundar a análise de complexidade computacional em termos de FLOPs e utilizando DSPG, o algoritmo projetado que se mostrou mais promissor dentre os estudados.

- Alguns trabalhos recentes estudam a utilização de técnicas de *Machine Le-*

arning em aplicações em telecomunicações (O'Shea; Hoydis, 2017; Wang et al., 2017; RAMANATHAN; JAYAKUMAR, 2017); sendo esse um campo de estudo promissor a ser explorado.

Referências

ANTONIOU, A.; LU, W.-S. *Practical Optimization: Algorithms and Engineering Applications*. 1st. ed. New York, NY, USA: Springer, 2007. ISBN 0387711066, 9780387711065.

BERTSEKAS, D. P. Projected newton methods for optimization problems with simple constraints. In: *1981 20th IEEE Conf. Decision Control including Symp. Adaptive Processes*. [S.l.: s.n.], 1981. p. 762–767.

BONYADI, M. R.; MICHALEWICZ, Z. Particle swarm optimization for single objective continuous space problems: A review. *Evolutionary Computation*, v. 25, n. 1, p. 1–54, 2017. PMID: 26953883.

BOYD, S.; VANDENBERGHE, L. *Convex Optimization*. New York, NY, USA: Cambridge University Press, 2004. ISBN 9780521833783.

CHO, Y. S.; KIM, J.; YANG, W. Y.; KANG, C. G. *MIMO-OFDM Wireless Communications with MATLAB*. [S.l.]: Wiley Publishing, 2010. ISBN 0470825618, 9780470825617.

CHOCKALINGAM, A.; RAJAN, B. S. *Large MIMO Systems*. New York, NY, USA: Cambridge University Press, 2014. ISBN 1107026652, 9781107026650.

CLERC, M.; KENNEDY, J. The particle swarm - explosion, stability, and convergence in a multidimensional complex space. *IEEE Transactions on Evolutionary Computation*, v. 6, n. 1, p. 58–73, Feb 2002. ISSN 1089-778X.

CUI, T.; HO, T.; TELLAMBURA, C. Linear programming detection and decoding for MIMO systems. In: *2006 IEEE Int. Symp. on Inf. Theory*. [S.l.: s.n.], 2006. p. 1783–1787. ISSN 2157-8095.

ELGHARIANI, A.; ZOLTOWSKI, M. Low complexity detection algorithms in large-scale MIMO systems. *IEEE Trans. Wireless Commun.*, v. 15, n. 3, p. 1689–1702, March 2016. ISSN 1536-1276.

FILHO, J. C. M.; SOUZA, R. N. de; ABRAO, T. Ant colony input parameters optimization for multiuser detection in ds/cdma systems. *Expert Systems with Applications*, v. 39, n. 17, p. 12876 – 12884, 2012. ISSN 0957-4174.

FOSCHINI, G. J. Layered space-time architecture for wireless communication in a fading environment when using multi-element antennas. *Bell Labs Technical Journal*, v. 1, n. 2, p. 41–59, Autumn 1996. ISSN 1089-7089.

GOLDBERG, D. E. *Genetic Algorithms in Search, Optimization and Machine Learning*. 1st. ed. Boston, MA, USA: Addison-Wesley Longman Publishing Co., Inc., 1989. ISBN 0201157675.

GOLDSMITH, A. *Wireless Communications*. [S.l.]: Cambridge University Press, 2005. ISBN 9780521837163.

GOLUB, G. H.; LOAN, C. F. V. *Matrix Computations*. 4. ed. [S.l.]: Johns Hopkins University Press, 2013. ISBN 9781421408590.

GORE, A. P. R. N. D. *Introduction to space-time wireless communications*. Repr. with corr. [S.l.]: Cambridge University Press, 2003. ISBN 9780521826150,0-521-06593-3,0521826152,9780521065931.

GRANT, M.; BOYD, S. *CVX: Matlab Software for Disciplined Convex Programming, version 2.1*. dez. 2014. `http://cvxr.com/cvx`.

GUPTA, A.; JHA, R. K. A survey of 5g network: Architecture and emerging technologies. *IEEE Access*, v. 3, p. 1206–1232, 2015. ISSN 2169-3536.

HAMPTON, J. R. *Introduction to MIMO Communications*. New York, NY, USA: Cambridge University Press, 2014. ISBN 1107042836, 9781107042834.

KENNEDY, J.; EBERHART, R. C. Particle swarm optimization. In: *Proceedings of the 1995 IEEE International Conference on Neural Networks*. Perth, Australia, IEEE Service Center, Piscataway, NJ: [s.n.], 1995. v. 4, p. 1942–1948.

KHAN, A. A.; NAEEM, M.; SHAH, S. I. A particle swarm algorithm for symbols detection in wideband spatial multiplexing systems. In: *Proceedings of the 9th Annual Conference on Genetic and Evolutionary Computation*. New York, NY, USA: ACM, 2007. (GECCO '07), p. 63–69. ISBN 978-1-59593-697-4. Disponível em: <http://doi.acm.org/10.1145/1276958.1276968>.

KIM, D.; SRA, S.; DHILLON, I. S. Tackling Box-Constrained Optimization via a New Projected Quasi-Newton Approach. *SIAM J. Sci. Comput.*, v. 32, n. 6, p. 3548–3563, 2010. ISSN 1064-8275.

LAU, M. S. K.; YUE, S. P.; LING, K. V.; MACIEJOWSKI, J. M. A comparison of interior point and active set methods for FPGA implementation of model predictive control. In: *2009 European Control Conf. (ECC)*. [S.l.: s.n.], 2009. p. 156–161.

LEVIN, G.; LOYKA, S. On capacity-maximizing angular densities of multipath in mimo channels. In: *2010 IEEE 72nd Vehicular Technology Conference - Fall*. [S.l.: s.n.], 2010. p. 1–5. ISSN 1090-3038.

LUO, Z. Q.; MA, W. K.; SO, A. M. C.; YE, Y.; ZHANG, S. Semidefinite relaxation of quadratic optimization problems. *IEEE Signal Process. Mag.*, v. 27, n. 3, p. 20–34, May 2010. ISSN 1053-5888.

MA, W.-K.; SU, C.-C.; JALDEN, J.; CHI, C.-Y. Some results on 16-QAM MIMO detection using semidefinite relaxation. In: *2008 IEEE International Conference on Acoustics, Speech and Signal Processing*. [S.l.: s.n.], 2008. p. 2673–2676. ISSN 1520-6149.

MANDLOI, M.; BHATIA, V. Low-complexity near-optimal iterative sequential detection for uplink massive MIMO systems. *IEEE Commun. Lett.*, v. 21, n. 3, p. 568–571, March 2017. ISSN 1089-7798.

MARZETTA, T. L. Noncooperative cellular wireless with unlimited numbers of base station antennas. *IEEE Transactions on Wireless Communications*, v. 9, n. 11, p. 3590–3600, November 2010. ISSN 1536-1276.

MARZETTA, T. L.; LARSSON, E. G.; YANG, H.; NGO, H. Q. *Fundamentals of Massive MIMO*. [S.l.]: Cambridge University Press, 2016.

MATLAB. *Linprog: Solve linear programming problems*. Accessed in 2018-11-18. Disponível em: <https://www.mathworks.com/help/optim/ug/linprog.html>.

MATLAB. *Lsqlin: Solve constrained linear least-squares problems*. Accessed in 2018-11-18. Disponível em: <https://www.mathworks.com/help/optim/ug/lsqlin.html>.

NEGRAO, J. L.; MUSSI, A. M.; ABRAO, T. Semidefinite relaxation for large scale MIMO detection. In: *XXXIV Simp. Br. Telecom. - SBrT2016*. [S.l.: s.n.], 2016.

NOCEDAL, J.; WRIGHT, S. *Numerical Optimization*. New York, NY, USA: Springer-Verlag New York, 2006. (Springer Series in Operations Research and Financial Engineering). ISBN 9780387400655.

O'Shea, T.; Hoydis, J. An introduction to deep learning for the physical layer. *IEEE Transactions on Cognitive Communications and Networking*, v. 3, n. 4, p. 563–575, Dec 2017. ISSN 2332-7731.

RAMANATHAN, R.; JAYAKUMAR, M. A support vector regression approach to detection in large-mimo systems. *Telecommunication Systems*, v. 64, n. 4, p. 709–717, Apr 2017. ISSN 1572-9451. Disponível em: <https://doi.org/10.1007/s11235-016-0202-2>.

RUSEK, F.; PERSSON, D.; LAU, B. K.; LARSSON, E. G.; MARZETTA, T. L.; EDFORS, O.; TUFVESSON, F. Scaling up mimo: Opportunities and challenges with very large arrays. *IEEE Signal Processing Magazine*, v. 30, n. 1, p. 40–60, Jan 2013. ISSN 1053-5888.

SCHMIDT, M.; KIM, D.; SRA, S. Projected newton-type methods in machine learning. In: MAX-PLANCK-GESELLSCHAFT. *Optimization for Machine Learning*. Cambridge, MA, USA: MIT Press, 2011. p. 305–330.

SEYMAN, M. N.; TASPINAR, N. Symbol detection using the differential evolution algorithm in mimo-ofdm systems. *Turkish Journal of Electrical Engineering and Computer Science*, v. 21, p. 373 – 380, 2014. ISSN 1300-0632.

Shafi, M.; Molisch, A. F.; Smith, P. J.; Haustein, T.; Zhu, P.; De Silva, P.; Tufvesson, F.; Benjebbour, A.; Wunder, G. 5g: A tutorial overview of standards, trials, challenges, deployment, and practice. *IEEE Journal on Selected Areas in Communications*, v. 35, n. 6, p. 1201–1221, June 2017. ISSN 0733-8716.

SHI, Y.; EBERHART, R. A modified particle swarm optimizer. In: *1998 IEEE International Conference on Evolutionary Computation Proceedings. IEEE World Congress on Computational Intelligence (Cat. No.98TH8360)*. [S.l.: s.n.], 1998. p. 69–73.

SIDIROPOULOS, N. D.; LUO, Z. Q. A semidefinite relaxation approach to MIMO detection for high-order QAM constellations. *IEEE Signal Process. Lett.*, v. 13, n. 9, p. 525–528, Sept 2006. ISSN 1070-9908.

STORN, R.; PRICE, K. Differential evolution – a simple and efficient heuristic for global optimization over continuous spaces. *Journal of Global Optimization*, v. 11, n. 4, p. 341–359, Dec 1997. ISSN 1573-2916. Disponível em: <https://doi.org/10.1023/A:1008202821328>.

TANG, C.; LIU, C.; YUAN, L.; XING, Z. High precision low complexity matrix inversion based on newton iteration for data detection in the massive MIMO. *IEEE Commun. Lett.*, v. 20, n. 3, p. 490–493, March 2016. ISSN 1089-7798.

TELATAR, E. Capacity of multi-antenna gaussian channels. *European Transactions on Telecommunications*, Wiley Subscription Services, Inc., A Wiley Company, v. 10, n. 6, p. 585–595, 1999. ISSN 1541-8251. Disponível em: <http://dx.doi.org/10.1002/ett.4460100604>.

TRELEA, I. C. The particle swarm optimization algorithm: convergence analysis and parameter selection. *Information Processing Letters*, v. 85, n. 6, p. 317 – 325, 2003. ISSN 0020-0190.

TRIMECHE, A.; BOUHLEL, A.; SAKLY, A.; MTIBAA, A. The particle swarm optimization (pso) for symbol detection in mimo-ofdm system. *International Journal of Information Security*, v. 4, n. 1, p. 38–45, March 2013.

TÜTÜNCÜ, R. H.; TOH, K. C.; TODD, M. J. Solving semidefinite-quadratic-linear programs using SDPT3. *Math. Program.*, v. 95, n. 2, p. 189–217, Feb 2003. ISSN 1436-4646.

Wang, T.; Wen, C.; Wang, H.; Gao, F.; Jiang, T.; Jin, S. Deep learning for wireless physical layer: Opportunities and challenges. *China Communications*, v. 14, n. 11, p. 92–111, Nov 2017. ISSN 1673-5447.

WU, M.; YIN, B.; WANG, G.; DICK, C.; CAVALLARO, J. R.; STUDER, C. Large-scale MIMO detection for 3GPP LTE: Algorithms and FPGA implementations. *IEEE J. Sel. Topics Signal Process.*, v. 8, n. 5, p. 916–929, Oct 2014. ISSN 1932-4553.

ZELST, a. V.; HAMMERSCHMIDT, J. A single coefficient spatial correlation model for multiple-input multiple-output (MIMO) radio channels. *27th General Assembly of the International Union of Radio Science (URSI)*, n. 1, p. 2–5, 2002. Disponível em: <http://www.avzelst.nl/ursi_ga2002_a_van_zelst.pdf>.

Zhang, Y. H.; Lu, W. .; Gulliver, T. A. Integer QP relaxation-based algorithms for intercarrier-interference reduction in OFDM systems. *Canadian J. Elect. Comput. Eng.*, v. 32, n. 4, p. 199–205, Fall 2007. ISSN 0840-8688.

Apêndice A – Trabalhos Desenvolvidos

Neste apêndice são apresentados os trabalhos em desenvolvimento ou já publicados durante o Mestrado Acadêmico.

A.1 *Efficient Detectors for MIMO-OFDM Systems under Spatial Correlation Antenna Arrays*

Título:	*Efficient Detectors for MIMO-OFDM Systems under Spatial Correlation Antenna Arrays*
Autores:	David Marques Guerra, **Rafael Masashi Fukuda**, Ricardo Tadashi Kobayashi e Taufik Abrão
Revista:	*Electronics and Telecommunications Research Institute* (ETRI)
Status:	Publicado
DOI:	https://doi.org/10.4218/etrij.2018-0005
Qualis:	A2 Qualis-Eng.IV CAPES

Neste trabalho, algoritmos heurísticos PSO e DE são aplicados para o problema da detecção em sistemas MIMO-OFDM em cenários com correlação espacial entre as antenas. Questões como a escolha dos parâmetros de entrada do PSO e DE, visando uma comparação justa entre as heurísticas são abordadas. De maneira geral, o aumento da correlação provoca a degradação em performance dos detectores; foram observadas diferenças marginais de performance entre a configuração ULA e URA. Ambos os detectores heurísticos apresentaram desempenho melhor que os detectores lineares; entre os heurísticos, o PSO apresentou um melhor compromisso entre complexidade e desempenho, pois é capaz de atingir desempenho semelhante ao DE com menor complexidade.

Received: 7 January 2018 | Revised: 28 February 2018 | Accepted: 9 April 2018

DOI: 10.4218/etrij.2018-0005

ORIGINAL ARTICLE

WILEY ETRI Journal

Efficient detectors for MIMO-OFDM systems under spatial correlation antenna arrays

David William Marques Guerra | Rafael Masashi Fukuda | Ricardo Tadashi Kobayashi | Taufik Abrão

Electrical Engineering Department, State University of Londrina, Londrina, Paraná, Brazil.

Correspondence
Taufik Abrão, Electrical Engineering Department (DEEL), State University of Londrina, Londrina, Paraná, Brazil.
Email: taufik@uel.br

This work analyzes the performance of implementable detectors for the multiple-input multiple-output (MIMO) orthogonal frequency division multiplexing (OFDM) technique under specific and realistic operation system conditions, including antenna correlation and array configuration. A time-domain channel model was used to evaluate the system performance under realistic communication channel and system scenarios, including different channel correlation, modulation order, and antenna array configurations. Several MIMO-OFDM detectors were analyzed for the purpose of achieving high performance combined with high capacity systems and manageable computational complexity. Numerical Monte Carlo simulations demonstrate the channel selectivity effect, while the impact of the number of antennas, adoption of linear against heuristic-based detection schemes, and the spatial correlation effect under linear and planar antenna arrays are analyzed in the MIMO-OFDM context.

KEYWORDS
BER performance, heuristic detector, linear detector, MIMO-OFDM, multipath channel, spatial correlation

1 | INTRODUCTION

Orthogonal frequency division multiplexing (OFDM) is a modulation scheme widely used in many communication systems, including several commercial applications such as wireless networks (Wi-Fi 802.11) and cellular systems (LTE) [1]. In those systems, it is also common to combine the OFDM with multiple-input multiple-output (MIMO), which can improve the spectral efficiency of the system [2,3]. However, to couple the OFDM to the MIMO system, it is necessary to understand the basics of SISO channel and SISO-OFDM.

Usually, inside an OFDM system, a large number N of subcarriers is deployed in order to achieve a flat fading condition on each subchannel. This is particularly important in realistic scenarios, where the wireless channel introduces dispersion effects on the signal, creating selective channels. In [4], a SISO-OFDM system was simulated to show how the number of subcarriers influences its performance on a multipath fading indoor channel based on the Saleh-Valenzuela model, but not considering the Doppler frequency.

In flat fading channels, the coherence bandwidth of the channel $(\Delta B)_c$ is larger than W, the bandwidth of the signal. Hence, all frequency components of the signal experience the same magnitude of fading. On the other hand, in frequency-selective fading channels, $(\Delta B)_c < W$ occurs. As a consequence, different frequency components of the signal experience correlated fading.

In OFDM systems, to mitigate the intersymbol interference (ISI) caused by multipath fading, it is necessary to use a guard interval. The most used type of guard interval on OFDM systems is the cyclic prefix (CP), as described analytically in [5].

One of the most recent well-established data transmission structures is the multiple-input multiple-output (MIMO) system, which uses multiple antennas at the transmitter and receiver sides to transfer data over a wire or wireless channels. MIMO systems are able to increase data rates by means of multiplexing or to improve performance/reliability through a diversity mode [6]. The data increase can be achieved sending different data via different antennas. By simultaneously sending the same data via multiple antennas, the reliability is increased by exploiting diversities such as time and space diversity. In spatial multiplexing, the signal that reaches at each receive antenna suffers interference from the other $N_t - 1$ antennas, where N_t represents the number of transmitting antennas. Hence, the purpose of demultiplexing-detection schemes is to mitigate the effects of the interference [7]. Hence, on the receiver side, there are a large number of MIMO detection techniques available. In this work, several MIMO-OFDM detectors are characterized and numerically evaluated under specific but realistic channel and system scenarios, including the maximum likelihood (ML), linear zero-forcing (ZF), and linear minimum mean-square error (MMSE) detectors. Moreover, two MIMO-OFDM detectors based on evolutionary heuristic approaches also have been analyzed, namely, the *particle swarm optimization* (PSO) detector and *differential evolution* (DE) detector.

Indeed, because the ML detector solution requires an exhaustive search through all possible symbol combinations [8], while linear closed solutions such as ZF and MMSE result in a poor performance for highly correlated channels [9], evolutionary heuristic algorithms are strong candidates for producing better solutions than linear detectors, and they result in reduced computational complexity compared to ML because heuristic approaches do not evaluate all possibilities.

The PSO algorithm has already been applied to solve the detection problem in MIMO-OFDM systems in [8,10]. In [8], the PSO, and in [11], the binary PSO, were evaluated and the numerical results of bit error rate (BER) and computational complexity were analyzed. In [10], the performances of DE, PSO, and the genetic algorithm were compared. On the other hand, in our work, the performance-complexity tradeoff of the evolutionary heuristic PSO and DE MIMO-OFDM detectors are analyzed under practical and useful scenarios, that is, considering spatial correlated channels and other linear conventional MIMO-OFDM detectors. The system model in a real-valued representation is considered while the selection procedure for the heuristic input parameters of the PSO and DE algorithms are addressed accordingly. Besides, to the best of our knowledge, there are no studies considering a comparative analysis of evolutionary heuristics and classical MIMO-OFDM detectors operating under spatial correlation antenna arrays.

The contribution of this work is threefold. First, we analyze and compare the performance and implementability of several MIMO-OFDM detectors, including linear and evolutionary heuristic approaches, operating under realistic system configurations. Second, the influence of parameters related to the distance between the antennas, which determine the spatial antenna correlation, is discussed; two antenna array configurations are considered, the *uniform linear array* (ULA) [12] and *uniform rectangular array* (URA) [13]. Last, a systematic procedure is developed and used to calibrate the input parameters of both evolutionary heuristic PSO and DE detectors with the aim of establishing a fair performance comparison between the linear and heuristic MIMO-OFDM detectors.

The rest of this work is organized as follows. In Section 2, the OFDM system is revised and the TD channel emulator is explored. The spatial channel correlation, ML, ZF, MMSE, as well as the evolutionary heuristic PSO and DE detectors are described in Section 3. Extensive numerical simulation results are analyzed in Section 5, including reliability evaluation, the channel selectivity effect, BER performance comparison regarding spatial correlation, modulation order, and sensibility analysis. Conclusions and final remarks are offered in Section 6.

2 | OFDM TRANSMISSION AND MIMO CHANNEL

OFDM is one type of multicarrier modulation that can be easily implemented using discrete Fourier transform (DFT) and its inverse (IDFT), or their equivalents, the fast Fourier transform (FFT) and inverse FFT (IFFT). OFDM modulation consists of parallel data transmission with some modulation such as M-QAM or M-PSK applying an IFFT to transform a signal in the FD into one in the TD. Thereafter, the CP is added. Data are converted into an analog signal. Finally, the signal is multiplied to a carrier by frequency f_c for transmission.

On the receiver side, signal $r(t)$ represents the transmitted signal $s(t)$ corrupted by noise. Signal $r(t)$ is multiplied by $\cos(2\pi f_c t)$, passes through a low-pass filter, is converted to digital information, the CP is removed, and the serial data is converted into parallel data. A DFT is performed, the symbols are converted to serial symbols and demodulated according to their respective scheme of modulation, and the information bits can then be estimated.

In order to mitigate ISI, some strategies such as cyclic suffix, silence, or the most common CP can be adopted.

CP consists of copying the last μ elements of the input sequence $s[n]$ and adding them to the start of $s[n]$, where $h[n] = h[0], h[1], \ldots, h[\mu]$ represents a channel impulse response of length $\mu + 1$. After the CP addition, the OFDM symbol becomes $\tilde{s}[n]$, with length $[N + \mu]$. Observe

that the CP is an overhead and does not carry any information, which reduces the spectral efficiency.

The choice of the number of subcarriers N depends on the channel characteristics. For the design of an OFDM system, two properties of the channel are considered, which are the maximum delay spread (τ_{max}) and the maximum Doppler frequency (f_d). OFDM systems require that N must be large enough so each subcarrier experiences a flat fading condition. Each subcarrier has a bandwidth B that is smaller than the system total bandwidth, centered at a frequency $\omega_1, \omega_2, \ldots, \omega_n$. Subcarriers with a bandwidth of B can be overlapped at a maximum rate of 50%.

2.1 | MIMO-OFDM system

The combination of an OFDM system with the use of multiple antennas at the transmitter and receiver results in a MIMO-OFDM system (Figure 1) with N_t transmit and N_r receive antennas. A QAM modulator and multiplexing configuration, where different data are sent through different antennas resulting in higher data rates than single-input single-output (SISO) channel configuration, have been considered.

On the transmitter side, the data feeds a serial-to-parallel converter, resulting in N_t data streams that are modulated in a similar way as OFDM SISO: the bit stream is modulated, symbols are converted to parallel, IDFT is performed, the CP is added, and the signal is multiplied by the carrier with frequency f_c and finally transmitted. On the receiver side, the signal is converted to baseband, transformed into digital, the CP is removed, the signals serve as a MIMO detector, and finally, the symbols are demodulated deploying QAM demodulator.

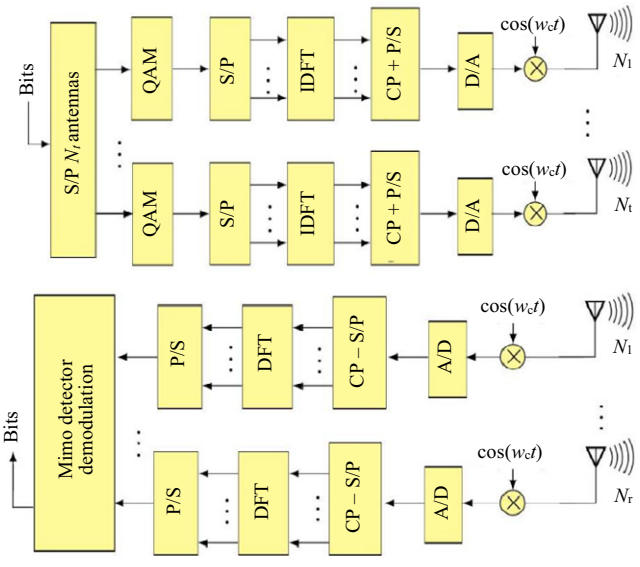

FIGURE 1 Block diagram of a MIMO-OFDM system

Because the OFDM technique allows parallel transmission over several subchannels, we can model a MIMO-OFDM system with N subcarriers in the TD as [14,15]:

$$\mathbf{y}[n] = \mathbf{H}[n]\mathbf{x}[n] + \mathbf{z}[n], \quad n = 0, 1, \ldots, N-1, \tag{1}$$

where n is the subcarrier index, $\mathbf{y}[n] \in \mathbb{C}^{N_r \times 1}$ denotes the received signals, $\mathbf{H}[n] \in \mathbb{C}^{N_r \times N_t}$ denotes the channel matrix gains, $\mathbf{x}[n] \in \mathbb{C}^{N_r \times 1}$ denotes the transmit symbols, and $\mathbf{z}[n] \in \mathbb{C}^{N_r \times 1}$ is Gaussian noise with zero mean and variance σ_z^2.

Therefore, we can interpret a MIMO system for each subcarrier, as illustrated in Figure 2. Thus, a MIMO-OFDM symbol block is composed of $N_r \times N_t$ OFDM symbols. Finally, it is important to note that if the number of subcarriers is insufficient to make the channel of each subcarrier flat, channel equalization cannot be implemented correctly.

Implementable MIMO-OFDM detectors operating in realistic fading channels and practical system configuration are discussed in Section 3.

3 | MIMO SPATIAL CORRELATION AND LINEAR DETECTORS

3.1 | MIMO-OFDM spatial correlation model

In channel modeling, the correlation among transmit and/or receive antennas is an important aspect to be considered in realistic MIMO channels and systems [16]. To model and evaluate the spatial antenna correlation, the Kronecker operator is deployed as:

$$\mathbf{H}_{corr}[n] = \sqrt{\mathbf{R}_r}\mathbf{G}[n]\sqrt{\mathbf{R}_t^H}, \tag{2}$$

where $\mathbf{H}_{corr}[n]$ is the correlated channel of the nth subcarrier, uncorrelated channel matrix $\mathbf{G}$ is composed of independent and identically distributed entries, $\sqrt{\mathbf{R}_r}$ and $\sqrt{\mathbf{R}_t}$ are the square root of the spatial correlation matrices at the transmitter and receiver antennas, respectively.

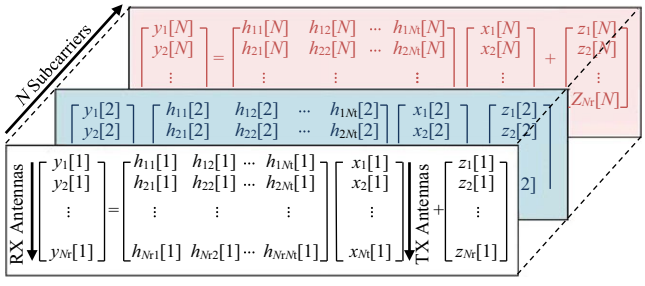

FIGURE 2 MIMO-OFDM problem

3.2 | Uniform linear antenna array (ULA)

A spatial correlation model for ULA was proposed in [12]. This model considers that the antennas are arranged equidistantly, where d_t and d_r represent the spacing between the transmitting and receiving antennas, respectively. For simplicity of analysis, assuming the same number of antennas at the transmitter and receiver ($N_t = N_r$) side, while the spatial correlation matrix of the transmitter and receiver antennas are assumed to be equal $\sqrt{\mathbf{R}_r} = \sqrt{\mathbf{R}_t}$. The spatial correlation matrix results Toeplitz, being expressed by:

$$\mathbf{R}_t = \mathbf{R}_r = \begin{bmatrix} 1 & \rho & \rho^4 & \cdots & \rho^{(N_t-1)^2} \\ \rho & 1 & \rho & \ddots & \vdots \\ \rho^4 & \rho & 1 & \cdots & \rho^4 \\ \vdots & \vdots & \vdots & \cdots & \rho \\ \rho^{(N_t-1)^2} & \cdots & \rho^4 & \rho & 1 \end{bmatrix} \quad (3)$$

where $\rho \in [0, 1]$ represents the normalized correlation index between antennas.

3.3 | Uniform rectangular antenna array (URA)

An approximation for the URA correlation model was proposed in [13]. This model assumes that the URA matrix correlation between the antennas is obtained from the Kronecker product of 2 ULA correlation matrices. Considering an URA configuration on the XY plane with n_x and n_y antenna elements along X and Y coordinates, respectively, we have an array with $n = n_x \times n_x$ antennas. Further, the correlation between the elements along the X coordinate does not depend on Y and is given by matrix $\mathbf{R}_x$, and the correlation along Y coordinate does not depend on X and is given by matrix $\mathbf{R}_y$. As a result, the Kronecker model approximation for the URA correlation matrix is as follows:

$$\mathbf{R}_r = \mathbf{R}_x \otimes \mathbf{R}_y, \quad (4)$$

where $\otimes$ is the Kronecker product.

3.4 | Maximum likelihood (ML) MIMO detector

The ML detector provides the best performance, but its complexity makes it impractical for real applications. This detector calculates all the possible symbols combinations and chooses the one symbol vector $\mathbf{x}$ that provides the minimum Euclidian distance between the received data $\mathbf{y}$ and the reconstructed data defined by the channel matrix $\mathbf{H}$ and symbol-vector candidate $\mathbf{x}$. Hence, the estimated symbol $\tilde{\mathbf{x}}$ can be mathematically expressed by

$$\tilde{\mathbf{x}} = \min_{\mathbf{x}} \|\mathbf{y} - \mathbf{H}\mathbf{x}\|^2. \quad (5)$$

3.5. | Zero-forcing (ZF) MIMO detector

Considering a MIMO system operating under multiplexing mode, the data that reach the receptor are the linear superposition of the signals of all the N_t antennas [7]. The ZF detector ignores the additive noise $\mathbf{z}$ in (1) and solves the linear system by multiplying the received signal by the inverse matrix, which is defined, according to the Moore–Penrose inverse, as:

$$\mathbf{H}_{zf}^{\dagger} = (\mathbf{H}^H\mathbf{H})^{-1}\mathbf{H}^H. \quad (6)$$

The estimated symbol is given by

$$\tilde{\mathbf{x}} = \mathbf{H}_{zf}^{\dagger}\mathbf{y}. \quad (7)$$

3.6 | Minimum mean-square error (MMSE) MIMO detector

The MMSE detector considers the thermal noise channel statistics. This method tries to minimize the squared error between the true and estimated values of the transmitted symbols, $\mathbf{x}$ and $\tilde{\mathbf{x}}$, respectively [7] via optimization

$$\mathbf{H}_{mmse}^{\dagger} = \min_{\mathbf{W}} \mathbb{E}\|\mathbf{x} - \mathbf{W}\mathbf{y}\|. \quad (8)$$

Hence, solving this MMSE optimization problem, the MIMO channel matrix results in the MMSE pseudoinverse matrix described by

$$\mathbf{H}_{mmse}^{\dagger} = \left(\mathbf{H}^H\mathbf{H} + \frac{N_0}{E_s}\mathbf{I}\right)^{-1}\mathbf{H}^H, \quad (9)$$

where $\frac{N_0}{E_s}$ is the inverse of the signal-to-noise ratio (SNR). Finally, the estimated symbol under linear MMSE MIMO detection is obtained in the same way as in (7) and is give by:

$$\tilde{\mathbf{x}} = \mathbf{H}_{mmse}^{\dagger}\mathbf{y}. \quad (10)$$

4 | HEURISTIC-BASED MIMO-OFDM DETECTORS

In this section, the heuristic PSO and DE algorithms are described in the context of the MIMO-OFDM detection problem. The complex system model is described in a well-known equivalent real-valued representation, for example, in [17]. The deployment of the fitness function to evaluate the candidate solution provided by heuristic

algorithms is illustrated. PSO and DE algorithms are presented afterwards, while the input parameter tuning problem for the evolutionary heuristic algorithms is addressed.

4.1 | Real value representation

The MIMO-OFDM system presented in (1) can be represented using a real-valued matrix and vectors in the form

$$\boldsymbol{\upsilon}[n] = \mathcal{H}[n]\boldsymbol{\gamma}[n] + \boldsymbol{\xi}[n], \tag{11}$$

with

$$\mathcal{H}[n] = \begin{bmatrix} \Re\{\mathbf{H}[n]\} & -\Im\{\mathbf{H}[n]\} \\ \Im\{\mathbf{H}[n]\} & \Re\{\mathbf{H}[n]\} \end{bmatrix}, \boldsymbol{\upsilon}[n] = \begin{bmatrix} \Re\{\mathbf{y}[n]\} \\ \Im\{\mathbf{y}[n]\} \end{bmatrix},$$
$$\boldsymbol{\gamma}[n] = \begin{bmatrix} \Re\{\mathbf{x}[n]\} \\ \Im\{\mathbf{x}[n]\} \end{bmatrix}, \boldsymbol{\xi}[n] = \begin{bmatrix} \Re\{\mathbf{z}[n]\} \\ \Im\{\mathbf{z}[n]\} \end{bmatrix},$$

where $\mathcal{H}[n] \in \mathbb{R}^{2N_r \times 1}$ is the real-valued representation of the channel matrix, vectors $\boldsymbol{\gamma}[n]$, $\boldsymbol{\xi}[n] \in \mathbb{R}^{2N_r \times 1}$ are the real-valued representations of the received signal and additive noise, respectively, and $\boldsymbol{\upsilon}[n] \in \mathbb{R}^{2N_r \times 1}$ is the real-valued original information.

4.2 | Fitness function

The fitness function evaluates the quality of the estimated symbol and guides the evolutionary heuristic search on the candidate-solution feasible subspace. For the detection problem, the fitness function is based on the Euclidean distance between the received signal and the reconstructed one [8,10,11]. Considering $\boldsymbol{\zeta}_k$, the kth candidate solution of an evolutionary heuristic, namely a particle in PSO or individual in DE, the fitness function is calculated as follows:

$$f(\boldsymbol{\zeta}_k) = \|\boldsymbol{\upsilon}[n] - \mathcal{H}[n]\boldsymbol{\zeta}_k\|^2. \tag{12}$$

For the detection problem, a minimization problem is considered, and lower values of the fitness function are desired.

4.3 | PSO-based detection algorithm

PSO was proposed by [18] considering a population-based approach, emulating bird flocking and fish schooling behavior. The PSO algorithm calculates the velocity and position of each particle inside the swarm; using a matrix representation [19], they are given, respectively, by

$$\mathbf{V} = w\mathbf{V} + c_1\mathbf{U}_1 \odot (\mathbf{M}_{\text{pb}} - \mathbf{P}) + c_2\mathbf{U}_2 \odot (\mathbf{M}_{\text{gb}} - \mathbf{P}), \tag{13}$$

and

$$\mathbf{P} = \mathbf{P} + \mathbf{V}, \tag{14}$$

where $\odot$ denotes the Hadamard product, w, c_1, and c_2 represent inertia, cognitive, and social factors, respectively; $\mathbf{U}_1$ and $\mathbf{U}_2$ are random matrices with elements following uniform distributions $\mathbf{U}_i \sim \mathcal{U}[0;1]$; $\mathbf{M}_{\text{pb}}$ is a matrix that stores the values of the personal best of each particle and $\mathbf{M}_{\text{gb}}$ is a matrix constructed of the positions of the global best particle $\mathbf{p}_{\text{gb}}$, given in the form $\mathbf{M}_{gb} = [\mathbf{p}_{\text{gb}} \cdots \mathbf{p}_{\text{gb}}] \in \mathbb{R}^{N_{\text{dim}} \times N_{\text{pop}}}$. Matrix $\mathbf{P}$ is a real-valued matrix representing positions, while $\mathbf{V}$ represents the particle velocity matrix; explicitly,

$$\mathbf{P} = [\mathbf{p}_1 \ldots \mathbf{p}_{N_{\text{pop}}}], \mathbf{V} = [\mathbf{v}_1 \ldots \mathbf{v}_{N_{\text{pop}}}] \in \mathbb{R}^{N_{\text{dim}} \times N_{\text{pop}}},$$

where vectors $\mathbf{p}_k, \mathbf{v}_k \in \mathbb{R}^{N_{\text{dim}} \times 1}$ with $k = 1, \ldots, N_{\text{pop}}$ represent the position and velocity of the kth particle, with N_{pop} representing the population size and N_{dim} denoting the dimensionality of the problem.

In order to avoid the possibly that the velocity vector grows to infinity [20], a limitation of the velocity $[-V_{\max}, V_{\max}]$ [21] was considered, where $V_{\max}$ represents the maximum achievable velocity of the N_{pop} particles. Regarding the inertia parameter, it can be a constant or a linear or nonlinear function [22]. In this work, to give to the algorithm exploitation ability at the beginning and exploration for fine search near the solution [21], a strategy of decreasing the inertia factor at each iteration by $0.99w$ is considered.

The initialization of both implemented PSO and DE heuristic algorithms was the same; the position of the particles $\mathbf{P}$ and initial population in DE are generated randomly following a uniform distribution inside the search space of the problem [23]. These positions are set as the personal best position of the particle in matrix $\mathbf{M}_{\text{pb}}$. The fitness function in (12) is evaluated ($\boldsymbol{\zeta}_k = \mathbf{p}_k$, $k = 1, \ldots, N_{\text{iter}}$), the position of the particle that produces the lowest value (since we are dealing with a minimization problem) is set as the global best position $\mathbf{p}_{\text{gb}}$, and the matrix $\mathbf{M}_{\text{gb}}$ is formed.

After evaluation of (13) and (14), matrices $\mathbf{M}_{\text{pb}}$ and $\mathbf{M}_{\text{gb}}$ are updated (if needed) and the process is repeated until the stop criteria is met. In our implementation, a stop criterion based on a predefined maximum number of evaluations N_{iter} is used. Hence, after N_{iter} iterations, the output of the evolutionary heuristic algorithm is the vector of best position $\mathbf{p}_{\text{gb}}$, which is the estimated symbol $\tilde{\mathbf{x}}$ in the MIMO-OFDM detection problem.

Pseudocode summarizing the procedure for the evolutionary heuristic PSO algorithm is presented in Algorithm 1.

Algorithm 1. PSO

1: Input parameters: c_1, c_2, w, N_{pop}, N_{iter}
2: Generate initial positions $\mathbf{P}$
3: Fitness function evaluation and initialization of $\mathbf{M}_{\text{pb}}$ and $\mathbf{M}_{\text{gb}}$
4: for 1 to N_{iter} do
5: Calculate velocity using (13)
6: Calculate position using (14)
7: Evaluate fitness function (12) for all particles p_k
8: Update personal best matrix $\mathbf{M}_{\text{pb}}$
9: Update global best matrix $\mathbf{M}_{\text{gb}}$
10: Velocity limitation
11: Inertia factor reduction
12: end for
13: Output: $\mathbf{p}_{\text{gp}}$

4.4 | DE-based detection algorithm

DE is an evolutionary population-based heuristic that relies on a population of individuals to find a global optimum. The algorithm relies on the operations of mutation, crossover, and selection to produce more suitable individuals through N_{gen} generations.

The DE algorithm was presented in [23] and operates as follows. There are $N_{\text{ind}} \geq 4$ vectors of individuals that are represented as $\boldsymbol{\iota}_k \in \mathbb{R}^{N_{\text{dim}} \times 1}, k = 1, \ldots, N_{\text{ind}}$, where N_{dim} represents the dimensionality of the problem. Here, following the procedure defined in [23], the `rand/1/bin` strategy is employed. Strategies to escape local optima that are adopted in the DE-based detector are described in the following.

4.4.1 | Mutation

The kth mutation vector $\boldsymbol{\upsilon}$ is constructed as:

$$\boldsymbol{\upsilon}_k = \boldsymbol{\iota}_{r_1} + F_{\text{mut}}(\boldsymbol{\iota}_{r_2} - \boldsymbol{\iota}_{r_3}), \tag{15}$$

where $k \neq r_1 \neq r_2 \neq r_3$ and $k = 1, \ldots, N_{\text{ind}}$. Variables r_1, r_2, and r_3 are integer random indexes uniformly distributed inside the interval $[1, 2, \ldots, N_{\text{ind}}]$ and $F_{\text{mut}} \in [0, 2]$ represents the mutation scale factor.

4.4.2 | Crossover

The kth crossover vector $\boldsymbol{\psi}_k (k = 1, \ldots, N_{\text{ind}})$ is constructed as follows. The ith element, $i = 1, \ldots, N_{\text{dim}}$ of the kth crossover vector $\boldsymbol{\psi}_k$ is selected given the following rule:

$$\psi_{ik} = \begin{cases} \nu_{ik} & \text{if } rand \in [0,1] \leq F_{\text{cr}} \text{ or } i = r_4 \\ \iota_{ik} & \text{if } rand \in [0,1] > F_{\text{cr}} \text{ and } i \neq r_4 \end{cases} \tag{16}$$

where $rand \sim \mathcal{U}[0,1]$, r_4 is uniformly distributed in the interval [0;1], r_4 is an integer randomly generated in the interval $[1, \ldots, N_{\text{dim}}]$, and the crossover factor is defined by $F_{\text{cr}} \in [0, 1]$. As pointed out in [23], the crossover vector has at least one element from the mutation vector, that is, $i = r_4$.

4.4.3 | Selection

The next generation of individuals $\boldsymbol{\iota}_k^g$ is constructed as follows:

$$\boldsymbol{\iota}_k^g = \begin{cases} \boldsymbol{\psi}_k & \text{if } f(\boldsymbol{\psi}_k) < f(\boldsymbol{\iota}_k) \\ \boldsymbol{\iota}_k & \text{otherwise} \end{cases}. \tag{17}$$

The fitness function in (12) evaluates $\boldsymbol{\iota}_k$ and $\boldsymbol{\psi}_k$. Vectors that produce more suitable values (smaller values) are selected and a new generation of individuals is produced.

After the execution of N_{gen} iterations, the best individual, in other words, the individual corresponding to the lowest value of the fitness function in (12) is the output of the algorithm and the estimated symbol $\tilde{\mathbf{x}}$ of the MIMO-OFDM detection problem. Pseudocode synthesizing the DE steps is presented in Algorithm 2.

Algorithm 2 DE

1: Input parameters: F_{cr}, F_{mut}, N_{ind}, N_{gen}
2: Generate initial individuals
3: for 1 to N_{gen} do
4: Mutation using (15), $k = 1, \ldots, N_{\text{ind}}$
5: Crossover using (16), $i = 1, \ldots, N_{\text{ind}}$; $k = 1, \ldots, N_{\text{ind}}$
6: Select new individuals using (17), $k = 1, \ldots, N_{\text{ind}}$
7: end for
8: Output: best individual $\boldsymbol{\iota}$

4.5 | Input parameters

The choice of nonoptimal input parameter values could substantially degrade the performance results provided by the heuristic algorithm in a given application, as studied in [24] for the ant colony optimization algorithm. Besides, the PSO algorithm also suffers from alteration of its convergence properties when the input parameters are chosen incorrectly [20,25,26]. In the same way, the DE-based algorithm has recommended intervals of values to achieve fast convergence [23]. For instance, the number of individuals must be $N_{\text{ind}} \in \{5;10\}N_{\text{ind}}$, where N_{dim} is the problem dimension, as suggested in [23].

To fairly compare the selected evolutionary heuristic algorithms, and since such an approach is sensible with respect to the choice of the input parameter values, which can differ substantially considering the nature of different optimization problems, the input parameter tuning

procedure here is obtained numerically and discussed in Sections 5.1.1 and 5.1.2.

5 | NUMERICAL RESULTS

In this section, numerical simulation results of MIMO-OFDM system are discussed. Linear and evolutionary heuristic detector performance subject to spatial antenna correlation effect is compared.

5.1 | MIMO-OFDM reliability evaluation

The parameters adopted in the Monte Carlo simulations are shown in Table 1. Additionally, the system operates with perfect channel state information (CSI). Performance of such detectors is compared with the optimum maximum-likelihood (ML) MIMO-OFDM detector. The total power allocated was equally distributed (EPA) among the N_t antennas in order to promote a fair comparison.

TABLE 1 MIMO-OFDM simulation parameters

Parameter	Value
OFDM	
System bandwidth BW	20 MHz
Modulation order M	4-QAM
Delay spread τ_{rms}	5 1ns
# subcarriers N	64
$(\Delta B)_c$	3.125 MHz
Subcarrier flatness $\frac{(\Delta B)_c}{W/N}$	10
MIMO	
# antennas $N_t \times N_r$	2×2; 4×4; 8×8
Antenna array type	Linear (ULA); rectangular (URA)
Spatial correlation index	$\rho \in [0; 0.5; 0.9]$
Linear detectors	ZF & MMSE
Heuristic detectors	PSO & DE
Power allocation strategy	EPA
Channel	
Type	NLOS rayleigh channel
CSI knowledge	Perfect
Mobility (freq. Doppler)	$f_d = 0$ Hz
PSO detector	
Population size N_{pop}	40
Iterations N_{max}	100
Search space	[−1; 1]
Cognitive factor c_1	4
Social factor $c_2(\rho)$	1(0); 0.5(0.5); 1(0.9)
Inertia $w(\rho)$	1.5(0); 1.5(0.5); 3.5(0.9)
DE detector	
# generation N_{gen}	100
Crossover factor $F_{cr}(\rho)$	0.6(0); 0.6(0.5); 0.8(0.9)
Mutation factor $F_{mul}(\rho)$	0.6(0); 0.8(0.5); 1.8(0.9)
# individuals N_{ind}	40

Specifically, in the MIMO-OFDM detection problem with heuristics, a 4-QAM modulation format was considered, with valid symbols defined by $\{-1+1j, -1-1j, 1+1j, 1-1j\}$, while the search space was limited to the interval of integer values $[\pm 1]$. The heuristic algorithm was applied to each subcarrier as presented in the model description in (11), resulting in $N_{dim} = 2N_t$ symbols to be estimated per subcarrier. For the PSO detection algorithm, parameter $V_{max} = 1$ was used in the simulations, reflecting the dynamic range of each particle inside the search space [21].

5.1.1 | Input parameter calibration for PSO-aided MIMO-OFDM detector

First, a round of simulations was executed to tune the PSO input parameters. Here, these parameters were obtained numerically over 100 simulation runs and averaged to obtain the values in Figure 3. The start parameters were $N_{pop} = 40$, $c_1 = c_2$, $w = 1$, and $N_{iter} = 50$. In Figure 3, the PSO input parameters were altered considering a wide range of input parameter values. The scenario assumed was 4×4, 4-QAM modulation MIMO-OFDM, considering a system operating in a medium-high SNR, that is, $E_b/N_0 = 24$ dB, and different values of spatial correlation. Choosing PSO parameters that provide small values of BER yielded the input parameters shown in Table 1 and deployed in the numerical simulation setup discussed in this section. Related to the population size, even with a marginal decrease in BER, low values of N_{pop} are desirable because this parameter has a direct impact in the computational complexity of the algorithm, as detailed in Section 5.2.

In Figure 4, the convergence behavior for the PSO-based detector is analyzed. It can be observed that convergence depends on the level of E_b/N_0; the number of iterations for convergence increases with SNR, from $\approx$ 25 to 50 iterations when E_b/N_0 increases from 5 dB to 10 dB and 15 dB. Moreover, high values of spatial correlation ($\rho = 0.9$) seem to interfere substantially in the convergence speed of the PSO algorithm applied in the MIMO-OFDM detection problem. After around 40 iterations, there are small improvements in the solution (symbol detection) provided by PSO algorithm for any spatial correlation level.

5.1.2 | Input parameter calibration DE-aided MIMO-OFDM detector

A similar procedure was carried out to find the best input parameter values of the DE-based detector in the context of

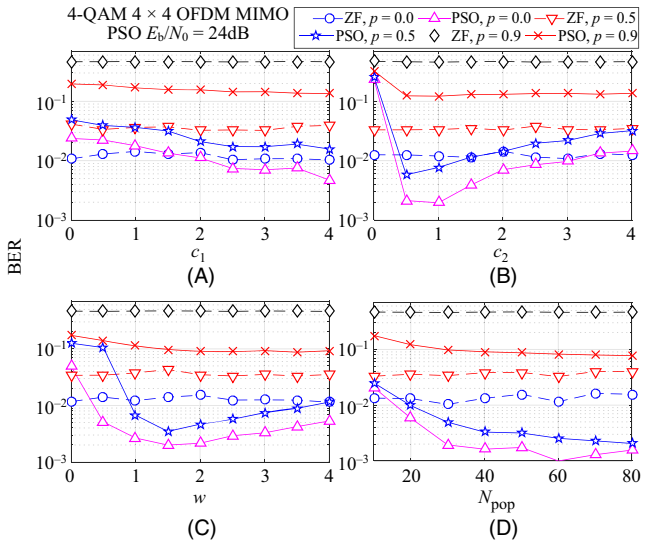

FIGURE 3 Calibration of PSO input parameter values for 4-QAM 4 × 4 MIMO-OFDM detection problem operating under medium-high SNR and different spatial correlation indexes

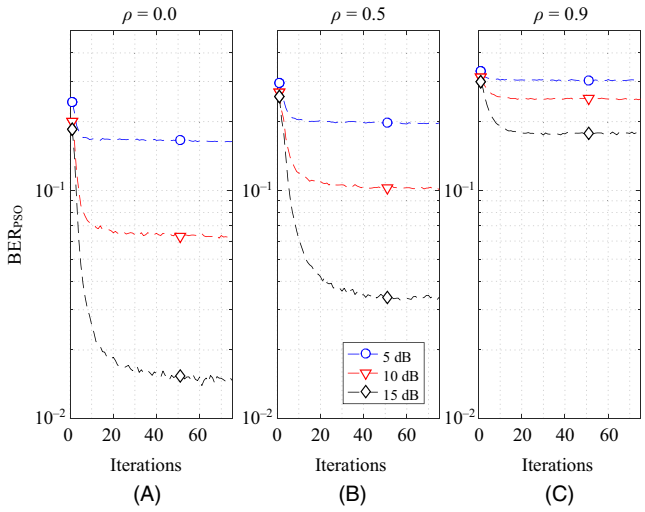

FIGURE 4 Convergence analysis for a 4-QAM, 4 × 4 MIMO-OFDM with PSO detector considering different values of E_b/N_0

MIMO-OFDM detection. This algorithm requires the parameters to be inside the intervals $F_{cr} \in [0, 1]$ and $F_{mul} \in [0, 2]$. Moreover, $N_{ind} \geq 4$ and it is recommended [23] that N_{ind} be between $5N_{dim}$ and $10N_{dim}$. The selected input parameters values were chosen to be those that minimize the BER and are presented in Table 1. Note that the optimum mutation factor value increases with antenna correlation index ρ. Figure 5 depicts the simulated BER curves for a wide range of input parameter values, showing the best values of such input parameters, that is, those values that minimize the BER. The calibration procedure is finished when the range of those input parameters is narrowed.

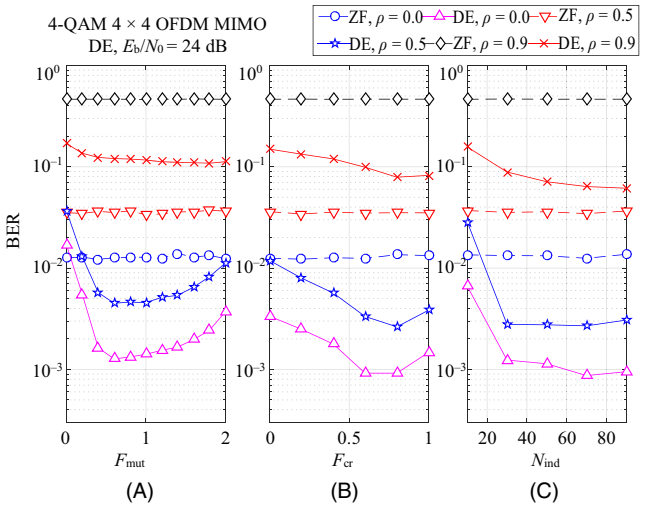

FIGURE 5 Calibration of the input parameters for the DE-aided MIMO-OFDM detector algorithm considering different values of spatial correlation

After the input parameter tuning procedure, the convergence of the DE-aided OFDM-MIMO detector algorithm is obtained, as depicted in Figure 6. Similar to the PSO convergence behavior, the convergence of the DE detector seems to be attained at around 40 iterations, being influenced mainly by the E_b/E_0 levels.

5.1.3 | Effect of spatial correlation on performance

In this section, the numerical simulation results for the BER performance were obtained under different correlation index ρ values, which represents the antenna separation on the transmitter and receiver sides, as depicted in Figure 7. As inferred previously from Figures 4 and 3, the spatial correlation deteriorates the BER performance; as ρ

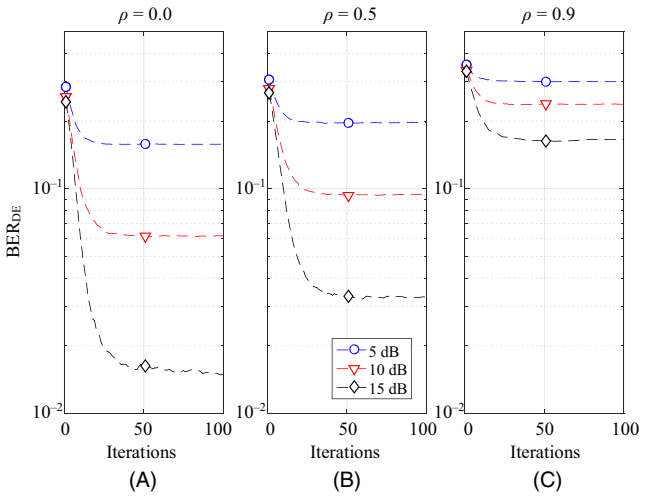

FIGURE 6 Convergence of the DE-aided detector for MIMO-OFDM systems for different spatial correlation values

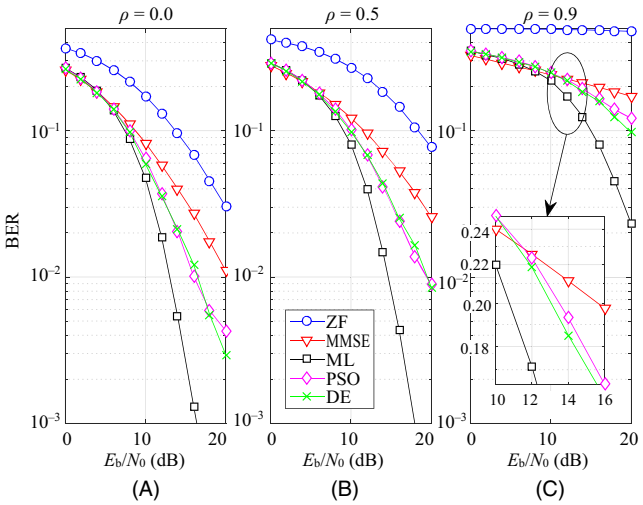

FIGURE 7 BER performance for 4-QAM, 4 × 4 ULA antenna MIMO-OFDM detectors under different values of spatial correlation and SNR

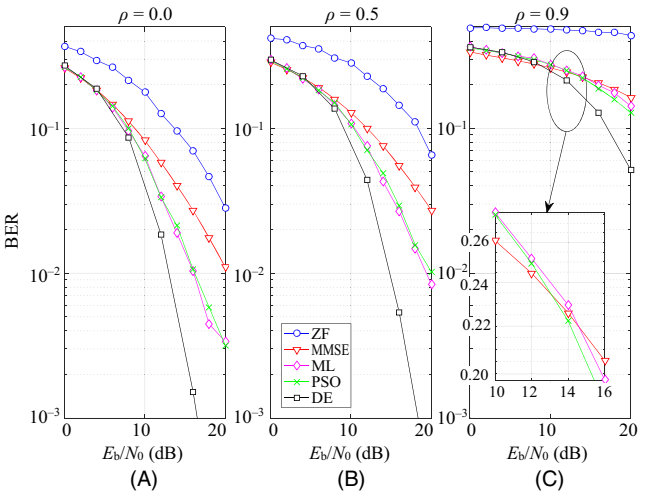

FIGURE 8 BER performance for 4-QAM 4 × 4 OFDM MIMO with linear and heuristic detectors for a URA configuration and different values of correlation and SNR

increases, the probability of error also increases. Under the most highly correlated channels $\rho = 0.9$, the ZF detector provides an unacceptable performance, even operating within the high E_b/E_0 region. The effect of degradation of spatial correlation on the performance also influences the ML detector's performance; however, the ML detector still attains a suitable performance considering uncoded system, at the cost of an enormous computational complexity. Alternatively, considering low-complexity evolutionary DE-based and PSO-aided detectors under the $\rho = 0$ scenario, PSO can outperform MMSE; however, in a highly correlated situation, this performance advantage becomes marginal, while the DE-based MIMO-OFDM detector performs marginally worse than MMSE for all SNR regions. Hence, under medium or even highly correlated MIMO channels, the linear MMSE and the PSO-based detectors represent good options regarding the performance-complexity tradeoff in MIMO-OFDM systems.

Figure 8 explores the BER performance considering planar arrays (URA) instead of a ULA. For high E_b/E_0, medium ρ, and a low number of antennas (4 × 4), the planar array configuration slightly outperforms the linear array design for ZF, MMSE, and PSO detectors (compare the BER performance of Figures 7 and 8). Note that the use of a URA system implies a slightly higher correlation among antennas compared to the ULA. Despite this, the URA performance remains very similar to that of the ULA and is even slightly better at high SNR.

5.1.4 | Sensitivity analysis

To compare the BER degradation with respect to array antenna correlation, the sensitivity of the detectors' performance regarding the level of correlation can be defined as:

$$\kappa_{\text{scn}} = \log_{10} \text{BER}_{\text{scn}} - \log_{10} \text{BER}_{\text{ref}}, \tag{18}$$

where BER_{ref} represents the reference BER value, and BER_{scn} is the BER in a specific scenario, including spatial correlation conditions or detector type.

For illustration purposes, two cases are studied: the degradation in performance when comparing the BER of each detector with respect to uncorrelated antennas ($\rho = 0$); and the degradation using the ML detector as a reference, since its performance is superior to that of the others. Figure 9 depicts both sensitivity scenarios.

κ_ρ: In Figure 9A, the sensitivity considering the performance of each detector at $\rho = 0$ as the correlation increases

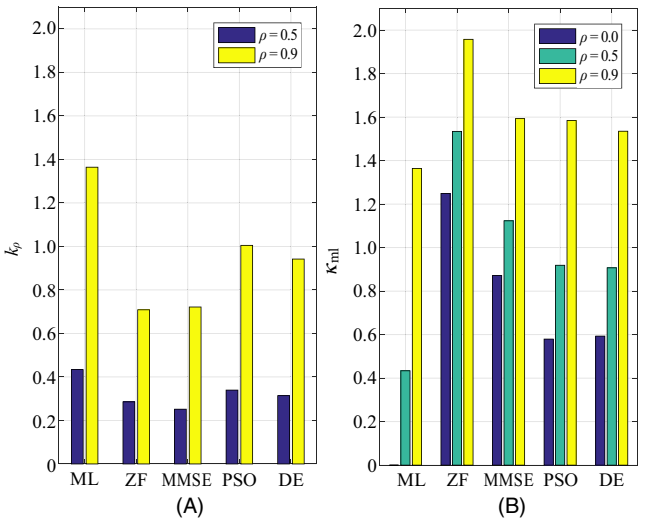

FIGURE 9 Sensitivity of detectors for two correlation scenarios: (A) κ_ρ, comparing each detector with its BER under $\rho = 0$ and (B) κ_{ml}, comparing detector performance with ML detector performance under $\rho = 0$

was numerically obtained. Hence, comparing the performance degradation sensitivity for each detector at $\rho = 0.5$ and $\rho = 0.9$, one can conclude that ML's sensitivity to increasing channel correlation is severely degraded compared with that of the linear and heuristic detectors because of its excellent performance under the $\rho = 0$ condition; while for the ZF detector, the degradation is small, since it already has poor performance compared to the other detectors. In short, the four MIMO-OFDM detectors are not robust to the spatial correlation channel effect.

κ_{ml}: In Figure 9B, sensitivity is shown, taking the ML detector BER performance with $\rho = 0$ as reference BER_{ref}. For medium correlation values ($\rho = 0.5$), the PSO is most near to ML's sensitivity performance degradation, and so κ_{ml} has relatively low results. For $\rho = 0.9$, the ZF detector performs poorly in terms of BER, resulting in a high sensitivity index κ_{ml}. The PSO-aided detector is more sensitive in terms of κ_ρ because its BER varies more as correlation increases, but less sensitive in terms of κ_{ml}, mainly for low and medium spatial correlation channel indexes ($\rho \leq 0.5$).

5.2 | Complexity analysis

To evaluate the complexity of the algorithms, the number of *floating point operations* (FLOPs), defined as a floating point addition, subtraction, multiplication, or division [27] between real numbers, are considered. Here, both the Hermitian and *if* conditional operators are disregarded. In a real implementation, some platforms may use hardware-based random number generators, where an electric circuit provides the random numbers; hence, the FLOP cost for random number generation was also disregarded in this analysis.

The FLOPs required for the main operations are summarized in Table 2 and the full complexity expressions are denoted by Υ. These values for the considered MIMO-OFDM detectors are presented in Table 3. To analyze the detectors' FLOP complexity for different numbers of antennas, Figure 10 depicts the linear and heuristic detector complexities assuming $N_{\text{dim}} = 2N_{\text{t}}$, $N_{\text{t}} = N_{\text{r}}$, and $N_{\text{ind}} = N_{\text{pop}} = 5N_{\text{dim}}$, and considering the number of iterations until convergence is obtained through simulations, as shown in Figures 4 and 6.

The ML detector computes all possible input matrices [6] resulting in the evaluation of (5) as $\mathcal{M}^{2N_{\text{t}}\times 1}$ times, where $\mathcal{M}$ represents the modulation order, making it the most computationally complex of the detectors considered. It can be observed that the DE algorithm requires more FLOPs than PSO since it evaluates two N_{pop} times the fitness function per iteration in (17) for individuals and crossover vectors. The complexity among the linear detectors is almost the same, differing by a scalar–matrix multiplication and matrix–matrix sum in (6) and (9).

TABLE 2 Number of FLOPs for vector and matrix operations: $\mathbf{w} \in \mathbb{R}^{q\times 1}, \mathbf{A} \in \mathbb{R}^{m\times q}, \mathbf{B} \in \mathbb{R}^{q\times p}, \mathbf{C} \in \mathbb{R}^{m\times p}, \mathbf{D} \in \mathbb{R}^{q\times q}$

Operation	# FLOPS
Matrix-matrix multiplication **AB**	$mp(2q-1)$
Matrix-vector multiplication **Aw**	$m(2q-1)$
Matrix multiply-add **AB** + **C**	$2mpq$
Square root $\sqrt{\cdot}$	8
Matrix inversion using LU factorization of **D** [28]	$2/3q^3 + q^2$
Norm-2, $\sqrt{\mathbf{w}^T\mathbf{w}}$	$2q - 1 + 8$

TABLE 3 Number of FLOPs per subcarrier for the MIMO-OFDM detectors, with $\mathcal{H} \in \mathbb{R}^{2N_{\text{r}}\times 2N_{\text{t}}}$, $\boldsymbol{\upsilon} \in \mathbb{R}^{2N_{\text{t}}\times 1}$, $N_{\text{dim}} = 2N_{\text{t}}$

Detector	Number of operations
$\Upsilon_{\text{ZF}}(N_{\text{t}}, N_{\text{r}})$	$\frac{16}{3}N_{\text{t}}^3 + 4N_{\text{t}}^3 + 32N_{\text{t}}^2N_{\text{r}} + 4N_{\text{t}}N_{\text{r}} - 2N_{\text{t}}$
$\Upsilon_{\text{MMSE}}(N_{\text{t}}, N_{\text{r}})$	$\frac{16}{3}N_{\text{t}}^3 + 8N_{\text{t}}^2 + 32N_{\text{t}}^2N_{\text{r}} + 4N_{\text{t}}N_{\text{r}}$
$\Upsilon_{\text{PSO}}(N_{\text{t}}, N_{\text{r}}, N_{\text{pop}}, \mathcal{I})$	$N_{\text{pop}}\mathcal{I}(8n_{\text{t}}N_{\text{r}} + 20N_{\text{t}} + 4N_{\text{r}} + 7)$
$\Upsilon_{\text{DE}}(N_{\text{t}}, N_{\text{r}}, N_{\text{ind}}, \mathcal{I})$	$N_{\text{ind}}\mathcal{I}(16N_{\text{t}}N_{\text{r}} + 12N_{\text{t}} + 8N_{\text{r}} + 14)$
$\Upsilon_{\text{ML}}(N_{\text{t}}, N_{\text{r}}, \mathcal{M})$	$\mathcal{M}^{2N_{\text{t}}}(8N_{\text{t}}N_{\text{r}} + 4N_{\text{r}} + 7)$

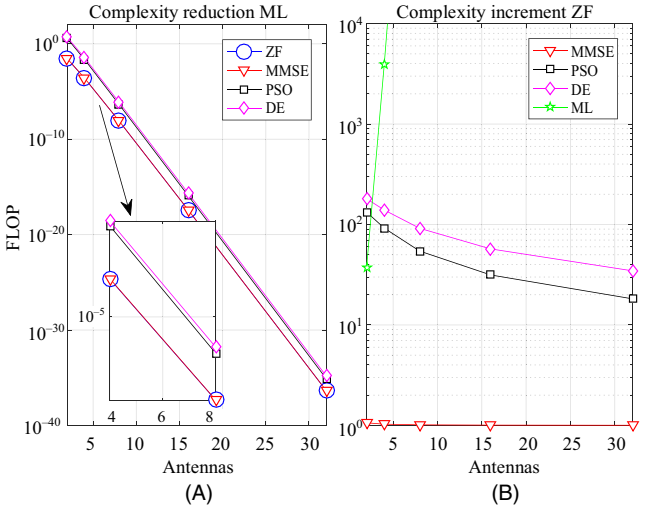

FIGURE 10 Relative complexity of MIMO-OFDM detectors considering different numbers of antennas for linear and heuristic detectors in a point-to-point scenario: $N_{\text{t}} = N_{\text{r}}$, $N_{\text{dim}} = 2N_{\text{t}}, N_{\text{ind}} = N_{\text{pop}} = 5N_{\text{dim}}, \mathcal{I} = 50, \mathcal{M} = 4$.

Relative complexity is depicted in Figure 10. On the left side, the complexity reduction relative to ML and linear/heuristic detectors, evaluated as $\Upsilon_{\text{det}}/\Upsilon_{\text{ml}}$, are shown. All the studied MIMO-OFDM detectors decrease complexity with respect to the ML detector. Note that PSO provides slightly more reduction than DE, and linear detectors provide more than the heuristics, at the cost of BER performance. On the right side, the complexity increases relative to the linear low-complexity ZF MIMO-OFDM detector $\Upsilon_{\text{det}}/\Upsilon_{\text{zf}}$ is determined. Note that the linear MMSE detector has a

complexity that is near to that of ZF resulting in values close to one, while the ML detector complexity increases rapidly as the number of antennas increases. The heuristic PSO detector increments complexity more slowly than the DE detector at almost the same BER performance, offering a good complexity tradeoff between computational complexity vs performance, mainly when the number of antennas increases (such as in massive MIMO systems).

6. | CONCLUSIONS

The analysis of an OFDM scheme was developed considering NLOS Rayleigh fading channel conditions. Extensive simulations were deployed and suitable input parameters for the evolutionary heuristics PSO and DE were chosen numerically for the MIMO-OFDM detection problem. The convergence of a PSO-based detector depends mainly on the E_b/N_0 level, requiring more iterations as the SNR increases.

Spatial correlation degrades the performance of the analyzed MIMO-OFDM detectors. For the uncorrelated scenario ($\rho = 0$), the PSO-aided detector outperforms linear detectors ZF and MMSE. However, for high correlation ($\rho = 0.9$), the PSO detector gain in terms of BER performance becomes marginal. The performance degradation as correlation increases is quantified by the sensitivity of the detectors for different levels of correlation.

Planar antenna arrays marginally outperform the linear array configurations for the ZF, MMSE, PSO, and DE MIMO-OFDM detectors considering high SNR operation region and low number of antennas. When the number of antennas increases, such outperformance may become noticeable. Although the correlation among antennas is slightly higher in the URA, this difference is not enough to deteriorate the performance of the system.

Comparing the complexity of the detector algorithms, the linear MMSE detector provides better performance than the linear ZF for almost the same computational complexity. Among the representative evolutionary heuristic MIMO-OFDM detectors, the PSO provides lower increments in complexity with respect to the DE detector, and almost the same (similar) BER performance for all the system and channel scenarios analyzed, both offering a suitable computational complexity vs performance tradeoff, even under medium spatial antenna correlation levels.

ACKNOWLEDGEMENTS

This work was supported in part by the National Council for Scientific and Technological Development (CNPq) of Brazil (Grants 130464/2015-5 and 304066/2015-0), in part by Araucaria Foundation, PR, (Grant 302/2012), and by Londrina State University - Paraná State Government, Brazil.

REFERENCES

1. L. L. Hanzo et al., *MIMO-OFDM for LTE, WiFi and WiMAX: Coherent versus non-coherent and cooperative turbo transceivers*, Wiley-IEEE Press, Torquay, UK, 2011.
2. G. Foschini and M. Gans, *On limits of wireless communications in a fading environment when using multiple antennas*, Wirel. Pers. Commun. **6** (1998), no. 3, 311–335.
3. E. Telatar, *Capacity of multi-antenna Gaussian channels*, Eur. Trans. Telecommun. **10** (1999), no. 6, 585–595.
4. M. A. Saeed, B. M. Ali, and M. H. Habaebi, *Performance evaluation of OFDM schemes over multipath fading channels, Asia-Pacific Conf. Commun. (IEEE Cat. No.03EX732)*, Penang, Malaysia, Sept. 21–24, 2003, pp. 415–419.
5. H. Steendam and M. Moeneclaey, *Analysis and optimization of the performance of OFDM on frequency-selective time-selective fading channels*, IEEE Trans. Commun. **47** (1999), no. 12, 1811–1819.
6. A. Goldsmith, *Wireless communications*, Cambridge University Press, New York, NY, USA, 2005.
7. J. R. Hampton, *Introduction to MIMO communications*, Cambridge University Press, New York, NY, USA, 2014.
8. A. Trimeche et al., *The particle swarm optimization (PSO) for symbol detection in MIMO-OFDM system*, Int. J. Inform. Secur. **4** (2013), no. 1, 38–45.
9. D. W. M. Guerra et al., Linear detection analysis in MIMO-OFDM with spatial correlation, *12th IEEE Int. Conf. Ind. Appicat. (INDUSCON)*, Curitiba, Brazil, 2016, pp. 1–8.
10. M. N. Seyman and N. Taspinar, *Symbol detection using the differential evolution algorithm in MIMO-OFDM Systems*, Turkish J. Elect. Eng Comp. Sci. **21** (2014), 373–380.
11. A. A. Khan, M. Naeem, and S. I. Shah, A particle swarm algorithm for symbols detection in wideband spatial multiplexing systems, *9th Annu. Conf. Genet. Evol. Comput. (GECCO '07)*, New York, NY, USA, 2007, pp. 63–69.
12. V. Zelst and J. Hammerschmidt, A single coefficient spatial correlation model for multiple-input multiple-output (Mimo) radio channels, *27th Gen. Assem. Int. Union Radio Sci. (URSI)*, Maastricht, Netherlands, Aug. 17–24, 2002, pp. 2–5.
13. G. Levin and S. Loyka, On capacity-maximizing angular densities of multipath in MIMO channels, *IEEE 72nd Veh. Tech. Conf.—Fall*, Ottawa, Canada, Sept. 2010, pp. 1–5.
14. J. Janhunen et al., *Fixed- and floating-point processor comparison for MIMO-OFDM detector*, IEEE J. Sel. Top. Signal Proc. **5** (2011) no. 8, 1588–1598.
15. A. P. R. N. D. Gore, *Introduction to space-time wireless communications*, Cambridge University Press, Cambridge, UK, 2003.
16. Y. S. Cho et al., *MIMO-OFDM wireless communications with MATLAB*, Wiley Publishing, Noida, India, 2010.
17. J. G. Proakis and M. Salehi, *Digital communications*, 5th ed., McGraw-Hill, New York, USA, 2008.
18. J. Kennedy and R. C. Eberhart, Particle swarm optimization, *IEEE Int. Conf. Neural Netw.*, Perth, Australia, Nov, 27-Dec. 1, 1995, pp. 1942–1948.
19. S. Cheng and Y. Shi, *Normalized population diversity in particle swarm optimization*, Springer Berlin Heidelberg, Berlin, Germany, 2011, pp. 38–45.
20. M. R. Bonyadi and Z. Michalewicz, *Particle swarm optimization for single objective continuous space problems: A review*, Evol. Comput. **25** (2017), no. 1, 1–54.

21. Y. Shi and R. C. Eberhart, Parameter selection in particle swarm optimization, *Evol. Prog. VII*, V. W. Porto, N. Saravanan, D. Waagen and A. E. Eiben, Eds., Springer Berlin Heidelberg, Berlin, Germany, 1998, pp. 591–600.
22. Y. Shi and R. Eberhart, A modified particle swarm optimizer, *IEEE Int. Conf. Evol. Comput. Proc. IEEE World Cong. Comput. Intell. (Cat. No. 98TH8360)*, Anchorage, AK, USA, May 4–9, 1998, pp. 69–73.
23. R. Storn and K. Price, *Differential evolution – A simple and efficient heuristic for global optimization over continuous spaces*, J. Glob. Optim. **11** (1997), no. 4, 341–359.
24. J. C. M. Filho, R. N. deSouza, and T. Abrão, *Ant colony input parameters optimization for multiuser detection in DS/CDMA systems*, Expert Sys. Appl. **39** (2012), no. 17, 12876–12884.
25. M. Clerc and J. Kennedy, *The particle swarm—Explosion, stability, and convergence in a multidimensional complex space*, IEEE Trans. Evol. Comput. **6** (2002), no. 1, 58–73.
26. I. C. Trelea, *The particle swarm optimization algorithm: Convergence analysis and parameter selection*, Inform. Proc. Lett. **85** (2003), no. 6, 317–325.
27. G. H. Golub and C. F. Van Loan, *Matrix computations*, 4th ed., Johns Hopkins University Press, Baltimore, USA, 2013.
28. S. Boyd and L. Vandenberghe, Numerical linear algebra background, available at http://www.seas.ucla.edu/~vandenbe/ee236b/lectures/num-lin-alg.pdf (Accessed Apr. 23, 2018).

AUTHOR BIOGRAPHIES

David William Marques Guerra received his BS degree in electrical engineering from the State University of Londrina, Brazil, in 2017, where he is currently working toward his MS degree in electrical engineering. His research interests lie in telecommunication systems, more precisely in wireless communications and signal processing, including multicarrier systems, MIMO systems, 5G, and the optimization aspects of communications systems and signals.

Rafael Masashi Fukuda received his BS degree in electrical engineering from the State University of Londrina, Brazil, in 2017. Currently, he is working on his MS degree in electrical engineering. His interests include OFDM and MIMO systems, 4G and 5G wireless systems, signal processing, and heuristics and convex optimization techniques for wireless communication systems.

Ricardo Tadashi Kobayashi received his BTech and MS degrees, both in electrical engineering, from the State University of Londrina, Brazil, in 2014 and 2016, respectively. Currently, he is working toward his PhD in electrical engineering at the State University of Londrina. His research interests lie in communications and signal processing, including MIMO detection techniques, optimization aspects of communications, convex optimization, and cognitive radio techniques.

Taufik Abrão received his BS degree, MSc degree, and PhD in electrical engineering from the Polytechnic School of the University of São Paulo, Brazil, in 1992, 1996, and 2001, respectively. Since March 1997, he has been with the Communications Group, Department of Electrical Engineering, Londrina State University, Brazil, where he is currently an associate professor in Telecommunications and the head of the Telecommunications and Signal Processing Lab. In 2012, he was an Academic Visitor with the Southampton Wireless Research Group, University of Southampton, UK. From 2007 to 2008, he was a postdoctoral researcher with the Department of Signal Theory and Communications, Polytechnic University of Catalonia, Spain. He has participated in several projects funded by government agencies and industrial companies. He is involved in editorial board activities of six journals in the telecommunications area and has served as a TPC member in several symposiums and conferences. He has also served as an editor for the *IEEE Communications Surveys and Tutorials* since 2013, *IEEE Access* since 2016, *IET Journal of Engineering* since 2014, and *ETT-Wiley* since 2016. He is a member of SBrT and a senior member of the IEEE. His current research interests include communications and signal processing, especially multiuser detection and estimation, MC-CDMA and MIMO systems, cooperative communication and relaying, resource allocation, as well as the heuristic and convex optimization aspects of 3G and 4G wireless systems. He has supervised 24 MSc degree and 4 PhD students, as well as 2 postdocs, co-authored nine book chapters on mobile radio communications and over 180 research papers published in specialized/international journals and conferences (http://www.uel.br/pessoal/taufik).

A.2 *DE/PSO-aided Hybrid Linear Detectors for MIMO-OFDM Systems Under Correlated Arrays*

Título:	*DE/PSO-aided Hybrid Linear Detectors for MIMO-OFDM Systems Under Correlated Arrays*
Autores:	**Rafael Masashi Fukuda**, David Marques Guerra, Ricardo Tadashi Kobayashi e Taufik Abrão
Revista:	*Transactions on Emerging Telecommunications Technologies* (ETT)
Status:	Publicado
DOI:	https://doi.org/10.1002/ett.3495
Qualis:	A2 Qualis-Eng.IV CAPES

No segundo trabalho, os detectores híbridos, que são uma combinação entre detectores lineares e heurísticos, são estudados. As combinações de detectores lineares e heurísticos avaliadas foram PSO-MF, PSO-MMSE, DE-MF e DE-MMSE. O PSO-MMSE apresentou a melhor performance durante as simulações; o DE-MF e DE-MMSE apresentaram desempenho parecido, enquanto o PSO-MF apresentou performance próxima porém um pouco pior em termos de BER. Os detectores híbridos são capazes de melhorar o compromisso entre desempenho e complexidade, proporcionando performance melhor ou bastante próxima dos detectores com as heurísticas PSO e DE e apresentando uma complexidade computacional menor.

Received: 13 May 2018 | Accepted: 6 July 2018
DOI: 10.1002/ett.3495

RESEARCH ARTICLE

WILEY

DE/PSO-aided hybrid linear detectors for MIMO-OFDM systems under correlated arrays

Rafael Masashi Fukuda | David William Marques Guerra | Ricardo Tadashi Kobayashi | Taufik Abrão

Department of Electrical Engineering, State University of Londrina, Londrina, Brazil

Correspondence
Taufik Abrão, Department of Electrical Engineering, State University of Londrina, 86057-970 Londrina, Brazil.
Email: taufik@uel.br

Funding information
National Council for Scientific and Technological Development (CNPq) of Brazil, Grant/Award Number: 130464/2015-5 (scholarship) and 304066/2015-0 (research); Araucaria Foundation, PR, Grant/Award Number: 302/2012 (research); Londrina State University - Paraná State Government, Brazil

Abstract

In this paper, we analyze the performance of evolutionary heuristic-aided linear detectors deployed in multiple-input–multiple-output (MIMO) orthogonal frequency-division multiplexing (OFDM) systems, considering realistic operating scenarios. Hybrid linear-heuristic detectors under different initial solutions provided by linear detectors are considered, namely, differential evolution and particle swarm optimization. Numerical results demonstrated the applicability of hybrid detection approach, which can improve considerably the performance of minimum mean-square error and matched filter detectors. Furthermore, we discuss how the complexity of the presented algorithms scales with the number of antennas, besides of verifying the spatial correlation effects on MIMO-OFDM performance assisted by linear, heuristic, and hybrid detection schemes. The influence of the initial point in the performance improvement and complexity reduction is evaluated numerically.

1 | INTRODUCTION

Contemporary wireless communications systems, such as IEEE 802.11 and 4G LTE, deploy multicarrier modulation with the aim of transmitting data over frequency-selective channels. In this sense, orthogonal frequency-division multiplexing (OFDM) is the most popular choice and a suitable number of subcarriers are used to make subchannels frequency flat. Moreover, dispersion and other phenomena introduce undesirable effects that may limit the overall performance of a wireless system. From this perspective, Saeed et al[1] discuss how the number of subcarriers affects the transmission of an OFDM signal with equipped with a single antenna at both transmission sides transmitter-receiver (single input single output [SISO]).

In the search of more efficient systems, multiple-input–multiple-output (MIMO) systems were proposed and able to improve the spectral efficiency.[2] However, such benefits also require more sophisticated electrical circuitry and signal processing, which are needed to decouple signals from the different antennas.[3] The system may increase the throughput using multiplexing mode, where each antenna transmit different signals. Conversely, increasing the performance/reliability requires the transmission of the same information and exploiting diversity. Those characteristics are limited to the Diversity-multiplexing trade-off.[4] Herein, the multiplexing mode is considered, where the signal of the other $N_t - 1$ transmit antennas interferes each other. Thus, detection algorithms are required to reduce the effects of such interference[5,6] and are studied throughout this work.

In order to attain high levels of efficiency, the MIMO system considers the assumption of rich scattering (isotropic) scenario modeled as independent Rayleigh,[7] which is not always entirely valid in real applications. A rule of thumb

is the approximation of half-wavelength of separation between antennas[3] to achieve independent fading channels, but this distance may not be always respected, for example, due to space limitation of the receiver hardware, resulting in spatial correlation of the channel coefficients. In realistic scenarios, correlated models are good representations of field measurements[8] and thus considered in our numerical simulations.

Guerra et al[9] discuss how the performance of SISO-OFDM systems scale with the number of subcarriers. In the MIMO-OFDM context, the performance of zero forcing (ZF) and minimum mean-square error (MMSE) linear detectors is analyzed under spatial correlation scenarios. This work extends the results reported in the work of Guerra et al.[9] In particular and different from the aforementioned work,[9] herein, we propose a hybrid detection approach, where particle swarm optimization (PSO) and differential evolution (DE) evolutionary heuristics are combined with linear detectors (two detection steps), aiming to improve performance with reduced increment in complexity.

In detection problem, the maximum likelihood (ML) is known to provide optimal performance; however, its high computational complexity is prohibitive in real applications, specially when the problem dimension increases, eg, number of antennas, constellation size and number of subcarriers. Heuristic algorithms provide alternative good solutions with relatively low computational complexity. In the work of Khan et al,[10] PSO-aided detection is considered in MIMO and in the work of Trimeche et al[11] to MIMO-OFDM systems, providing lower computational complexity compared to ML detector. In the work of Seyman and Taspinar,[12] heuristic approaches DE, genetic algorithm, and PSO are applied to detection in MIMO-OFDM and performance in terms of bit error rate (BER) is evaluated. In the work of Khan et al,[13] binary PSO is applied to MIMO-OFDM and an algorithm considering the output of ZF-VBLAST is proposed and performance evaluated numerically.

The contributions of this paper are as follows. We analyze the influence on BER performance and computational complexity in terms of *floating points operations* (FLOPs) of different initial solution as input to the heuristic algorithms, ie, we have analyzed distinct initialization, including random guess, linear detector outputs, such as matched filter (MF) and MMSE solutions as input, while perform a comparison between those heuristic detectors in realistic scenario, ie, under spatial correlation between antennas. Moreover, aiming to attain a fair performance-complexity comparison, the input parameters of both heuristic strategies have been systematically chosen, since they directly impact on the algorithm performance and complexity, as studied in the work of Filho et al.[14]

The remainder of this work is organized as follows. Section 2 revisits briefly the OFDM scheme. Descriptions for the MIMO-OFDM system with spatial channel correlation are offered in Section 3. Moreover, Section 4 also describes the classical MIMO detectors and formulates heuristic aided detectors based on PSO and DE, including the hybrid linear-heuristic approaches. Extensive numerical results are discussed in Section 5, where BER performance comparison considering spatial correlation was systematically carried out. Besides, Section 5.3 carefully analyzes the resulting complexity of the MIMO-OFDM detectors. Final remarks and conclusions are offered in Section 6.

Notation 1. Throughout this paper, lowercase and uppercase bold-faced letters represent vectors and matrices, respectively. $\mathbb{C}$ and $\mathbb{R}$ represent the set of complex and real numbers; $\mathfrak{Re}\{.\}$ and $\mathfrak{Im}\{.\}$ represent the real and imaginary parts of a complex number. Operators $[.]^H$, $\|.\|$, $\circ$ and $\otimes$ represent Hermitian, Frobenius norm, Hadamard product, and Kronecker product, respectively. $\mathbb{E}\{.\}$ denotes expectation operator and $\sim \mathcal{U} \in [a, b]$ that a random variable follows a uniform distribution inside a specified interval.

2 | OFDM TRANSMISSION AND CHANNEL

A block diagram representing the MIMO-OFDM communication in multiplexing operation mode is exposed in Figure 1. At the transmitter side, the stream of bits is distributed throughout N_t transmitting substreams. Here, classical OFDM

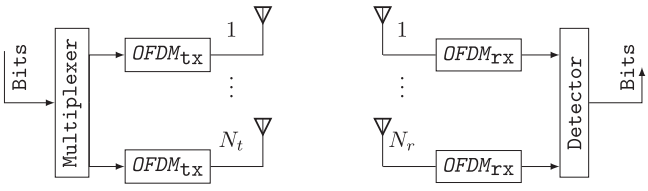

FIGURE 1 Multiple-input–multiple-output orthogonal frequency-division multiplexing (OFDM) block diagram

modulation is considered and described as follows. The signal passes through the $OFDM_{\text{tx}}$ block that represents the OFDM modulator, which includes the serial-to-parallel conversion, digital M-ary modulation, inverse discrete Fourier transform, cyclic prefix addition, parallel-to-serial conversion, and the transmission of the signal through the wireless channel. At the receiver, the signals of the N_r receive antennas are shifted to baseband, passed by the OFDM demodulator ($OFDM_{\text{rx}}$), which includes a serial-to-parallel followed by a discrete Fourier transform. Thus, cyclic prefix is discarded, the signal is serialized, demodulated, and it finally feeds the detection block, which is the focus of this work. Note that linear, heuristic, and hybrid detectors are discussed in more details in Section 4.

Among the different channel effects, the coherence time $(\Delta t)_c$ and the coherence band $(\Delta B)_{\text{C}}$ may influence parameters of an OFDM system. The coherence time scales directly with the maximum Doppler frequency while the mobility of a wireless terminal may cause problems such as the *carrier frequency offset*,[15] which is important for the performance of the system but not the focus of this paper. The coherence bandwidth is dictated by power delay profile (PDP) of the channel, which is measured empirically.[3] More specifically, the coherence bandwidth is evaluated based on the estimation of the delay spread of the PDP of a channel. This parameter influences directly on the number of subcarriers of the system, because, to achieve the flat-fading on every subchannel, the condition $B_{\text{sc}} \ll (\Delta B)_{\text{C}}$ requires N to be sufficiently large.[3] In special, this work deploys the IEEE 802.11b PDP model, which follows an exponential profile.[15]

3 | MIMO-OFDM MULTIPLEXING MODE AND SPATIAL CORRELATION

Considering N_t and N_r transmit and receive antennas, respectively, the signal received in a MIMO-OFDM channel on each subcarrier can be expressed as[16]

$$\mathbf{y}[n] = \mathbf{H}[n]\mathbf{x}[n] + \mathbf{z}[n], \tag{1}$$

where $\mathbf{y}[n] \in \mathbb{C}^{N_r \times 1}$ is the vector of the received signal, $\mathbf{H}[n] \in \mathbb{C}^{N_r \times N_t}$ is the channel matrix, $\mathbf{x}[n] \in \mathbb{C}^{N_t \times 1}$ the transmitted information, $\mathbf{z}[n] \in \mathbb{C}^{N_r \times 1}$ the Gaussian noise with zero mean and variance σ_z^2 through $n = 0, \ldots, N-1$ subcarriers.

In order to describe and evaluate spatial correlation between antennas, the Kronecker product is used as follows:

$$\mathbf{H}[n] = \sqrt{\mathbf{R}_r}\mathbf{G}[n]\sqrt{\mathbf{R}_t^H}, \tag{2}$$

where $\mathbf{G}$ is an uncorrelated channel matrix composed by independent and identically distributed entries, $\mathbf{R}_r$ and $\mathbf{R}_t$ are the spatial correlation matrices seen by the receiver and transmitter, respectively. The coefficients needed to construct the correlation matrix and the arrangement of the antennas (linear, rectangular) influences the entries of correlation matrices of the transmitter and receiver.

In the work of Van Zelst and Hammerschmidt,[17] an antenna correlation model is proposed for *uniform linear antenna* (ULA) array configurations. This model considers that the antennas are arranged equidistantly, where d_t and d_r represent the spacing between the transmitting and receiving antennas, linearly arranged, respectively. To simplify the analysis, we consider $N_t = N_r$, leading to Toeplitz symmetric correlation matrix

$$\mathbf{R}_t = \mathbf{R}_r = \begin{bmatrix} 1 & \rho & \rho^4 & \cdots & \rho^{(N_t-1)^2} \\ \rho & 1 & & & \vdots \\ \rho^4 & \rho & 1 & & \rho^4 \\ \vdots & \vdots & \vdots & \ddots & \rho \\ \rho^{(N_t-1)^2} & \cdots & \rho^4 & \rho & 1 \end{bmatrix}, \tag{3}$$

where $\rho \in [0, 1]$ denotes the correlation index between element antennas of a ULA array.

4 | MIMO-OFDM DETECTORS

In this section, linear- and heuristic-based detectors are discussed in details. Heuristic procedure involves the definition of a fitness function, deployed to evaluate the quality of the population/swarm and to decide which ones are more suitable to solve a given problem (in this paper, MIMO-OFDM detection). Furthermore, the model is rewritten in an equivalent real-valued representation and the PSO and DE heuristic procedures are detailed, while the utilization of different initial solution (hybrid approach) is briefly described.

4.1 | ML detector

Aiming to perform optimal symbol estimation, ML detection requires an exhaustive search over all symbol vector combinations. However, optimal performance comes at high computational complexity, which is not feasible for real-world systems. In the search, the vector offers the minimum Euclidean distance between the actual received signal $\mathbf{y}[n]$ and the estimated reconstructed received signal $\mathbf{H}[n]\mathbf{x}[n]$, assuming the transmission of a given candidate-signal vector $\mathbf{x}[n]$. Hence, ML symbols estimation for MIMO-OFDM systems can be formulated as the following problem:

$$\tilde{\mathbf{x}}[n] = \min_{\mathbf{x}} \|\mathbf{y}[n] - \mathbf{H}[n]\mathbf{x}[n]\|^2. \tag{4}$$

4.2 | Linear detectors

Since MIMO channels introduce linear superposition between the transmitted signals, detection algorithms must be deployed at the receiver side to mitigate inter-antenna interference while allowing the symbol reconstruction.[15] In this sense, the ZF is one of the simplest MIMO-OFDM equalizers, which uses the Moore-Penrose pseudo-inverse matrix to decouple the transmitted symbol vector, ie,

$$\mathbf{H}^{\dagger}_{\text{zf}}[n] = (\mathbf{H}[n]^H\mathbf{H}[n])^{-1}\mathbf{H}[n]^H. \tag{5}$$

Alternatively, the MMSE linear detector considers the statistical distribution of the noise. Therefore, this detector aims to minimize the distance between the actual transmitted signal and the estimated signal obtained through a linear equalization matrix.[2] Such optimization procedure can be defined by

$$\mathbf{H}^{\dagger}_{\text{mmse}}[n] = \min_{\mathbf{W}} \mathbb{E}\{\|\mathrm{x}[n] - \mathbf{W}\mathbf{y}[n]\|^2\}. \tag{6}$$

Thus, solving Equation (6) leads to the MMSE closed-form solution

$$\mathbf{H}^{\dagger}_{\text{mmse}}[n] = \left(\mathbf{H}^H[n]\mathbf{H}[n] + \frac{N_0}{E_S}\mathbf{I}\right)^{-1}\mathbf{H}^H[n]. \tag{7}$$

where $\frac{N_0}{E_S}$ is the inverse of the signal-to-noise ratio (SNR).

As another option, the MF is a classical method that provides optimum performance in the additive white Gaussian noise scenario and consists of the multiplication of the received signal by the transpose conjugate of the channel.

Finally, linear estimation can be generically described by

$$\tilde{\mathbf{x}}[n] = \mathbf{W}_{\text{lin}}[n]\mathbf{y}[n], \tag{8}$$

where $\mathbf{W}_{\text{lin}}[n] = \mathbf{H}^{\dagger}_{\text{zf}}[n]$ for the ZF detection, $\mathbf{W}_{\text{lin}}[n] = \mathbf{H}^{\dagger}_{\text{mmse}}[n]$ for the MMSE detection, and $\mathbf{W}_{\text{lin}} = \mathbf{H}^H[n]$ for the MF.

4.3 | Fitness function

To facilitate the application of the heuristic methods, Equation (1) can be denoted as an equivalent real-valued representation as follows:

$$\underline{\mathbf{y}}[n] = \begin{bmatrix} \mathfrak{Re}\{\mathbf{y}[n]\} \\ \mathfrak{Im}\{\mathbf{y}[n]\} \end{bmatrix}, \quad \underline{\mathbf{H}}[n] = \begin{bmatrix} \mathfrak{Re}\{\mathbf{H}[n]\} & -\mathfrak{Im}\{\mathbf{H}[n]\} \\ \mathfrak{Im}\{\mathbf{H}[n]\} & \mathfrak{Re}\{\mathbf{H}[n]\} \end{bmatrix}, \tag{9}$$

$$\underline{\mathbf{x}}[n] = \begin{bmatrix} \mathfrak{Re}\{\mathbf{x}[n]\} \\ \mathfrak{Im}\{\mathbf{x}[n]\} \end{bmatrix}, \qquad \underline{\mathbf{z}}[n] = \begin{bmatrix} \mathfrak{Re}\{\mathbf{z}[n]\} \\ \mathfrak{Im}\{\mathbf{z}[n]\} \end{bmatrix}, \tag{10}$$

where matrix $\underline{\mathbf{H}} \in \mathbb{R}^{2N_r \times 2N_t}$ and vectors $\underline{\mathbf{y}}[n] \in \mathbb{R}^{2N_r \times 1}$, $\underline{\mathbf{x}}[n]$, and $\underline{\mathbf{z}}[n] \in \mathbb{R}^{2N_t \times 1}$ are the real-valued representation of the channel, received signal, sent information, and thermal noise, respectively.

For the detection problem, generally, the fitness function is defined based on the Euclidean distance between the received signal and the estimated-reconstructed (candidate) symbol and is formulated as[11-13]

$$f(\boldsymbol{\zeta}) = \|\underline{\mathbf{y}}[n] - \underline{\mathbf{H}}[n]\boldsymbol{\zeta}\|^2, \tag{11}$$

where ζ denotes the entity that we want to evaluate, an specific position of particle in PSO and an individual in DE.

4.4 | Heuristic PSO-based detector

PSO is an evolutionary heuristic algorithm with adjustable parameters, such as cognitive and social factors (c_1 and c_2, respectively), related to the behavior of bird flocking and fish schooling. Associated to each particle, there is a velocity $\mathbf{v} \in \mathbb{R}^{N_{\text{dim}} \times 1}$, actual position $\mathbf{p} \in \mathbb{R}^{N_{\text{dim}} \times 1}$, and personal best position $\mathbf{p}_{\text{PB}} \in \mathbb{R}^{N_{\text{dim}} \times 1}$ associated, which are updated at each iteration of the algorithm as follows in matrix representation[18]:

$$\mathbf{V} = w\mathbf{V} + c_1\mathbf{U}_1 \circ (\mathbf{M}_{\text{PB}} - \mathbf{P}) + c_2\mathbf{U}_2 \circ (\mathbf{M}_{\text{GB}} - \mathbf{P}), \tag{12}$$

$$\mathbf{P} = \mathbf{P} + \mathbf{V}, \tag{13}$$

where N_{dim} denotes the dimensionality of the problem, w is the inertia factor; $\mathbf{U}_1$ and $\mathbf{U}_2$ are matrices compounded of elements $\sim \mathcal{U}[0, 1]$, $\mathbf{P} \in \mathbb{R}^{N_{\text{dim}} \times N_{\text{pop}}}$ and $\mathbf{V} \in \mathbb{R}^{N_{\text{dim}} \times N_{\text{pop}}}$ matrices store the position and velocity of N_{pop} particles of the swarm in each column, ie, $\mathbf{P} = [\mathbf{p}_1 \cdots \mathbf{p}_{N_{\text{pop}}}]$ and $\mathbf{V} = [\mathbf{v}_1 \cdots \mathbf{v}_{N_{\text{pop}}}]$. $\mathbf{M}_{\text{PB}}$ is a matrix constructed with the personal best position of each particle and the best position matrix is given by $\mathbf{M}_{\text{GB}} = [\mathbf{p}_{\text{GB}} \cdots \mathbf{p}_{\text{GB}}] \in \mathbb{R}^{N_{\text{dim}}} \times N_{\text{pop}}$, where vector $\mathbf{p}_{\text{GB}} \in \mathbb{R}^{N_{\text{dim}} \times 1}$ denotes the best position in the swarm, the global best (in a minimization problem, the position that provides the lowest value of the fitness function).

The w coefficient introduced in the work of Shi and Eberhart[19] can be a constant, linear, or nonlinear function, and it balances the global and local exploitation depending on its value.[20] Here, a nonlinear decreasing strategy of $0.99w$ is considered. Regarding the velocity, to avoid a possible increase to infinity, it was limited to the interval $[-V_{\text{MAX}}, V_{\text{MAX}}]$, with V_{MAX} representing the maximum possible velocity value.[20]

After the execution of N_{iter} times of the PSO algorithm (Algorithm 1), the output vector $\mathbf{p}_{\text{GB}}$ corresponds to the detected symbol using the PSO-aided detector $\tilde{\mathbf{x}}_{\text{PSO}}[n]$ in the MIMO-OFDM problem.

Algorithm 1 Particle swarm optimization

1: Input parameters: $c_1, c_2, w, N_{\text{pop}}, N_{\text{iter}}, \mathbf{P}$
2: Initialization of $\mathbf{M}_{\text{PB}}$ and $\mathbf{M}_{\text{GB}}$
3: **for** $1 \rightarrow N_{\text{iter}}$ **do**
4: Calculate velocity, Equation (12)
5: Calculate position, Equation (13)
6: Evaluate fitness function, Equation (11), for all particles
7: Update personal best matrix $\mathbf{M}_{\text{PB}}$
8: Update global best matrix $\mathbf{M}_{\text{GB}}$
9: **end for**
10: Output: $\mathbf{p}_{\text{GB}}$

4.5 | Heuristic DE-based detector

DE is a population-based heuristic proposed in the work of Storn and Price[21] that relies on operations mutation, crossover, and selection in order to avoid be trapped on local minima across the N_{gen} generations of the algorithm.

Consider $\boldsymbol{\iota}, \boldsymbol{\nu}, \boldsymbol{\psi}$ vectors with dimensions $N_{\text{dim}} \times 1$ that represent the individuals, mutation, and crossover vectors, while N_{ind} is the number of individuals. The operations of the DE algorithm (Algorithm 2) operating with the strategy `rand/1/bin` presented in the aforementioned work[21] are synthesized in the following.

4.5.1 | Mutation

At each iteration, the kth mutation vector is constructed as

$$\boldsymbol{\nu}_k = \boldsymbol{\iota}_{r_1} + F_{\text{mut}}(\boldsymbol{\iota}_{r_2} - \boldsymbol{\iota}_{r_3}), \tag{14}$$

where variables $r_1 \neq r_2 \neq r_3 \neq k, k = 1, \ldots, N_{\text{ind}}$; r_1, r_2, r_3 are integer random variables distributed as $\sim \mathcal{U}[1, N_{\text{ind}}]$, and $F_{\text{mut}} \in [0, 2]$ is the parameter representing the mutation scale factor.

4.5.2 | Crossover

The crossover vector is created from individual and mutation vectors following the rule

$$\psi_{ik} = \begin{cases} \nu_{ik}, & \text{if} \quad \text{rand} \in [0,1] \leq F_{\text{cr}} \text{ or } i = r_k \\ \iota_{ik}, & \text{if} \quad \text{rand} \in [0,1] > F_{\text{cr}} \text{ and } i \neq r_k, \end{cases} \tag{15}$$

where rand $\sim \mathcal{U} \in [0,1]$; r_k is an integer $\sim \mathcal{U}[1, N_{\text{dim}}]$ and $F_{\text{cr}} \in [0,1]$ is the crossover factor, one of the input parameters of the algorithm.

4.5.3 | Selection

The population of individuals of the next generation is selected by the following rule:

$$\boldsymbol{\iota}_k^{\text{G}} = \begin{cases} \boldsymbol{\psi}_k, & \text{if } f(\boldsymbol{\psi}_k) < f(\boldsymbol{\iota}_k) \\ \boldsymbol{\iota}_k, & \text{otherwise.} \end{cases} \tag{16}$$

Notice that, in order to select the next generation, the fitness function must evaluate both the individuals and the crossover vectors, which reflects in the computational complexity of the algorithm.

After the execution of DE procedure N_{gen} times, the best individual $\boldsymbol{\iota}$ corresponds to the detected (estimated) symbol $\tilde{\mathbf{x}}_{\text{DE}}[n]$ using the DE-aided detector in the MIMO-OFDM problem.

Algorithm 2 Differential evolution

1: Input parameters: $F_{\text{cr}}, F_{\text{mut}}, N_{\text{ind}}, N_{\text{gen}}, [\boldsymbol{\iota}_1 \cdots \boldsymbol{\iota}_{N_{\text{ind}}}]$
2: **for** $1 \rightarrow N_{\text{gen}}$ **do**
3: Mutation, Equation (14), $k = 1, \ldots, N_{\text{ind}}$
4: Crossover, Equation (15), $i = 1, \ldots, N_{\text{ind}}; k = 1, \ldots, N_{\text{ind}}$
5: Select new individuals, Equation (16), $k = 1, \ldots, N_{\text{ind}}$
6: **end for**
7: Output: best individual $\boldsymbol{\iota}$

4.6 | Hybrid detectors

To improve performance with a marginal increment on the computational complexity of the suboptimal MIMO-OFDM detectors, two efficient hybrid linear-heuristic algorithms are proposed and evaluated in the sequel. Starting from an initial solution provided by MMSE linear detector, a heuristic approach is applied in the subsequent stage aiming to improve the BER performance. In such hybrid configuration, the initial population/swarm in DE/PSO is generated adding random numbers with Gaussian distribution $\mathcal{N}(0,1)$ to the initial solution.[21]

In this work, different initial guess solution are considered and numerical simulation is discussed under the perspective of the *performance-complexity trade-off*. For that, numerical simulation results relating performance improvements and complex reduction are pointed out. Three different initializations have been considered herein.

1. *Random initialization*: initial positions (in the PSO) and population (DE) are generated using random variables uniformly distributed inside the search space.
2. *Hybrid approach*: two different initial points are performed, which are provided by linear detectors MF and MMSE, while the respective symbol is considered as one variable input to the heuristic algorithms.
3. *Perturbation on the MF/MMSE solutions*: the initial position of particles and initial population of individuals are obtained adding random Gaussian variables $\mathcal{N}(0,1)$ to the initial solution provided by MF/MMSE detector.[21]

The influence of those points on the BER performance and complexity of the algorithm are explored in Section 5.

TABLE 1 MIMO-OFDM simulation parameters

Parameter	Value
OFDM	
System bandwidth, BW	20 MHz
Constellation	4-QAM
Delay spread, τ_{RMS}	64 ns
Number of subcarriers, N	64
MIMO	
Number of antennas, $N_t \times N_r$	4×4
Spatial correlation index	$\rho \in [0; 0.5; 0.9]$
MIMO-OFDM detectors	MF, ZF, MMSE, PSO, DE, PSO-MF, PSO-MMSE, DE-MF, DE-MMSE
Power allocation strategy	Equal power allocation
Channel	
Type	NLOS Rayleigh channel
CSI knowledge	perfect
Heuristic Detectors Setup	
Population size $N_{\text{pop}} = N_{\text{ind}}$	40
Search space	$[-1; 1]$

Abbreviations: CSI, channel state information; DE, differential evolution; MF, matched filter; MIMO, multiple-input–multiple-output; MMSE, minimum mean-square error; NLOS, non–line-of-sight; OFDM, orthogonal frequency-division multiplexing; PSO, particle swarm optimization.

5 | NUMERICAL RESULTS

Throughout this section, MIMO-OFDM systems are simulated considering realistic scenarios and different symbol detection. Specifically, linear, evolutionary heuristic, and linear-heuristic detectors performance subject to spatial antenna correlation effect has been compared using BER and rates of convergence for heuristic and hybrid detector approaches. Moreover, for the heuristic-based MIMO-OFDM detectors, the calibration of input parameters is conducted for each heuristic algorithm and respective hybrid approaches and the convergence reduction is appointed. After finding the best input parameter for each heuristic-based detector, the performance of the PSO and DE detectors are compared with hybrid approaches, namely, PSO-MF, PSO-MMSE, DE-MF, and DE-MMSE considering correlation between antennas; the performance of hybrid approaches is evaluated considering different number of iterations. Finally, the computational complexity of the algorithms is compared in terms of number of operations.

Table 1 summarizes the simulation setup adopted in this work. Moreover, for a fair comparison, equal power allocation was deployed throughout the transmitting antennas.

5.1 | Input parameter calibration for heuristic-aided MIMO-OFDM detectors

As different parameters may influence in the convergence properties of the heuristic algorithms, they were obtained numerically using the following procedure.[14] Considering a set of start parameters, one by one is varied and the one that provides the lowest BER is considered in the variation of next parameter. The illustration of the procedure executed for PSO algorithm is presented in Figure 2 and for DE algorithm in Figure 3, considering different values of spatial correlation and different initial points discussed in details in Section 4.6. Observe that different initializations result in different initial parameters, which is more evident in the parameter F_{mul} for random and MF/MMSE initializations. Looking at the convergence in Figure 2D, one can notice that, with MF and MMSE initialization, the number of iterations until convergence is reduced in comparison with random initialization case and consequently the complexity of the algorithm; as the E_b/N_0 value increases, more iterations are required. The start and final values after the calibration procedure for both PSO and DE heuristic-based detectors are summarized in Tables 2 and 3.

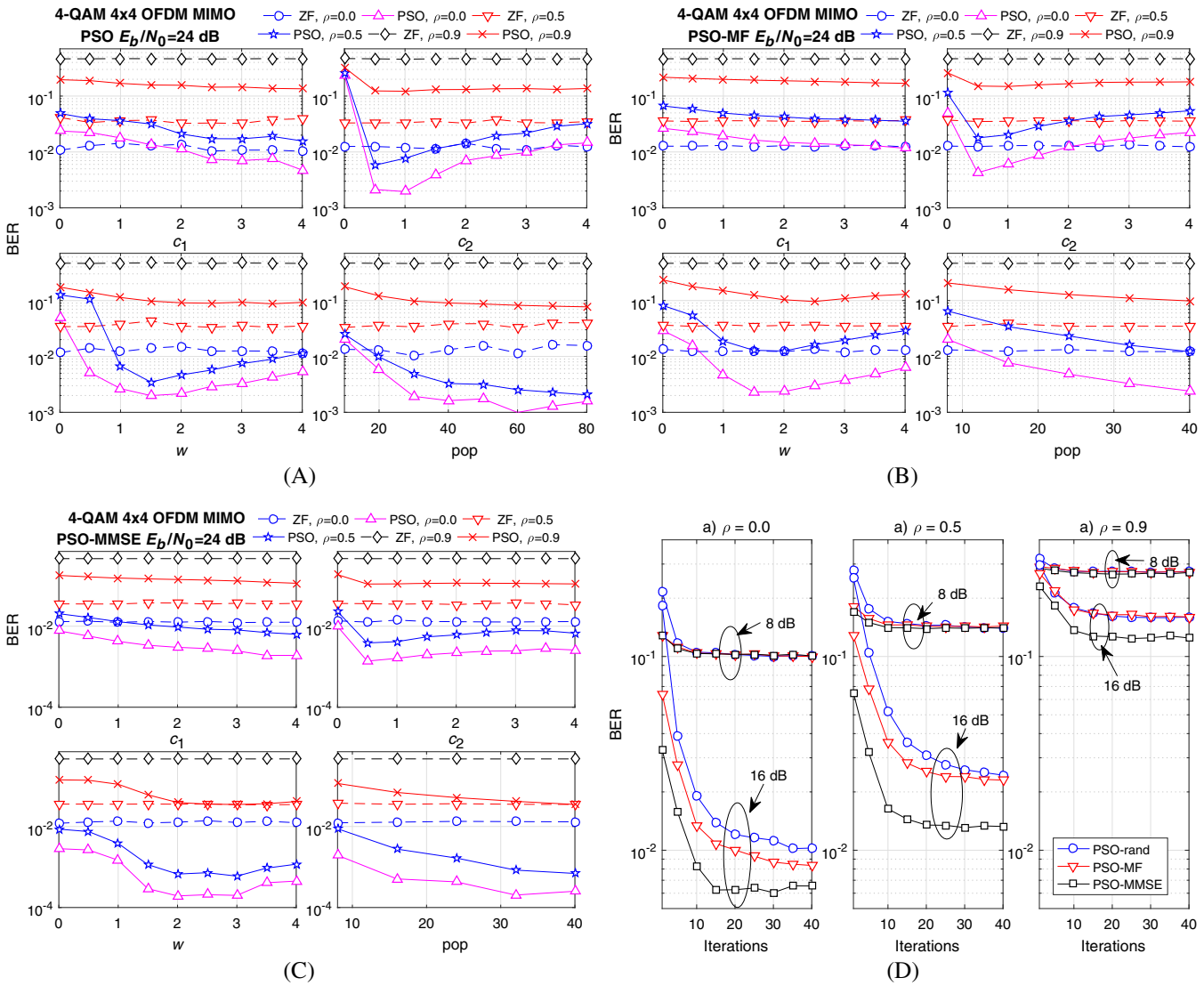

FIGURE 2 Calibration of input parameters values for 4-QAM 4 × 4 MIMO-OFDM PSO detection problem operating under medium-high signal-to-noise ratio and different spatial correlation indexes. A, Calibration: varying parameters and evaluating performance; B, Calibration of input parameter of PSO-MF algorithm; C, Calibration of input parameters considering PSO-MMSE algorithm; D, Convergence analysis for 4-QAM 4 × 4 MIMO-OFDM with PSO detector considering different values of E_b/N_0. BER, bit error rate; MF, matched filter; MIMO, multiple-input–multiple-output; MMSE, minimum mean-square error; OFDM, multiple-input–multiple-output; PSO, particle swarm optimization; ZF, zero forcing

5.2 | Performance analysis

After input parameters calibration, the BER performance of the heuristic and hybrid MIMO-OFDM detectors was numerically obtained. In Figures4A and 4B, the initial solution provided by the MMSE detector is considered. We observe that, as the number of iterations increase, the MMSE solution is refined, and after 15 iterations, the improvement in BER performance becomes marginal for both algorithms DE-MMSE and PSO-MMSE. In Figures 5A and 5B, a similar behavior is observed. We note that the initial point influences the performance of PSO-based detectors: indeed, the PSO-MMSE provides better results in terms of BER than PSO-MF, but this effect is marginal for DE-MF and DE-MMSE, where similar performance is achieved after 15 iterations.

In Figure 6, the performances of linear, heuristic, and hybrid MIMO-OFDM detection approaches are compared. We observe that PSO-MMSE provides the nearest ML performance and that the hybrid approaches provide similar or better approaches than conventional heuristics. For highly correlated scenarios, the overall performance is worsened. For PSO-MMSE, the gain in performance is evident in contrast to other linear and heuristic detectors.

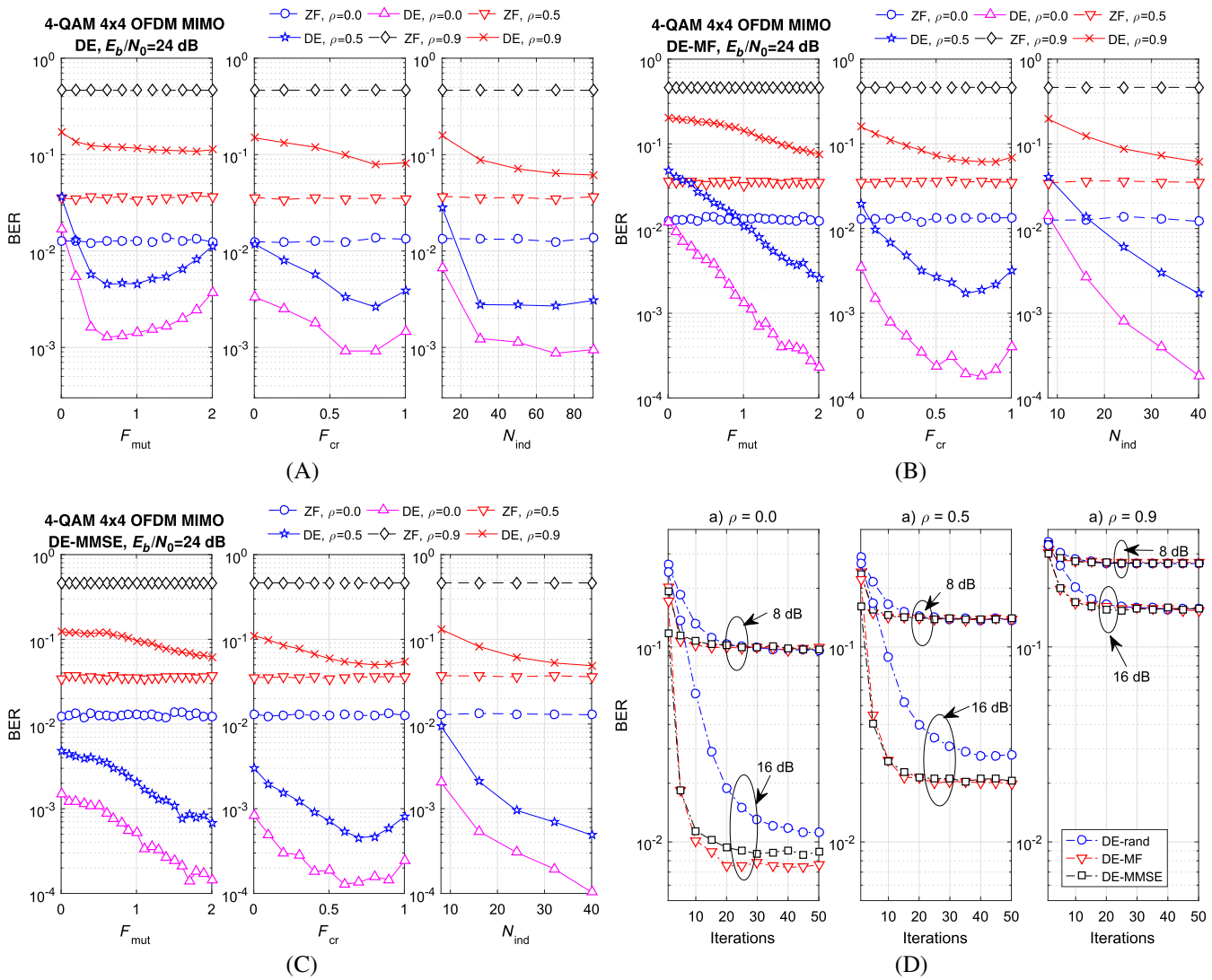

FIGURE 3 Calibration of input parameters of DE heuristic applied to MIMO-OFDM detection for different values of correlation. A, Calibration of input parameters of DE with uniformly random initialization; B, Calibration of input parameters of DE with MF initialization; C, Calibration of input parameters of DE with MMSE initialization; D, Convergence of DE-aided detector for MIMO-OFDM systems for different spatial correlation values. BER, bit error rate; DE, differential evolution; MF, matched filter; MIMO, multiple-input–multiple-output; MMSE, minimum mean-square error; ZF, zero forcing

In general, spatial correlation degrades considerably the performance of all the studied detectors. However, hybrid heuristic-linear MIMO-OFDM detectors are suitable choices for MIMO systems operating under low or even moderate antenna correlation.

5.3 | Complexity analysis

To analyze the complexity of the detection algorithms, the number of FLOPs among real numbers is considered. The FLOPs are described as floating point addition, subtraction, multiplication, or division operations.[22] In this evaluation, Hermitian operator and `if` conditional step were disregarded. In practice, some platforms use hardware random number generators, where an electric circuit provides random numbers generation, and so the FLOPs cost to generate random numbers was also ignored.

Table 4 describes the number of FLOPs needed for the main operations considered herein, whereas in Table 5, the full complexity expressions (Υ) for the analyzed MIMO-OFDM detectors are shown. In Figure 7, the complexity is described considering typical values, ie, $N_{\text{dim}} = 2N_t; N_t = N_r; N_{\text{ind}} = N_{\text{pop}} = 5 \cdot N_{\text{dim}}$ and admitting the number of iterations up to

TABLE 2 Input parameters of particle swarm optimization after calibration, considering $E_b/N_0 = 24$ dB, different initial points and spatial correlation

Parameter	Value
$N_{\text{iter}}^{\text{start}}$	[100; 20]
c_1^{start}	2
c_2^{start}	2
w^{start}	1
$N_{\text{iter}}^{\text{rand}}$	100
c_1^{rand}	4
$c_2^{\text{rand}}(\rho)$	1 (0) 0.5 (0.5) 1 (0.9)
$w^{\text{rand}}(\rho)$	1.5 (0) 1.5 (0.5) 3.5 (0.9)
$N_{\text{iter}}^{\text{MF}}$	$\in [5; 25]$
c_1^{MF}	4
$c_2^{\text{MF}}(\rho)$	0.5 (0) 0.5 (0.5) 1 (0.9)
$w^{\text{MF}}(\rho)$	1.5 (0) 2 (0.5) 2.5 (0.9)
$N_{\text{iter}}^{\text{MMSE}}$	$\in [5; 25]$
$c_1^{\text{MMSE}}(\rho)$	3.5(0) 4(0.5) 4(0.9)
$c_2^{\text{MMSE}}(\rho)$	0.5 (0) 0.5 (0.5) 0.5 (0.9)
$w^{\text{MMSE}}(\rho)$	2 (0) 3 (0.5) 3 (0.9)

TABLE 3 Input parameters of differential evolution algorithm after calibration considering $E_b/N_0 = 24$ dB, different initial points and spatial correlation

Parameter	Value
$N_{\text{gen}}^{\text{start}}$	[100; 20]
$F_{\text{mut}}^{\text{start}}$	1
$F_{\text{cr}}^{\text{start}}$	0.5
$N_{\text{gen}}^{\text{rand}}$	100
$F_{\text{cr}}^{\text{rand}}(\rho)$	0.6 (0) 0.6 (0.5) 0.8 (0.9)
$F_{\text{mut}}^{\text{rand}}(\rho)$	0.6 (0) 0.8 (0.5) 1.8 (0.9)
$N_{\text{gen}}^{\text{MF}}$	$\in [5; 25]$
$F_{\text{mut}}^{\text{MF}}(\rho)$	2 (0) 2 (0.5) 2 (0.9)
$F_{\text{cr}}^{\text{MF}}(\rho)$	0.8 (0) 0.7 (0.5) 0.9 (0.9)
$N_{\text{gen}}^{\text{MMSE}}$	$\in [5; 25]$
$F_{\text{mut}}^{\text{MMSE}}(\rho)$	1.7 (0) 2 (0.5) 2 (0.9)
$F_{\text{cr}}^{\text{MMSE}}(\rho)$	0.6 (0) 0.7 (0.5) 0.8 (0.9)

the convergence obtained previously through simulations, as shown in Figure 2D, Figure 3D for the heuristic algorithms, and for the hybrid algorithm in Figures 4 and 5.

From Table 5, it can be observed that DE algorithm requires more FLOPs than PSO since it evaluates $2N_{\text{pop}}$ times the fitness function per iteration in Equation (16) for individuals and crossover vectors. The complexity between the linear detectors is almost the same, differing from each other by an scalar-matrix multiplication and matrix-matrix sum in Equations (5) and (7). Moreover, observing the hybrid heuristic-linear MIMO-OFDM detector in Figures 4 and 5, the improvement in performance starts to stagnate around 15 iterations, and so $\mathcal{I}_{\text{hyb}} = 15$ has been considered as the number of iterations of the hybrid algorithm to attain the best performance-complexity trade-off.

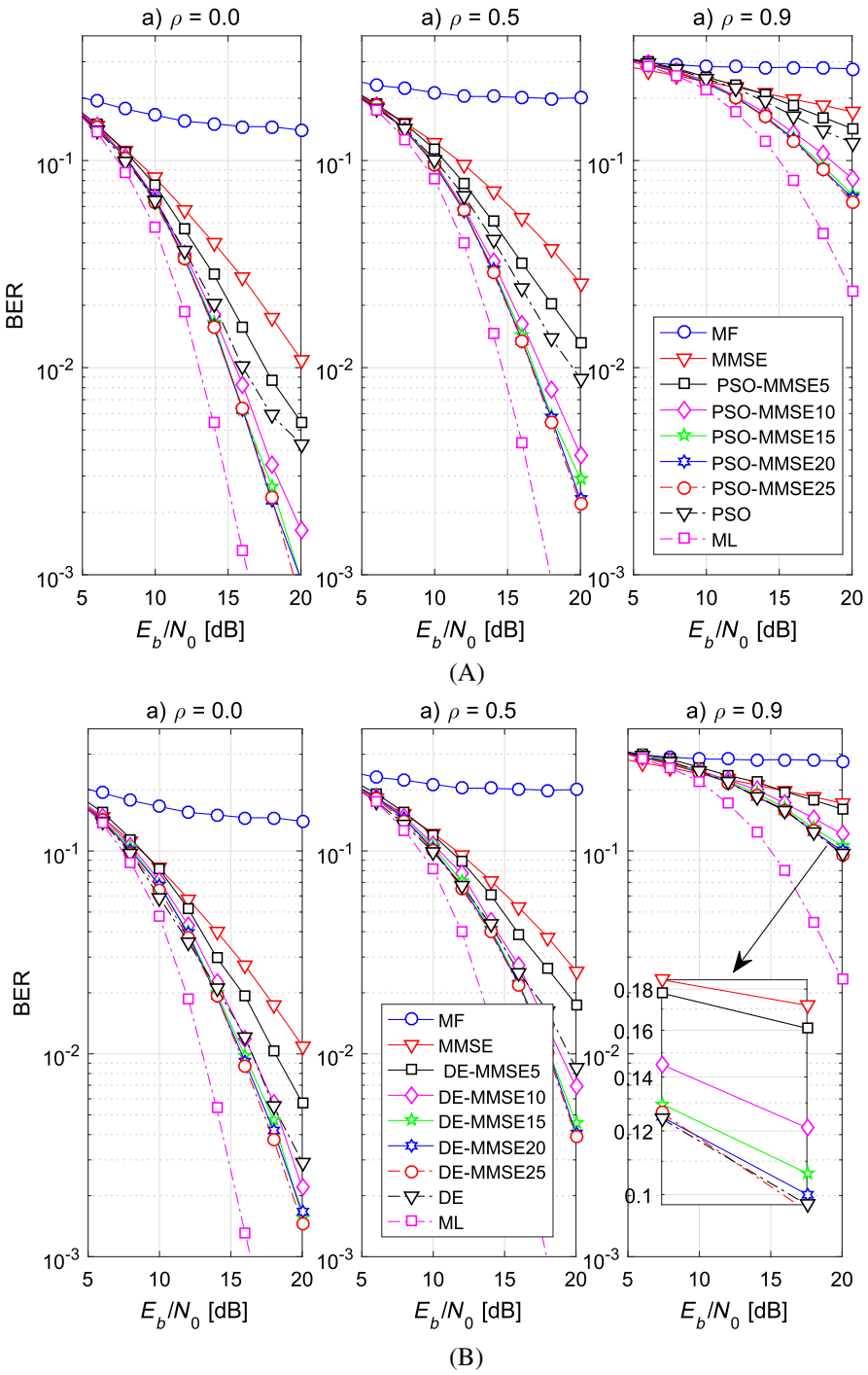

FIGURE 4 Performance of the MMSE-hybrid algorithm considering uniform linear antenna array with different values of E_b/N_0, spatial correlation and increasing number of iterations. A, Performance of hybrid algorithm PSO-MMSE; B, Performance of hybrid algorithm DE-MMSE. BER, bit error rate; DE, differential evolution; MF, matched filter; ML, maximum likelihood; MMSE, minimum mean-square error; PSO, particle swarm optimization

Heuristic detection algorithms produce better BER performance at the cost of an incremental computational complexity compared with linear detectors ZF and MMSE, mainly due to the population/swarm size (around 5 to $10 \cdot N_{\text{dim}}$) and the number of iterations necessary to attain convergence. In order to reduce the complexity, both hybrid linear-heuristic algorithms combing MF/MMSE and evolutionary-heuristic techniques were analyzed. The PSO-MF provides computational complexity near the linear approaches for $N_t = 256$ antennas. PSO-MMSE has similar computational complexity than DE-MF.

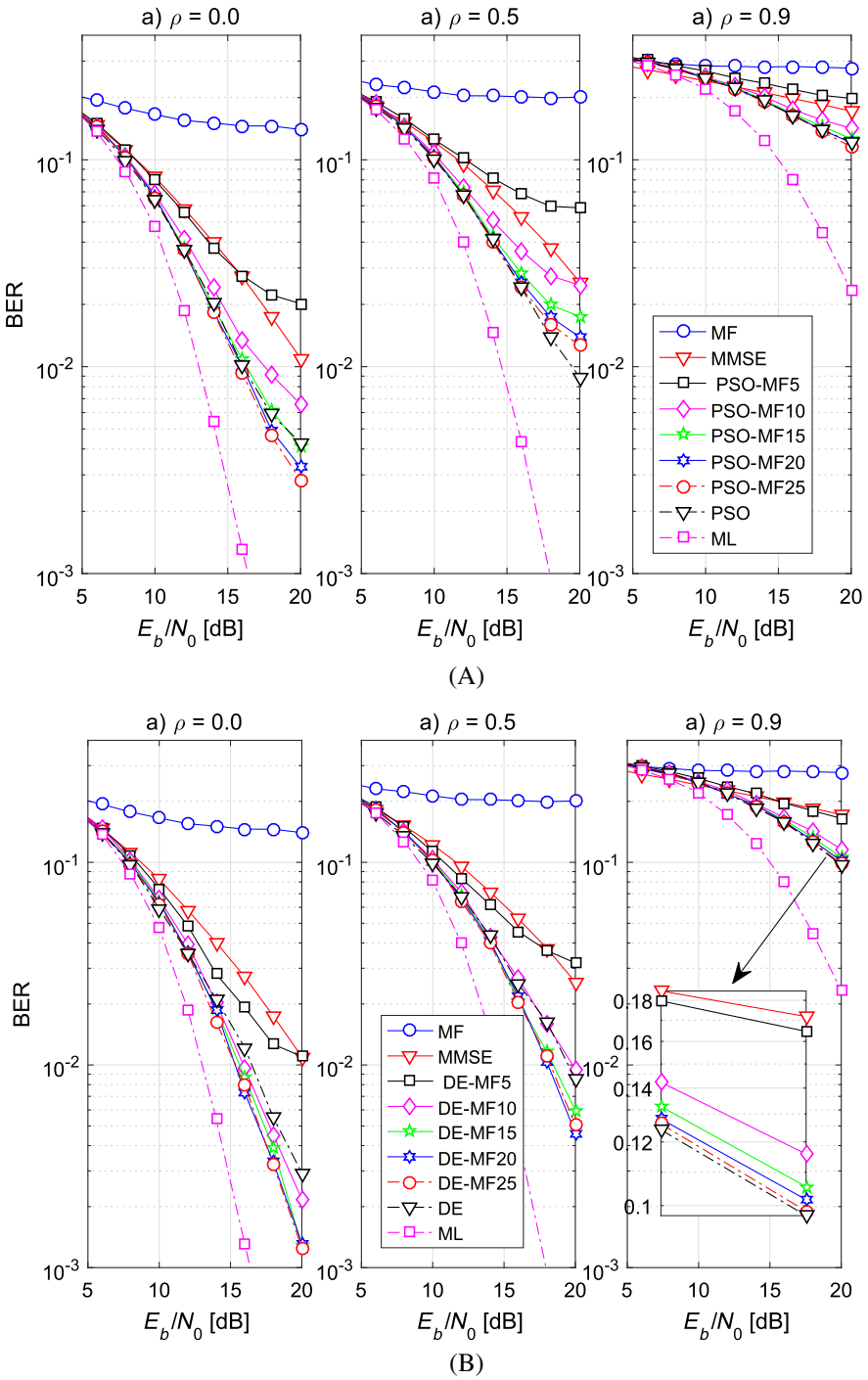

FIGURE 5 Performance of the MF-hybrid algorithm considering uniform linear antenna with different values of E_b/N_0, spatial correlation and increasing number of iterations. A, Performance of hybrid algorithm PSO-MF; B, Performance of hybrid algorithm DE-MF. BER, bit error rate; DE, differential evolution; MF, matched filter; ML, maximum likelihood; MMSE, minimum mean-square error; PSO, particle swarm optimization

Although linear MMSE and heuristic algorithms have slightly more computational complexity than other linear approaches, there is also improvement in BER performance. Moreover, evolutionary heuristics may be more flexible to be implemented in hardware. Parallelization, the possibility to deal with nondifferentiable and nonlinear functions[21] and the possibility to truncate the number of iterations to achieve different performance-complexity trade-offs in scenarios that do not require very low levels of BER, for example, with MF hybrid, may be good choices for real applications.

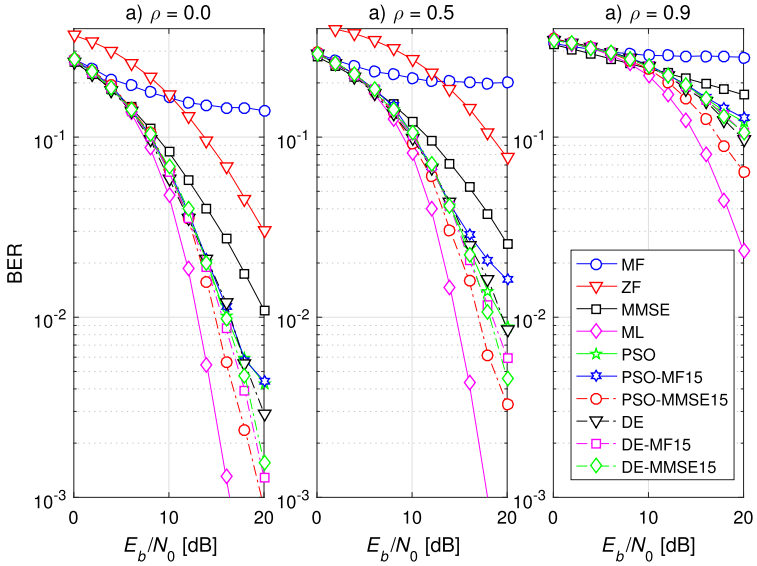

FIGURE 6 Bit-error-rate (BER) performance for 4-QAM 4 × 4 linear array (uniform linear antenna) antennas MIMO-OFDM for different detectors under different values of spatial correlation and signal-to-noise ratio. DE, differential evolution; MF, matched filter; ML, maximum likelihood; MIMO, multiple-input–multiple-output; MMSE, minimum mean-square error; PSO, particle swarm optimization; ZF, zero forcing

TABLE 4 Number of floating points operations (FLOPs), considering vector and matrices $\mathbf{w} \in \mathbb{R}^{q\times 1}, \mathbf{A} \in \mathbb{R}^{m\times q}, \mathbf{B} \in \mathbb{R}^{q\times p}, \mathbf{C} \in \mathbb{R}^{m\times p}, \mathbf{D} \in \mathbb{R}^{q\times q}$

Operation	# FLOPs
Square root $\sqrt{.}$	8
Norm-2, $\sqrt{\mathbf{w}^T\mathbf{w}}$	$2n - 1 + 8$
Matrix-vector multiply **Aw**	$m(2q - 1)$
Matrix-matrix multiply **AB**	$mp(2q - 1)$
Matrix multiply-add **AB+C**	$2mpq$
Matrix inversion with LU factorization of $\mathbf{D}$[23]	$2/3q^3 + 2q^2$

TABLE 5 Number of floating points operations per subcarrier for the multiple-input–multiple-output orthogonal frequency-division multiplexing detectors, with $\underline{\mathbf{H}} \in \mathbb{R}^{2N_r\times 2N_t}, \underline{\mathbf{y}} \in \mathbb{R}^{2N_r\times 1}, N_{\text{dim}} = 2N_t$

Detector	Number of Operations
$\Upsilon_{\text{MF}}(N_t, N_r)$	$2N_t(4N_r - 1)$
$\Upsilon_{\text{ZF}}(N_t, N_r)$	$\frac{16}{3}N_t^3 + 4N_t^2 + 32N_t^2N_r + 4N_tN_r - 2N_t$
$\Upsilon_{\text{MMSE}}(N_t, N_r)$	$\frac{16}{3}N_t^3 + 8N_t^2 + 32N_t^2N_r + 4N_tN_r$
$\Upsilon_{\text{PSO}}(N_t, N_r, N_{\text{pop}}, \mathcal{I})$	$N_{\text{pop}}\mathcal{I}(8N_tN_r + 20N_t + 4N_r + 7)$
$\Upsilon_{\text{DE}}(N_t, N_r, N_{\text{ind}}, \mathcal{I})$	$N_{\text{ind}}\mathcal{I}(16N_tN_r + 12N_t + 8N_r + 14)$
$\Upsilon_{\text{PSO-MMSE}}(N_t, N_r, N_{\text{pop}}, \mathcal{I}_{\text{hyb}})$	$\Upsilon_{\text{PSO}}(N_t, N_r, N_{\text{pop}}, \mathcal{I}_{\text{hyb}}) + \Upsilon_{\text{MMSE}}(N_t, N_r)$
$\Upsilon_{\text{DE-MMSE}}(N_t, N_r, N_{\text{ind}}, \mathcal{I}_{\text{hyb}})$	$\Upsilon_{\text{DE}}(N_t, N_r, N_{\text{ind}}, \mathcal{I}_{\text{hyb}}) + \Upsilon_{\text{MMSE}}(N_t, N_r)$
$\Upsilon_{\text{PSO-MF}}(N_t, N_r, N_{\text{pop}}, \mathcal{I}_{\text{hyb}})$	$\Upsilon_{\text{PSO}}(N_t, N_r, 1N_{\text{pop}}, \mathcal{I}_{\text{hyb}}) + \Upsilon_{\text{MF}}(N_t, N_r)$
$\Upsilon_{\text{DE-MF}}(N_t, N_r, N_{\text{ind}}, \mathcal{I}_{\text{hyb}})$	$\Upsilon_{\text{DE}}(N_t, N_r, N_{\text{ind}}, \mathcal{I}_{\text{hyb}}) + \Upsilon_{\text{MF}}(N_t, N_r)$
$\Upsilon_{\text{ML}}(N_t, N_r, \mathcal{M})$	$\mathcal{M}^{2N_t}(8N_tN_r + 4N_r + 7)$

$\mathcal{I}$: number of iterations for conventional algorithms; $\mathcal{I}_{\text{hyb}}$: number of iterations for the hybrid algorithm

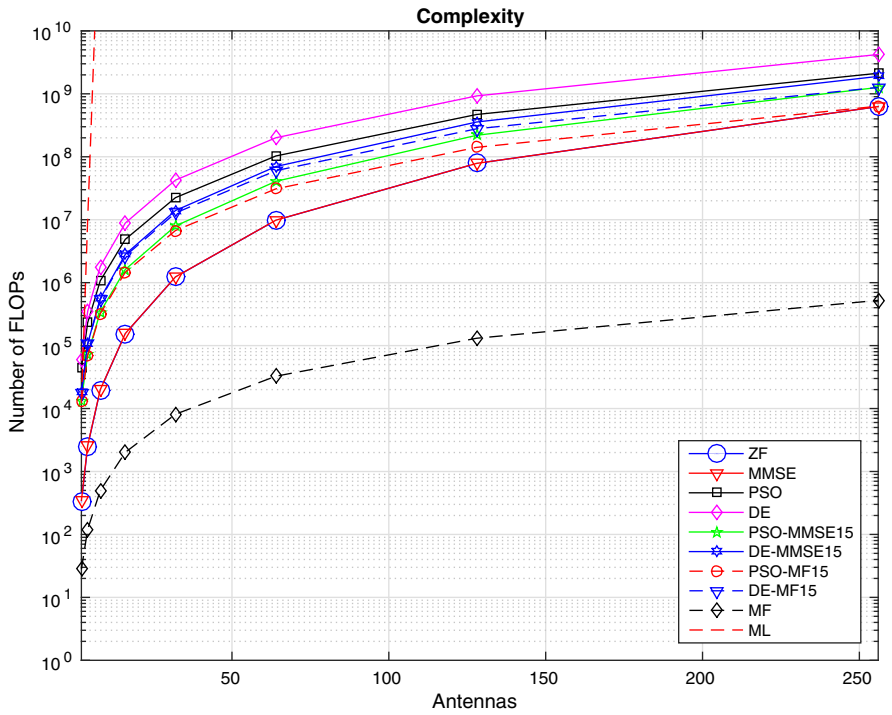

FIGURE 7 MIMO-OFDM complexity considering an increasing number of antennas for linear, heuristic, and hybrid detectors in a point-to-point scenario; $N_t = N_r, N_{\text{dim}} = 2N_t, N_{\text{pop}} = N_{\text{ind}} = 5 \cdot N_{\text{dim}}, \mathcal{I} = 50, \mathcal{I}_{\text{hyb}} = 15$. DE, differential evolution; FLOPs, floating points operations; MF, matched filter; MIMO, multiple-input–multiple-output; ML, maximum likelihood; MMSE, minimum mean-square error; OFDM, orthogonal frequency-division multiplexing; PSO, particle swarm optimization; ZF, zero forcing

6 | CONCLUSIONS

Extensive simulations were deployed and suitable evolutionary heuristic PSO and DE input parameter calibration were chosen numerically aiming to find suitably and of practical interest solutions for the MIMO-OFDM detection problem. Hybrid approaches considering MF and MMSE as initial solutions have been also considered, where the linear initial solution is improved while the number of iterations of heuristic algorithms reduced.

Among the analyzed MIMO-OFDM detectors, the hybrid PSO-MMSE provided the near-ML performance for the considered scenarios, ie, $\rho = 0$ (uncorrelated), $\rho = 5$, and $\rho = 0.9$. However, the BER performance has demonstrated to be sensible to the initialization. For PSO-MF, the performance was similar to conventional PSO, with the advantage of reduced number of iterations until convergence. For DE, almost the same BER performance was achieved using MF and MMSE.

In terms of complexity, ZF and MMSE require almost the same number of FLOPs, although MMSE requires some statistical knowledge of the channel condition. Among the heuristic detectors, DE requires more FLOPs in comparison with the PSO, mainly because the number of fitness function evaluations is higher, since in DE, it is calculated for the $\boldsymbol{\iota}_k$ and $\boldsymbol{\psi}_k, k = 1, \ldots, N_{\text{ind}}$ per iteration of the algorithm, in comparison to N_{pop} per iteration with PSO (in the simulations, $N_{\text{pop}} = N_{\text{ind}}$).

To improve the complexity-performance trade-off, this work proposed and evaluated two linear-heuristic hybrid algorithms suitable to solve the MIMO-OFDM detection problem. Starting from a solution obtained from the MMSE and MF linear detectors, the DE and PSO heuristics were executed in order to further improve the BER performance while they were able to improve substantially the performance-complexity trade-off even under low and medium spatial correlation scenarios. Numerical simulations have demonstrated that, with both hybrid algorithms, the number of iterations required to the convergence is reduced, achieving similar and slightly better performance in the DE and PSO-hybrid detectors when compared to the conventional DE and PSO.

ACKNOWLEDGEMENTS

This work was supported in part by the National Council for Scientific and Technological Development (CNPq) of Brazil under grants 130464/2015-5 (scholarship) and 304066/2015-0 (research), in part the by Araucaria Foundation, PR, under grant 302/2012 (research), and by the Londrina State University - Paraná State Government, Brazil.

ORCID


Taufik Abrão http://orcid.org/0000-0001-8678-2805

REFERENCES

1. Saeed MA, Ali BM, Habaebi MH. Performance evaluation of OFDM schemes over multipath fading channels. Paper presented at: 9th Asia-Pacific Conference on Communication; 2003; Penang, Malaysia.
2. Hampton JR. *Introduction to MIMO Communications*. New York, NY: Cambridge University Press; 2014.
3. Goldsmith A. *Wireless Communications*. New York, NY: Cambridge University Press; 2005.
4. Tse DNC, Viswanath P, Zheng L. Diversity-multiplexing tradeoff in multiple-access channels. *IEEE Trans Inf Theory*. 2004;50(9):1859-1874.
5. Choi J, Bai L. *Low Complexity MIMO Detection*. 1st ed. Berlin, Germany: Springer-Verlag; 2012.
6. Kobayashi RT, Ciriaco F, Abrão T. Efficient near-optimum detectors for large MIMO systems under correlated channels. *Wirel Pers Commun*. 2015;83(2):1287-1311. https://doi.org/10.1007/s11277-015-2450-y
7. Marzetta T, Larsson EG, Yang H, Ngo HQ. *Fundamentals of Massive MIMO*. New York, NY: Cambridge University Press; 2016.
8. Chizhik D, Ling J, Wolniansky PW, Valenzuela RA, Costa N, Huber K. Multiple-input-multiple-output measurements and modeling in Manhattan. *IEEE J Sel Areas Commun*. 2003;21(3):321-331.
9. Guerra DWM, Fukuda RM, Kobayashi RT, Abrão T. Linear detection analysis in MIMO-OFDM with spatial correlation. Paper presented at: 2016 12th IEEE International Conference on Industry Applications (INDUSCON); 2016; Curitiba, Brazil.
10. Khan AA, Naeem M, Bashir S, Shah SI. Optimized detection in multi-antenna system using particle swarm algorithm. *World Acad Sci Eng Tech*. 2008;2(2):296-300.
11. Trimeche A, Bouhlel A, Sakly A, Mtibaa A. The particle swarm optimization (PSO) for symbol detection in MIMO-OFDM system. *J Inf Secur Res*. 2013;4(1):38-45.
12. Seyman MN, Taspinar N. Symbol detection using the differential evolution algorithm in MIMO-OFDM systems. *Turkish J Electr Eng Comput Sci*. 2013;21:373-380.
13. Khan AA, Naeem M, Shah SI. A particle swarm algorithm for symbols detection in wideband spatial multiplexing systems. In: Proceedings of the 9th Annual Conference on Genetic and Evolutionary Computation (GECCO '07); 2007; New York, NY. http://doi.acm.org/10.1145/1276958.1276968
14. Filho JCM, De Souza RN, Abrão T. Ant colony input parameters optimization for multiuser detection in DS/CDMA systems. *Expert Syst Appl*. 2012;39(17):12876-12884.
15. Cho YS, Kim J, Yang WY, Kang CG. *MIMO-OFDM Wireless Communications with MATLAB*. Singapore: Wiley Publishing; 2010.
16. Paulraj A, Nabar R, Gore D. *Introduction to Space-Time Wireless Communications*. Cambridge, UK: Cambridge University Press; 2003.
17. Van Zelst A, Hammerschmidt JS. A single coefficient spatial correlation model for multiple-input multiple-output (MIMO) radio channels. Paper presented at: 27th General Assembly of the International Union of Radio Science (URSI); 2002; Maastricht, The Netherlands.
18. Cheng S, Shi Y. normalized population diversity in particle swarm optimization. In: *Advances in Swarm Intelligence*. Berlin, Germany: Springer; 2011:38-45.
19. Shi Y, Eberhart R. A modified particle swarm optimizer. Paper presented at: 1998 IEEE International Conference on Evolutionary Computation Proceedings. IEEE World Congress on Computational Intelligence (Cat. No.98TH8360); 1998; Anchorage, AK.
20. Shi Y, Eberhart RC. Parameter selection in particle swarm optimization. In: Porto VW, Saravanan N, Waagen D, Eiben AE, eds. *Evolutionary Programming VII*. Berlin, Germany: Springer; 1998:591-600.
21. Storn R, Price K. Differential evolution – a simple and efficient heuristic for global optimization over continuous spaces. *J Glob Optim*. 1997;11(4):341-359. https://doi.org/10.1023/A:1008202821328
22. Golub GH, Van Loan CF. *Matrix Computations*. 4th ed. Baltimore, MD: Johns Hopkins University Press; 2013.
23. Boyd S, Vandenberghe L. Numerical linear algebra background. http://www.seas.ucla.edu/~vandenbe/ee236b/lectures/num-lin-alg.pdf. Accessed on April 25, 2018.

How to cite this article: Fukuda RM, Guerra DWM, Kobayashi RT, Abrão T. DE/PSO-aided hybrid linear detectors for MIMO-OFDM systems under correlated arrays. *Trans Emerging Tel Tech*. 2018;e3495. https://doi.org/10.1002/ett.3495

A.3 *Linear, Quadratic and Semidefinite Programming Massive MIMO Detectors: Reliability and Complexity*

Título:	*Linear, Quadratic and Semidefinite Programming Massive MIMO Detectors: Reliability and Complexity*
Autores:	**Rafael Masashi Fukuda** e Taufik Abrão
Revista:	IEEE Access
Status:	Aceito (disponível em *early access*)
DOI:	10.1109/ACCESS.2019.2902521
Qualis:	A2 Qualis-Eng.IV CAPES

No terceiro trabalho, o problema da detecção em sistemas M-MIMO foi estudado utilizando algoritmos de otimização convexa. Na primeira parte, as formulações LPℓ1, LP$\ell\infty$, SDP e QP foram simuladas em um cenário realista composto de erro na estimativa do canal, correlação espacial, alterações no carregamento do sistema, e altas ordens de modulação QAM. Na segunda parte, os algoritmos projetados são aplicados para a formulação QP. A complexidade computacional depende do número de iterações N_{iter} e do número de execuções da busca em linha m_{iter}. A utilização dos algoritmos projetados é recomendada em cenários onde $N_{\text{iter}} m_{\text{iter}} < K$ para a complexidade computacional ser menor que a complexidade dos detectores lineares. Através de simulações numéricas, constatou-se que a complexidade do DSPG foi menor para cenários $M = 256, K = 64$, onde o número de FLOPs para o DSPG se mostrou menor que o MMSE.

This article has been accepted for publication in a future issue of this journal, but has not been fully edited. Content may change prior to final publication. Citation information: DOI 10.1109/ACCESS.2019.2902521, IEEE Access

Date of publication xxxx 00, 0000, date of current version xxxx 00, 0000.

Digital Object Identifier 10.1109/ACCESS.2017.DOI

Linear, Quadratic and Semidefinite Programming Massive MIMO Detectors: Reliability and Complexity

RAFAEL MASASHI FUKUDA[1], TAUFIK ABRAO (SENIOR MEMBER, IEEE)[1]
[1]Electrical Engineering Department, State University of Londrina, Parana, Brazil. Email: rafaelmasashi@gmail.com; taufik@uel.br

Corresponding author: Taufik Abrao (e-mail: taufik@uel.br).

This work was supported in part by the National Council for Scientific and Technological Development (CNPq) of Brazil under Grant 304066/2015-0; by the State University of Londrina (UEL), and by the State Government of Parana.

ABSTRACT One of the downsides of the massive Multiple Input Multiple Output (M-MIMO) system is its computational complexity. Considering that techniques and different algorithms proposed in the literature applied to conventional MIMO may be not well suited or readily applicable to M-MIMO systems, in this work, the application of different formulations inside the convex optimization framework are investigated. This work is divided in two parts. In the first part, Linear programming (LP), quadratic programming (QP) and Semidefinite Programming (SDP) are explored in an M-MIMO environment with high order modulation and under realistic channel conditions, i.e., considering spatial correlation, error in the channel estimation, as well as different system loading. The bit-error-rate (BER) is evaluated numerically through Monte Carlo simulations (MCS). In the second part, algorithms to solve the QP formulation are explored and computational complexity in terms of floating-point operations (flops) are compared with linear detectors. Those algorithms have interesting aspects when applied to our specific problem (M-MIMO detection formulated as QP), such as the exploitation of the structure of the problem (*simple constraints*) and the improvement of the rate of convergence due to the well-conditioned Gram matrix (channel hardening). The number of iterations is higher when the number of users K becomes similar to the number of base station antennas M (i.e., $K \approx M$) than the case $K \ll M$; the number of iterations increases slowly as the number of users K and base station antennas M increases while keeping a low system loading. The QP with projected algorithms presented better performance than MMSE when $K \approx M$, and promising computational complexity for scenarios with increasing K and low system loading.

INDEX TERMS Massive MIMO communication, Low-complexity Detectors, Convex Optimization, Linear Programming, Quadratic Programming, Semidefinite Programming.

I. INTRODUCTION

MULTIPLE input multiple output (MIMO) system with large number of antennas, often called Massive MIMO (M-MIMO), or even large-scale MIMO (LS-MIMO), is a promising technology where the great number of antennas provides several advantages, such as improved energy and spectrum efficiency, disappearance of thermal and fading noise effects [1], [2], to name a few.

However, among the benefits, new problems arise. One of the challenges in M-MIMO is the computational complexity required to process the information from the great number of antennas [2], [3]. This problem is even more accentuated in the case of detection which is known for being a non-polynomial (NP-hard) problem with optimal brute force solution given by the maximum likelihood (ML) detector that is unfeasible even for a not so high number of antennas, users and modulation order combinations.

Although there are many techniques applied for *conventional* MIMO, such as linear detectors with matched filter (MF), zero forcing (ZF), minimum mean square error (MMSE), tree-search based algorithms including sphere decoding (SD), heuristics, detectors-based on convex optimization approach, and the possibility to combine with transmit preprocessing techniques, e.g. precoding and cod-

This article has been accepted for publication in a future issue of this journal, but has not been fully edited. Content may change prior to final publication. Citation information: DOI 10.1109/ACCESS.2019.2902521, IEEE Access

ing to further improve the performance, detection is still an active field because most of the available algorithms apply to conventional MIMO systems and may not be well suited or readily applicable for M-MIMO systems (such as ML and SD) [3]. Hence, new and innovative detection algorithms must explore some of the specific features of M-MIMO structure.

In a multiuser M-MIMO scenario with low number of users and large number of antennas, linear detectors such as ZF and MF are known for providing near-optimal performance [4]. Some algorithms tries to explore the channel hardening feature of the M-MIMO system that results in a well-conditioned Gram matrix $\mathbf{H}^H\mathbf{H}$ [4], [5] approximating the matrix inversion operation using techniques such as Neumann series [6], the Gauss-Seidel algorithm [7], and variations considering Newton algorithm such as [8], [9] and Newton-Schultz [10]. However, in those scenarios, a very small number of users K limits the potential gains in spectral efficiency since the capacity is proportional to the minimum between K and base station antennas M, i.e., $\min(K, M)$ [5] and, as the number of users increases, as in ultra-crowded heterogeneous machine type communication (mTC) and enhanced mobile broadband (eMBB) scenarios, the reliability and the performance of such detectors deteriorate [8], [11].

Another strategy to avoid the ML solution is the use of convex optimization algorithms, such as linear programming (LP) [12], [13], quadratic programming (QP) [14]–[16] and semidefinite programming (SDP) [17]–[20]. With the relaxation of some constraints, detectors can be formulated as convex optimization problems taking advantage of its solid theory and extensive literature (e.g., [21]–[23]) and making use of well-known polynomial-time algorithms [24], many of them conceived and applied to solve large scale problems [25]–[27].

Regard LP, a detection scheme is investigated considering the ℓ_1-norm in conventional MIMO scenario with 8×8 antennas in [12]. The detection problem is reformulated first as a mixed integer linear programming (MILP) and after, the discrete constraint is relaxed and the problem is cast into LP, which can be solved using interior point methods.

In [15], authors use a QP detector in an Orthogonal Frequency Division Multiplexing (OFDM) context aiming to reduce the interference among subcarriers, while in [14], authors compare a QP and two other modified QP detectors with heuristics LAS and RTS (heuristics are not the focus of our paper) in an M-MIMO context. Although authors consider spatial correlation and different modulation orders, they do not explore error in the channel estimation and different system loading scenario.

The SDP detector is well-known in the literature and provides good performance results with an increased computational cost. The formulation in [17] is simple compared with other approaches [20]; it was tested for 16×16 MIMO system [17], for a 40×40 system [18], and for 128×128 in [19], however only considering a symmetric system with same number of antennas.

In order to solve LP, QP and SDP, interior-point algorithms can be applied [22], [23]. Particularly, the Mehrotra's Predictor Corrector (MPC) is the usual choice, and has been implemented in commands *linprog, lsqlin* in Matlab [28]–[30] to solve LP and QP, and in SDP3 to solve SDP [31]. Generally, interior-point methods involve the solution of a linear system of equations, hence have similar computational complexity order compared to linear detectors [14], and even greater in the case of SDP [18], [32].

General purpose solvers might be computationally expensive [27]; some algorithms are created considering the structure of the formulated problem, for example, the Two Metric Projection (TMP) [33] proposed to solve problems with *simple* constraints, such as nonnegative and box constraints [25]. With different scaling matrices, the TMP can become a Projected Gradient (PG) [26] or Projected Newton (PN) [25] algorithm (which are referred throughout the text as projected algorithms). TMP is capable to solve constrained problems similarly as its unconstrained counterpart and has advantages over manifold suboptimization and active set algorithms that require at least the number of constraints to converge [25]. Some application of those projected algorithms include large-scale problems arising in the machine learning field [26], quasi-Newton variations applied to image deblurring examples [27] and PG applied in beamforming [34].

This work is structured in two parts: in the first, the performance of different detectors formulated as optimization problems LP, QP and SDP in an M-MIMO context are studied in a variety of scenarios. In the second part, observing that the QP formulation presents the least number of variables, projected algorithms are applied to solve the QP formulation and its characteristics observed through numerical simulations.

The *contributions* of this work are threefold. **a**) An M-MIMO detector based on LP formulation is proposed using ℓ_∞-norm (LP$\ell\infty$), and its performance-complexity trade-off is compared with LP ℓ_1-norm (originally proposed in [12] for conventional MIMO systems), QP and SDP-based detectors. Those detectors are considered in the new large scale MIMO context operating under realistic scenarios composed by channel correlation, error in the channel state information (CSI) estimation, and different number of users, including ($K \ll M$) and crowded scenarios ($K \approx M$), and also under different modulation orders. **b**) In the second part of the work, we focus on the application of projected algorithms to solve specifically the QP due to its reduced problem size compared with LP and SDP formulations and suitable performance. We characterize the application of solvers for QP and unveils the influence of the condition number of the Gram matrix (channel hardening effect) on the rate of convergence through numerical simulations. **c**) We have characterized both the convergence and complexity-performance trade-off of the proposed efficient M-MIMO detectors compared with the linear detectors under different

This article has been accepted for publication in a future issue of this journal, but has not been fully edited. Content may change prior to final publication. Citation information: DOI 10.1109/ACCESS.2019.2902521, IEEE Access

system loading.

Our work differs from others presented in the literature; for instance, in [35], the Newton's Method (NM) is applied to LS-MIMO detection considering an optimization problem formulation where the constraints are discarded, hence solving an *unconstrained* problem. Herein, we use TMP and variations including PN, an algorithm adapted to solve *constrained* problems. In [8]–[10], NM and Newton-Schultz iterative algorithms are applied to M-MIMO detection problems in order to approximate the inverse of the channel matrix; however, differently from these approaches, we focus on the solution of an optimization problem.

The remainder of this paper is organized as follows. In section II the system model is described. Mathematical formulation of LP$\ell 1$, LP$\ell\infty$, QP, SDP-based M-MIMO detectors are presented in section III. Specific algorithms (solvers) applied to solve the optimization formulations LP, QP and SDP are detailed in section IV. Simulation results are divided in two parts. In the first part, the performance of the detectors are analyzed in subsection V-A, while the characterization and performance of projected algorithms are presented in subsection V-B. Computational complexity are analyzed in section VI. Final remarks and conclusions are offered in section VII.

Notation: bold lower case and bold upper case letters $\mathbf{a}$,$\mathbf{A}$ represent column vectors and matrices, respectively. The ith element of vector is written in italic a^i, bold numbers denote a vector of the number (for example $\mathbf{3} = [3 \dots 3]^T$), and $\mathbf{I}$ is the identity matrix.

II. UL M-MIMO SYSTEM MODEL

Considering a real-valued representation of an uplink (UL) M-MIMO system operating in multiplexing mode with single-antenna multiuser transmitters given by:

$$\mathbf{y} = \mathbf{H}\mathbf{x} + \mathbf{z}, \tag{1}$$

where $\mathbf{y}$ and $\mathbf{z} \in \mathbb{R}^{2M}, \mathbf{x} \in \mathbb{R}^{2K}$ and $\mathbf{H} \in \mathbb{R}^{2M \times 2K}$ represent the received signal, additive noise with variance σ_z^2, transmitted information and channel matrix, respectively; K represent number of user equipments (UEs), and M is the number of base station (BS) antennas.

In real applications, the separation between antennas can be smaller than half of the wavelength of the signal and spatial antenna correlation may occur [36]. Here we consider a uniform linear array (ULA) and the Kronecker model [36]; the correlated channel matrix is given by

$$\mathbf{H} = \sqrt{\mathbf{R}_M}\underline{\mathbf{H}}\sqrt{\mathbf{R}_K}, \tag{2}$$

where $\underline{\mathbf{H}}$, $\mathbf{R}_M$ and $\mathbf{R}_K$ represent the small-scale fading matrix with independent and identically distributed (iid) entries, the correlation matrices of the BS and UE, respectively. In the multiuser scenario considered, the Toeplitz symmetric matrix $\mathbf{R}_M$ is given by [37]

$$\mathbf{R}_M = \begin{bmatrix} 1 & \dots & \rho^{(M-1)^2} \\ \vdots & \ddots & \vdots \\ \rho^{(M-1)^2} & \dots & 1 \end{bmatrix}, \tag{3}$$

where $\rho \in [0, 1]$ is the correlation factor and here $\mathbf{R}_K = \mathbf{I}$, because users are autonomous and far from each other and, hence, not spatially correlated. Note that inside an uncorrelated scenario, $\mathbf{H} = \underline{\mathbf{H}}$.

Moreover, errors in the channel estimation are also considered as [38]

$$\widetilde{\mathbf{H}} = \sqrt{1-\tau^2}\mathbf{H} + \tau\mathbf{N}, \tag{4}$$

where $\mathbf{N} \sim \mathcal{N}(0, 1)$ and $\tau \in [0, 1]$ is the channel estimation quality parameter; for instance, $\tau = 0$ represents perfect knowledge of CSI, $\tau = 0.1$ means deviation of 10% in average from the perfect channel estimation.

III. M-MIMO DETECTORS

In order to recover the transmitted information, the ML detector denoted as the optimization problem

$$\begin{aligned} \underset{\mathbf{x}}{\text{minimize}} \quad & \|\mathbf{y} - \mathbf{H}\mathbf{x}\|_p^2 \\ \text{s.t.} \quad & \mathbf{x} \in \mathcal{B} \end{aligned} \tag{5}$$

can be applied. The symbol $\mathcal{B}$ is related to the digital modulation and represents the set of constellation symbols (for a numerical example, 16-QAM has $\mathcal{B} = \{\pm 1; \pm 3\}$ in the equivalent real-valued representation) and p denotes the norm.

A. QUADRATIC PROGRAMMING

Equation (5) is an integer programming problem; in order to solve it, the usual approach (e.g. [12], [15], [17]) is to relax the integer constraint into a bound constraint considering $\mathbf{x}$ a continuous variable. This results in a QP with linear (affine) inequalities

$$\begin{aligned} \underset{\mathbf{x}}{\text{minimize}} \quad & \|\mathbf{y} - \mathbf{H}\mathbf{x}\|_p^2 \\ \text{s.t.} \quad & \mathbf{b}_1 \leq \mathbf{x} \leq \mathbf{b}_2, \end{aligned} \tag{6}$$

which, opening the quadratic term of the objective function and reorganizing the constraints, becomes the problem

$$\begin{aligned} \underset{\mathbf{x}}{\text{minimize}} \quad & \mathbf{x}^T\mathbf{H}^T\mathbf{H}\mathbf{x} - 2\mathbf{y}^T\mathbf{H}\mathbf{x} \\ \text{s.t.} \quad & \begin{bmatrix} \mathbf{I} \\ -\mathbf{I} \end{bmatrix} \mathbf{x} \leq \begin{bmatrix} \mathbf{b}_2 \\ -\mathbf{b}_1 \end{bmatrix} \end{aligned} \tag{7}$$

where the term $\mathbf{y}^T\mathbf{y}$ is omitted from the objective function because it does not change the optimal point, $\mathbf{b}_1 \in \mathbb{R}^{2K}$ and $\mathbf{b}_2 \in \mathbb{R}^{2K}$ are vectors of the lower and upper values of the set $\mathcal{B}$ with $\mathbf{b}_1 \leq \mathbf{b}_2$ (for example in 16-QAM, $\mathbf{b}_1 = -\mathbf{3}$ and $\mathbf{b}_2 = \mathbf{3}$). The problem in (6) is a QP, and can also be called constrained least squares (CLS) [21] problem or box constrained QP (BCQP) [39]. Problem (6) is the

This article has been accepted for publication in a future issue of this journal, but has not been fully edited. Content may change prior to final publication. Citation information: DOI 10.1109/ACCESS.2019.2902521, IEEE Access

minimization of a quadratic function of $\mathbf{x}$ with Hessian in the form of a symmetric and semidefinite positive Gram[1] matrix $\mathbf{H}^T\mathbf{H}$ over a convex set (i.e., a polyhedron, which is the intersection of a finite number of halfspaces and hyperplanes), and hence, constitutes a convex optimization problem that can be solved using well-known algorithms. Notice that when the Hessian is indefinite, the problem is nonconvex[2] and can have stationary points and/or local minima [23], [39], [41].

B. LINEAR PROGRAMMING

Observing that the norm operator is always nonnegative and minimize the norm is equivalent to minimize the square of the norm [21], the optimization problem (6) can be equivalently expressed as

$$\begin{aligned} \underset{\mathbf{x}}{\text{minimize}} \quad & \|\mathbf{y}-\mathbf{H}\mathbf{x}\|_p \\ \text{s.t.} \quad & \mathbf{b}_1 \leq \mathbf{x} \leq \mathbf{b}_2. \end{aligned} \tag{8}$$

The problem (8) can be recast as LP in two different ways depending on the norm, namely sum of absolute residuals approximation for ℓ_1 norm ($p=1$) and Chebyshev approximation for ℓ_∞ norm ($p=\infty$) [21].

1) LP with ℓ_1-norm

The detection problem (8) can be expressed in the LP form [12]

$$\begin{aligned} \underset{\mathbf{x},\mathbf{t}}{\text{minimize}} \quad & \mathbf{1}^T\mathbf{t} \\ \text{s.t.} \quad & -\mathbf{t} \leq \mathbf{y}-\mathbf{H}\mathbf{x} \leq \mathbf{t} \\ & \mathbf{b}_1 \leq \mathbf{x} \leq \mathbf{b}_2, \end{aligned} \tag{9}$$

where variables in the vector $\mathbf{t} \in \mathbb{R}^{2M}$ are the new optimization variables, jointly with the original variables $\mathbf{x}$.

Many solvers accept LP problems in a specific format such as equality or inequality form. Redefining variables, problem (9) can be expressed in the LP *standard inequality form*

$$\begin{aligned} \underset{\mathbf{x}_{\ell_1}}{\text{minimize}} \quad & \mathbf{c}_{\ell_1}^T\mathbf{x}_{\ell_1} \\ \text{s.t.} \quad & \mathbf{A}_{\ell_1}\mathbf{x}_{\ell_1} \leq \mathbf{b}, \end{aligned} \tag{10}$$

where

$$\mathbf{c}_{\ell_1} = \begin{bmatrix}\mathbf{0}\\ \mathbf{1}\end{bmatrix}, \mathbf{A}_{\ell_1} = \begin{bmatrix}\mathbf{H} & -\mathbf{I}\\ -\mathbf{H} & -\mathbf{I}\\ \mathbf{I} & \mathbf{0}\\ -\mathbf{I} & \mathbf{0}\end{bmatrix}, \mathbf{x}_{\ell_1} = \begin{bmatrix}\mathbf{x}\\ \mathbf{t}\end{bmatrix}, \mathbf{b} = \begin{bmatrix}\mathbf{y}\\ -\mathbf{y}\\ \mathbf{b}_2\\ -\mathbf{b}_1\end{bmatrix}.$$

After the solution $\mathbf{x}^\star_{\ell_1}$ is found, the first $2K$ elements corresponding to $\mathbf{x}$ are extracted and converted from real to complex to form the estimated data symbols.

[1]Note that every Gram matrix is semidefinite positive [40, Theorem 7.2.10].

[2]The convexity of a function can be verified applying the second order conditions over the objective function; e.g., for problem (7), $\nabla^2 f(\mathbf{x}) = \mathbf{H}^T\mathbf{H} \succeq 0$.

2) LP with ℓ_∞-norm

Following a similar procedure, the LP detector based on ℓ_∞ norm is detailed. The cast to LP of the Chebyshev approximation [21] including the constellation symbol constraint becomes

$$\begin{aligned} \underset{\mathbf{x},t}{\text{minimize}} \quad & t \\ \text{s.t.} \quad & -\mathbf{1}t \leq \mathbf{y}-\mathbf{H}\mathbf{x} \leq \mathbf{1}t \\ & \mathbf{b}_1 \leq \mathbf{x} \leq \mathbf{b}_2. \end{aligned} \tag{11}$$

The problem (11) expressed in the *standard inequality form* is

$$\begin{aligned} \underset{\mathbf{x}_{\ell_\infty}}{\text{minimize}} \quad & \mathbf{c}_{\ell_\infty}^T\mathbf{x}_{\ell_\infty} \\ \text{s.t.} \quad & \mathbf{A}_{\ell_\infty}\mathbf{x}_{\ell_\infty} \leq \mathbf{b}, \end{aligned} \tag{12}$$

where:

$$\mathbf{c}_{\ell_\infty} = \begin{bmatrix}\mathbf{0}\\ 1\end{bmatrix}, \mathbf{A}_{\ell_\infty} = \begin{bmatrix}\mathbf{H} & -\mathbf{1}\\ -\mathbf{H} & -\mathbf{1}\\ \mathbf{I} & \mathbf{0}\\ -\mathbf{I} & \mathbf{0}\end{bmatrix}, \mathbf{x}_{\ell_\infty} = \begin{bmatrix}\mathbf{x}\\ t\end{bmatrix}.$$

After the solution $\mathbf{x}^\star_{\ell_\infty}$ is found, the last element is discarded and the vector is converted from real to complex to form the estimated symbol obtained through the LPℓ_∞ detector.

C. SEMIDEFINITE PROGRAMMING

The SDP is a powerful mathematical method [18] that has a competitive performance in MIMO detectors for high order modulations because of its polynomial worst-case complexity in contrast to ML that has an exponential complexity depending on the constellation size [17]. Here we consider [17] due to its simplicity and equivalence with other representations [20].

Considering the relaxation of the rank restriction in SDP formulation and the relaxation of the constellation symbols, it is possible to reformulate the detection problem for high-order modulation as the following SDP optimization problem [17]:

$$\begin{aligned} \underset{\mathbf{X}}{\text{minimize}} \quad & \text{trace}(\mathbf{L}\mathbf{X}) \\ \text{s.t.} \quad & \mathbf{X} \succeq \mathbf{0} \\ & \mathbf{X}(N,N) = 1 \\ & b_1^{\mathcal{B}^2} \leq \mathbf{X}(i,i) \leq b_2^{\mathcal{B}^2}, \end{aligned} \tag{13}$$

where $\mathbf{X}$ is the $N \times N$ unknown variable, $N = 2K+1$, the index $i = 1, \ldots, N-1$, scalars $b_1^{\mathcal{B}^2}$ and $b_2^{\mathcal{B}^2}$ represent the lower and upper limits of the set $\mathcal{B}^2$ (for example, 16-QAM has a set $\mathcal{B}^2 = \{1, 9\}$, so $b_1^{\mathcal{B}^2} = 1$ and $b_2^{\mathcal{B}^2} = 9$) and

$$\mathbf{L} = \begin{bmatrix}\mathbf{H}^T\mathbf{H} & -\mathbf{H}^T\mathbf{y}\\ -\mathbf{y}^T\mathbf{H} & 0\end{bmatrix}. \tag{14}$$

The method considered here to extract the solution vector from $\mathbf{X}$ is the rank-1 approximation [18],

$$\mathbf{x}^\star_{\text{SDP}} = \mathbf{v}_1\sqrt{\lambda}_1, \tag{15}$$

This article has been accepted for publication in a future issue of this journal, but has not been fully edited. Content may change prior to final publication. Citation information: DOI 10.1109/ACCESS.2019.2902521, IEEE Access

where λ_1 denotes the maximum eigenvalue and $\mathbf{v}_1$ is its associated eigenvector.

D. CLASSICAL LINEAR M-MIMO DETECTORS

For reference purpose, the classical linear detectors ZF and MMSE are considered and the estimated symbol is given in the form $\tilde{\mathbf{x}} = \mathbf{W}_{lin}\mathbf{y}$. The matrix $\mathbf{W}_{lin}$ is expressed by:

$$\mathbf{W}_{lin} = \begin{cases} (\mathbf{H}^T\mathbf{H})^{-1}\mathbf{H}^T, & \text{ZF detector,} \\ \left(\mathbf{H}^T\mathbf{H} + \dfrac{\sigma_z^2}{E_s}\mathbf{I}\right)^{-1}\mathbf{H}^T, & \text{MMSE detector,} \end{cases} \tag{16}$$

with E_s denoting the symbol energy. The ZF M-MIMO detector is obtained performing the pseudoinverse of the channel matrix, while the MMSE M-MIMO detector requires the second order channel statistics.

IV. SOLVERS FOR CONVEX OPTIMIZATION

In this section, algorithms usually implemented in general purpose solvers for LP, QP and SDP formulations are discussed. Algorithms implemented more frequently in subsection IV-A and the TMP exploring the simple constraints is detailed in subsection IV-B.

A. INTERIOR-POINT METHODS

Interior point methods appeared as a polynomial complexity approach to solve LP problems with efficiency better than simplex [22]; those algorithms were extended and are also capable to solve QP problems [22]–[24] and also SDP problems [22].

Among different algorithms, for example, barrier method, primal-dual path following, and the affine scaling method, the MPC is one of the most efficient implementations [22], [23] in this category; in Matlab platform, it is implemented with commands *lsqlin* and *linprog* [28]–[30] to solve to solve QP and LP, respectively. For SDP, the CVX, a package for specifying and solving convex programs [42], [43], was considered in the numerical simulations configured to use the SDPT3 solver, which also employs an MPC implementation [31].

Interior point methods solve a linear system of equations at each iteration, and has similar computational complexity order compared with linear detectors [14], [44] and is more computationally intensive in the SDP case, where specialized interior-point algorithms for SDP may require $\mathcal{O}(K^{3.5})$ [18], [32].

Table 1 summarizes the number of unknowns, constraints and computational complexity order of each formulation. The SDP-based detector must find a matrix of unknowns, and is the most complex among the studied detectors. The number of unknowns in the LPℓ1 formulation depends on M, which is large in M-MIMO systems and this impacts on computational complexity. The number of unknowns is similar between QP and LP$\ell\infty$, however, as shown later in section V, the performance of QP is better than LP$\ell\infty$. The QP formulation presents the least number of unknowns and constraints and is a good candidate to be an efficient detector with a good complexity-performance trade-off. In the next subsection, the application of TMP in the QP-based detector are detailed.

TABLE 1: Problem size in terms of number of variables and constraints and the associated complexity for M-MIMO detectors.

Detector	Variables	Constraints	Complexity
QP (6)	$2K$	$4K$	$\mathcal{O}(N_{iter}K^3)$
LPℓ1 (10)	$2K+2M$	$4M+4K$	$\mathcal{O}[N_{iter}(K+M)^3]$
LP$\ell\infty$ (12)	$2K+1$	$4M+4K$	$\mathcal{O}[N_{iter}(K+1)^3]$
SDP (13)	$(2K+1)^2$	$4K+1$	$\mathcal{O}(N_{iter}K^{3.5})$

B. TWO-METRIC PROJECTION ALGORITHMS

The TMP method is of practical application when the projection on the feasible set can be carrier easily [33], such as the box constraints in the QP-based detector (6). We have considered an initial[3] and feasible vector $\mathbf{x}_0 = \mathbf{0}$ in the middle of the feasible region (assuming a symmetric QAM constellation around zero, i.e. a 16-QAM with $\{\pm 1, \pm 3\}$). For different definitions of the direction matrix $\mathbf{D}$, we can obtain different algorithms, such as:

1) $\mathbf{D}_n = \mathbf{I}$, resulting in the PG method [26];
2) $\mathbf{D}_n = \left(\nabla^2 f(\mathbf{x})\right)^{-1} = (\mathbf{H}^T\mathbf{H})^{-1}$, the PN algorithm with complexity $2/3(2K)^3 + 2(2K)^2$ to perform LU factorization [21] for the matrix inverse calculation.
3) $\mathbf{D}_n = \dfrac{1}{\text{diag}(\nabla^2 f(\mathbf{x}))}$ scaling the gradient with the inverse of the diagonal, the Diagonally Scaled Projected Gradient (DSPG) method, which requires 2K flops after the precomputation of the Hessian;
4) Approximation of the inverse of the Hessian using Neumann series namely Projected Newton with Neumman Approximation (PNNA); under this approach it is affordable to consider 3 terms in the expansion resulting in cubic complexity [6] of $16K^3 + 12K^2 - 10$ flops.

Note that there are many possible variations, such as the approximation of Hessian (quasi-Newton method, e.g., BFGS [27]); approximations of the solution of the linear system of equations named truncated Newton; different line search algorithms can be employed beyond the Armijo-like rule, the utilization of an initial point (also called warm-start). Herein, we are not exhaustive, but trying promising combinations.

The steps of the TMP algorithm with the PN variation detailed in [25] are presented herein for completeness. When $\mathbf{D}_n = (\nabla^2 f(\mathbf{x}))^{-1}$ we have the PN; note the similarities when compared with the *unconstrained* counterpart NM: it is iterative, there is a search direction defined by matrix

[3]Note that depending on the constraints, more sophisticated strategies may be required to choose a feasible initial point, for example, the solution of an LP [44].

This article has been accepted for publication in a future issue of this journal, but has not been fully edited. Content may change prior to final publication. Citation information: DOI 10.1109/ACCESS.2019.2902521, IEEE Access

$\mathbf{D}_n$, a line search to find a step length α_n and an updating equation in a similar manner:

$$\mathbf{x}_{n+1}(\alpha_n) = [\mathbf{x}_n - \alpha_n \mathbf{D}_n \nabla f(\mathbf{x}_n)]^{\#}, \tag{17}$$

with the operator $[.]^{\#}$

$$[a^i]^{\#} = \begin{cases} b_2^i & \text{if } b_2^i \leq a^i \\ a^i & \text{if } b_1^i < a^i < b_2^i \\ b_1^i & \text{if } a^i \leq b_1^i, \end{cases} \tag{18}$$

keeping the solution inside the feasible region (the box constraints). At the nth iteration, the matrix $\mathbf{D}_n$ is diagonal with respect to subset of indexes $I_n^{\#}$ defined as

$$d^{ij} = 0, \quad \forall i \in I_n^{\#}, \quad j \neq i, \tag{19}$$

and set of indexes are chosen such as

$$I_n^{\#} = \left\{ i | \, b_1^i \leq x_n^i \leq b_1^i + \varepsilon_n \text{ and } \frac{\partial f(\mathbf{x}_n)}{\partial x^i} > 0 \quad \text{or} \right.$$
$$\left. b_2^i - \varepsilon_n \leq x_n^i \leq b_2^i \text{ and } \frac{\partial f(\mathbf{x}_n)}{\partial x^i} < 0 \right\} \tag{20}$$

with tolerance

$$\varepsilon_n = \min\{\varepsilon, \| \, [\mathbf{x}_n - \mathbf{M}_{\text{TM}} \nabla f(\mathbf{x}_n)]^{\#} \, \|_2\}, \tag{21}$$

where $\mathbf{M}_{\text{TM}}$ is a definite positive diagonal matrix that can be fixed or vary at each iteration; herein, it was considered as $\mathbf{I}$ as suggested in [25] for simplicity. The step length α_n is

$$\alpha_n = (\beta_{\text{TM}})^{m_n} \tag{22}$$

where m_n is the first m that attains the Armijo-like condition

$$f(\mathbf{x}_n) - f(\mathbf{x}(\beta_{\text{TM}}^m)) \geq \sigma_{\text{TM}} \left\{ \beta_{\text{TM}}^m \sum_{i \notin I_n^{\#}} \frac{\partial f(\mathbf{x}_n)}{\partial x^i} p_n^i + \right.$$
$$\left. \sum_{i \in I_n^{\#}} \frac{\partial f(\mathbf{x}_n)}{\partial x^i} \left[x_n^i - x_n^i(\beta_{\text{TM}}^m) \right] \right\} \tag{23}$$

and variables $\sigma_{\text{TM}} \in [0, \, 0.5], \beta_{\text{TM}} \in [0, \, 1]$; m_n is nonnegative and

$$\mathbf{p}_n = \mathbf{D}_n \nabla f(\mathbf{x}_n). \tag{24}$$

The algorithm terminates when a critical point $\mathbf{x}_{n+1} = \mathbf{x}_n$ is found [25]. Numerically, here we consider that the algorithm terminates if the condition holds approximately in the form

$$\|\mathbf{x}_{n+1} - \mathbf{x}_n\|_2 \leq \varepsilon_n. \tag{25}$$

The mentioned steps are synthetized in Algorithm 1. After the stop criteria is attained, the solution vector $\mathbf{x}_n$ is converted from real to complex form of the estimated data symbols. The computational complexity considered here is flops. Matrix and vector operations and some factorizations are found in [21, Appendix C]. Herein, the exponential operator $[.]^m$ and square root $\sqrt{[.]}$ (for calculation of ℓ_2-norm) are counted as 8 flops; `if` conditions are ignored, for example in (18), since they are not mathematical operations

Algorithm 1 Projected Newton Method for problem (7).

1: Input parameters: $\sigma_{\text{PN}}, \beta_{\text{PN}}, \mathbf{D}_n, \mathbf{x}_0, \varepsilon, N_{\max}, f(\mathbf{x}), \nabla f(\mathbf{x})$
2: Initialize $n = 0, \mathbf{x}_n = \mathbf{x}_0, \varepsilon_n$
3: **while** $n \leq N_{\max}$ **do**
4: Evaluate and store $\nabla f(\mathbf{x}_n)$ ▷ $8K^2$
5: Evaluate tolerance (21) ▷ $20K$
6: Check indexes (20)
7: Zeroing some elements of $\mathbf{D}_n$ eq.(19)
8: Evaluate (24) ▷ $(4K^2 - 2K)$, or $2K$ if $\mathbf{D}_n$ is diagonal
9: Line search (23) ▷ $8K^2 + 6K - 2 + m_{iter}(8K^2 + 10K + 10)$
10: Next iteration point (17) ▷ $10K$
11: **if** condition (25) is attained **then**
12: Store n inside N_{iter}
13: **end if**
14: **end while**
15: Output: $\mathbf{x}_n$

such as sum, subtraction, division, multiplication in the definition of flop [45].

Similar terms in the objective function (7) and its gradient $\nabla f(\mathbf{x})$ can be precomputed and stored before entering Algorithm 1; a fixed computational cost in evaluating $\mathbf{H}^T\mathbf{H}$ results in $8K^2M - 4K$, the precomputation of $\mathbf{H}^T\mathbf{y}$ represents $8MK - 2K$ and the sum after the multiplication by $\mathbf{x}_n$ spends $2K$ operations, resulting in a total of precomputation complexity of $\Upsilon_{fixed} = 8K^2M - 4K + 8MK$. The evaluation of the gradient $\nabla f(\mathbf{x}_n) = 2\mathbf{H}^T\mathbf{H}\mathbf{x}_n - 2\mathbf{H}^T\mathbf{y}$ requires only the evaluation of a matrix-vector multiplication of $\mathbf{x}_n$ per iteration. Hence, the total computational complexity of each algorithm is composed by a fixed amount Υ_{fixed} plus the construction of $\mathbf{D}_n$ and an iterative amount of operations described along Algorithm 1; the flops are summarized in Table 2, along with the flops count for linear detector MMSE, with N_{iter} representing the number of iterations till the condition (25) is attained and $m_{iter} = 1 + \overline{m_n}$, where $\overline{m_n}$ is the mean number of m_n line search evaluations that attains the condition (23) plus one because $m = 0$ is the first evaluation.

Note that inside the projected algorithms only Υ_{fixed} depends on M; equations inside Algorithm 1 involve the multiplication of matrices and vectors of size $2K$ and does not depend on M. The most costly part of the projected algorithms PN, PNNA, PG, DSPG applied to the M-MIMO detection is due to (23) calculation, which requires the evaluation of the objective function $N_{iter}m_{iter}$ times resulting in a complexity order of $\mathcal{O}(N_{max}m_nK^2)$.

The variable N_{iter} depends on the rate of convergence of each algorithm. PN is described as the fastest and PG the slowest among the studied projected algorithms; the rate of convergence of PG algorithm is given by [33]

$$\|\mathbf{x}_{n+1} - \mathbf{x}_{\text{QP}}^{\star}\|_2 \leq$$
$$\max\{\|1 - \alpha_n\lambda_{min}\|_1, \|1 - \alpha_n\lambda_{max}\|_1\} \, \|\mathbf{x}_n - \mathbf{x}_{\text{QP}}^{\star}\|_2, \tag{26}$$

where λ_{min} and λ_{max} denote the minimum and maximum eigenvalues of the Hessian matrix and $\mathbf{x}_{\text{QP}}^{\star}$ is the optimal

This article has been accepted for publication in a future issue of this journal, but has not been fully edited. Content may change prior to final publication. Citation information: DOI 10.1109/ACCESS.2019.2902521, IEEE Access

TABLE 2: Number of FLOPs for considered algorithms.

M-MIMO Detector	Number of Operations
$\Upsilon_{\text{PN}}(K, M, N_{iter}, m_{iter})$	$\Upsilon_{fixed} + \frac{16}{3}K^3 + 8K^2 + N_{iter}[20K^2 + 34K - 2 + m_{iter}(8K^2 + 10K + 10)]$
$\Upsilon_{\text{PNNA}}(K, M, N_{iter}, m_{iter})$	$\Upsilon_{fixed} + 16K^3 + 12K^2 - 10 + N_{iter}[20K^2 + 34K - 2 + m_{iter}(8K^2 + 10K + 10)]$
$\Upsilon_{\text{PG}}(K, M, N_{iter}, m_{iter})$	$\Upsilon_{fixed} + N_{iter}[16K^2 + 38K - 2 + m_{iter}(8K^2 + 10K + 10)]$
$\Upsilon_{\text{DSPG}}(K, M, N_{iter}, m_{iter})$	$\Upsilon_{fixed} + 2K + N_{iter}[16K^2 + 38K - 2 + m_{iter}(8K^2 + 10K + 10)]$
$\Upsilon_{\text{MMSE}}(K, M)$	$\Upsilon_{fixed} + \frac{16}{3}K^3 + 16K^2$

point for the QP formulation. Observing (26), the rate of convergence depends on the eigenvalues of the Hessian, which is the Gram matrix for QP, $\nabla^2 f(\mathbf{x}) = \mathbf{H}^T\mathbf{H}$. One can expect that changing the eigenvalues of the Hessian using different number of users $K \ll M$, the channel hardening effect occur changing the matrix condition number and influencing the rate of convergence of the projected algorithms. In that way, the number of iterations N_{iter} and evaluations m_{iter} are obtained numerically in order to characterize the full computational cost of the algorithm in section V.

Another detail to consider in the implementation is that the PN requires the Hessian to be definite positive and, in some scenarios, this condition may not be attained. So modifications in the Hessian matrix should be considered [22, Ch.5], where the Hessian is replaced by

$$\widehat{\nabla^2 f(\mathbf{x})} = \frac{\nabla^2 f(\mathbf{x}) + \gamma \mathbf{I}}{1 + \gamma} \tag{27}$$

before the calculation of the inverse in the matrix $\mathbf{D})n$ for PN, where large values of the regularization factor γ approximates the NM to a Steepest Descent. The value of γ was determined through numerical simulations.

V. NUMERICAL RESULTS

Monte Carlo simulations (MCS) were carried out to demonstrate the effectiveness of the proposed detectors in terms of performance-complexity trade-off; all the MCS have been conducted under uncoded information scenarios. The reliability of the studied detectors are presented in subsection V-A, while the characterization and performance of the projected algorithms are presented in subsection V-B.

A. PERFORMANCE EVALUATION

The main M-MIMO system parameters considered are presented in Table 3. A default set of parameters appears on the top, and, for each scenario, one parameter is changed at time in order to observe its effect on the system performance. The optimization problems (6), (10), (12) were treated using Matlab optimization solvers, *lsqlin* and *linprog* commands for QP and LP, respectively. The problem (13) was solved using CVX, a package for specifying and solving convex programs [42], [43] configured to use the SDPT3 solver [31].

In Fig.1, the BER performance for different values of signal-to-noise ratio (SNR) is presented for different detectors. Under uncorrelated scenarios and perfect CSI, the M-MIMO detectors with convex optimization formulation (LP, QP) presented better performance (lower BER) than linear detectors ZF and MMSE. Moreover, among the convex detectors, QP provided the best performance, followed by LPℓ_∞ and LPℓ_1 formulations.

TABLE 3: M-MIMO System and Channel MCS parameters.

Parameter	Value
Number of BS antennas, M	128
Number of UE terminals, K	128
Modulation order	16-QAM
Massive MIMO Detectors	Conventional: ZF, MMSE, LP ℓ_1, LP ℓ_∞, QP, SDP
LP, QP and SDP solver	*linprog*, *lsqlin*, CVX (SDPT3)
Channel condition ρ and τ	0
Scenarios	
Channel estimation quality, τ	[0; 0.05; 0.10]
Antenna correlation, ρ	[0; 0.5; 0.9]
Number of UE terminals, K	[128; 96; 64; 32]
Modulation order	[4; 16; 64] QAM

In Fig.1a, considering errors in CSI around 5 and 10%, the BER performance was impaired for all detectors, while a similar behavior in performance compared to perfect CSI has been observed; SDP provides the best performance among analyzed detectors followed by QP, LPℓ1, LP$\ell\infty$ and linear detectors. Indeed, the linear detector ZF provides the poorest performance among the studied detectors; its performance is degraded even further with the increase of the τ parameter.

Fig.1b exhibits the spatial antenna correlation impact on the BER performance; when $\rho = 0.5$, the overall performance is worsened; however, under extreme high correlated scenarios, i.e., $\rho = 0.9$, the performance of SDP, QP, LPℓ1 and LP$\ell\infty$ is worse than MMSE, while the LPℓ1 detector exhibits similar performance compared to QP and SDP.

In Fig.1c where the number of users are changed, the system loading $\frac{K}{M}$ is reduced progressively and the performance of linear detectors ZF and MMSE are significantly improved, surpassing LPℓ1 and LP$\ell\infty$ detectors and providing performance similar to QP and SDP detectors; and a different behavior compared to previous scenarios (Figs. 1a and 1b) is observed among LP detectors: as the number of users is reduced, the performance of LPℓ1 surpasses LP$\ell\infty$.

In Fig.1d, the modulation order was altered. In the low order modulation 4-QAM scenario, the improvement in performance of SDP compared with QP detector is more evident; performance of SDP and QP are better than linear detectors; moreover, the performance of LPℓ1 becomes very similar to LP$\ell\infty$, which is a different behavior compared

This article has been accepted for publication in a future issue of this journal, but has not been fully edited. Content may change prior to final publication. Citation information: DOI 10.1109/ACCESS.2019.2902521, IEEE Access

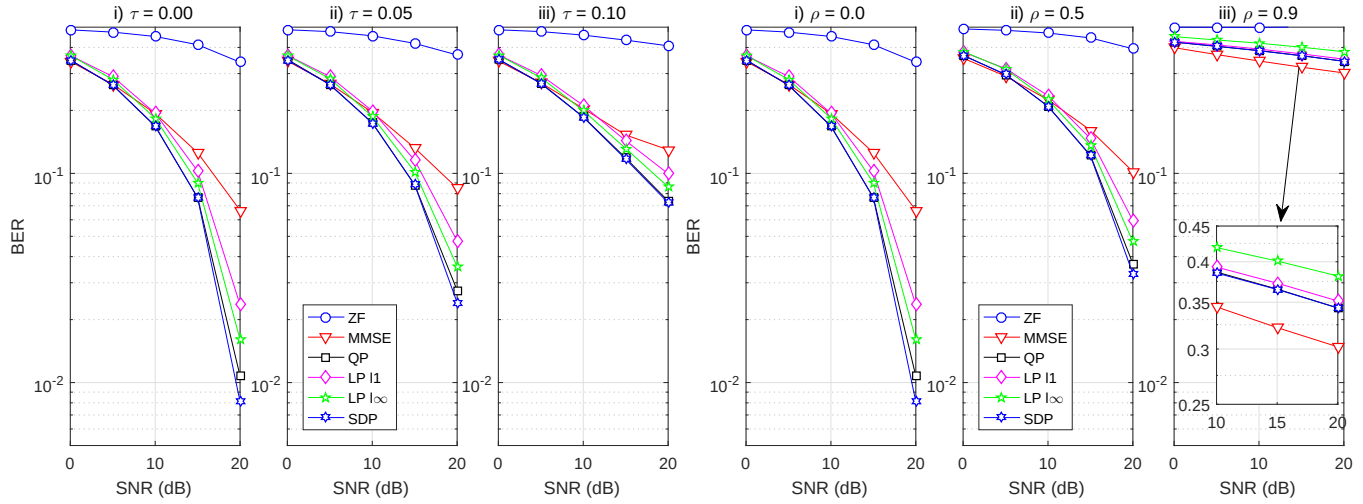

(a) Performance with error in the channel estimation.

(b) Performance with different correlation indexes.

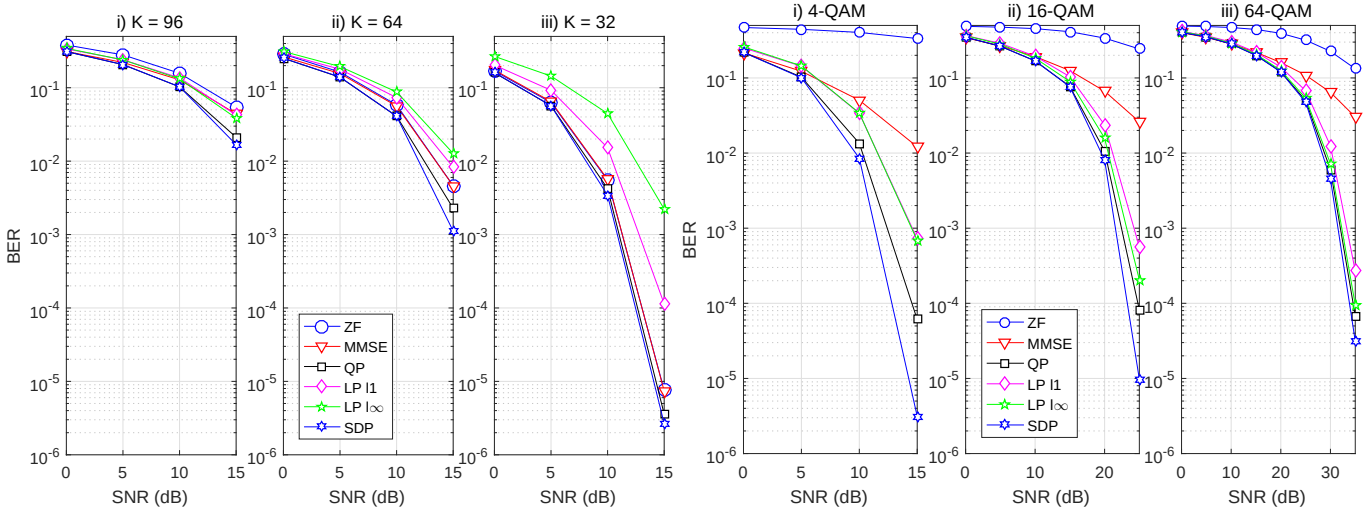

(c) Performance with different number of users.

(d) Performance with different values of modulation order.

FIGURE 1: Performance of 128×128 M-MIMO detectors under realistic channel and intended system conditions: spatial correlation, error in the channel estimation and reduced number of users (system loading) and digital modulation order.

with high order modulations (16-QAM and 64-QAM), where LP$\ell\infty$ provides superior performance compared with LPℓ1.

In summary, although SDP provides the best performance, this advantage is not very distinguishable compared with QP performance with high order modulation, i.e., 16-QAM in Figs. 1a, 1b, and 1c; it is more prominent in 4-QAM presented in Fig.1d. The QP detector provides suitable BER performance under scenarios with imperfect CSI, different system loading, at low or medium level of spatial correlation ($\rho \leq 0.5$) and only a slightly worse in performance than MMSE at the excessively correlated scenarios, i.e. $\rho = 0.9$. In the next subsection, projected algorithms are considered to solve the QP formulation in (7) focusing on the computational complexity while their solution quality and competitiveness are investigated and compared with the linear detector MMSE.

B. PROJECTED METHODS IN LS-MIMO DETECTION

In this subsection, MCS are performed focusing on computational complexity and characterization of parameters N_{iter} and m_{iter} in order to investigate the competitiveness of the projected algorithms applied to solve the QP formulation against linear detectors. The chosen scenarios are the ones that might interfere directly on the convergence properties as shown in (26): scenarios with different system loading $\frac{K}{M}$, including the intended use in LS-MIMO systems, where a large number of BS antennas serve a small number of users ($K \ll M$) and also when $K \approx M$ e.g., in crowded scenarios. First, numerical simulations were carried out in order to choose adequate input parameters for PG, DSPG, PNNA and PN algorithms. After that, the BER performance (deploying tuned parameters for a fair comparison) is computed and complexity compared in terms of flops. Finally, the performance with different number of users but a constant system loading is performed, to further evidence

This article has been accepted for publication in a future issue of this journal, but has not been fully edited. Content may change prior to final publication. Citation information: DOI 10.1109/ACCESS.2019.2902521, IEEE Access

TABLE 4: Scenario parameters for the calibration of input parameters for projected algorithms.

Parameter	Value
M	128
K	128
SNR	15 dB
Detectors	QP, MMSE
Algorithms for QP	PN, PNNA, DSPG, PG
Initial Values	
ε	10^{-2}
$\beta_{\text{TM}}^{start}$	0.5
$\sigma_{\text{TM}}^{start}$	0.3
N_{max}^{start}	10
γ^{start}	0
N_{max}	5
Intervals	
γ	$\in [0; 1.5]$
β_{TM}	$\in [0.1; 0.9]$
σ_{TM}	$\in [0.1; 0.4]$
ε	$\in [0.5; 0.0001]$
Scenarios	
Number of UE terminals, K	[128; 96; 64; 32]
Constant $\frac{K}{M} = \frac{1}{4}$	$M = [128; 256]$

that the number of iterations N_{iter} of projected algorithms depends mainly on the relation $\frac{K}{M}$ and the properties of the Hessian, but not so much on the dimensionality K of the QP problem.

1) Different Number of Users

Some algorithms are sensitive to the selection of input parameters, and an initial calibration may be required in order to improve the convergence speed. In [46], a methodology is proposed to tune the input parameters. Considering a certain interval for each parameter, one parameter is varied at time and the effect in performance is observed; the parameter that produces an adequate performance is chosen and the next input parameter is varied; two rounds of simulations are executed till the input parameters are chosen. Here, a similar procedure is deployed for $\gamma, \sigma_{\text{TM}}, \beta_{\text{TM}}, \varepsilon$ in order to characterize N_{iter} and m_{iter} for scenarios with different system loading. Considering an initial set of parameters depicted in Table 4, the procedure was executed first, for different system loading varying K, and after, for constant loading, changing both M and K.

In Fig. 2, the influence of the regularization factor γ in (27) is observed, where the Hessian was substituted by $\widehat{\nabla^2 f(\mathbf{x})}$ before the computation of $\mathbf{D}_n$ for PN and PNNA. The effect of γ is distinguishable in the scenario with $K = M$ for PN where the increase in γ results in better performance as shown in Fig. 2 i) and less line search evaluations depicted in Fig. 2 ii); after $\gamma = 1$ the improvements becomes smaller and so, $\gamma = 1$ is considered for PN in the $K = M$ scenario. Parameter γ does not seem to influence the performance for the other scenarios and other algorithms besides the PN, and also does not interfere in m_{iter} shown in 2 iii) for $K = 32$, so the value $\gamma = 0$ is considered for other algorithms and other scenarios.

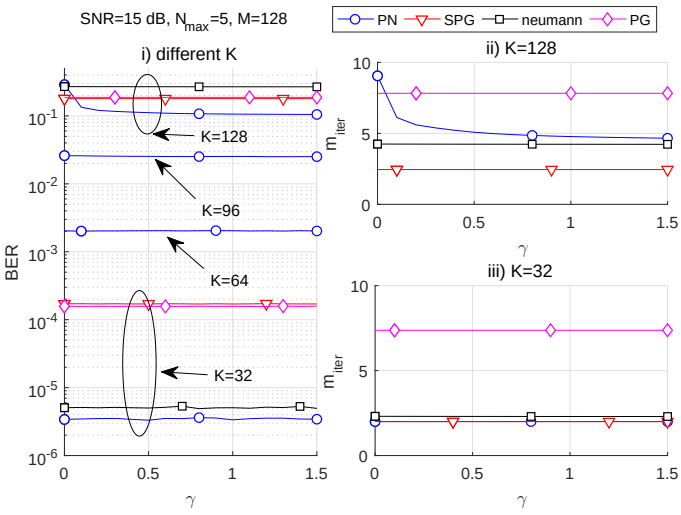

FIGURE 2: Influence of parameter γ for different simulation scenarios considered.

In Fig.3, the calibration of parameters $\sigma_{\text{TM}}, \beta_{\text{TM}}$ and ε are presented for $K = M$ and $K = \frac{M}{4}$; the procedure was also executed for $K = \frac{3M}{4}$ and $K = \frac{M}{2}$ but omitted herein for brevity. The left axis shows BER performance and the right axis the search evaluations m_{iter}, which impacts on the complexity. As β_{TM} increases, the evaluations of m_{iter} also increases, and more aggressively for PG. The parameter σ_{TM} is related to the step size in (22) and different values result in different performances for $K = 128$ and $K = 32$.

In the case of ε, $N_{max} = 5$ is not sufficient to achieve an MMSE performance for PG, DSPG and PNNA, and so, its effect is not clearly observed; the exception is the PN where the performance is slightly harmed when $\varepsilon = 0.5$. Therefore, the rate of convergence is characterized (parameters N_{iter} and m_{iter}), and a second round of simulations are executed with smaller values of ε. The information collected from the simulations illustrated in Fig. 3 and the two rounds for parameter ε shown in 4 is presented in Table 5.

Convergence for the M-MIMO detectors algorithms are presented in Fig. 4, where the BER performance is depicted as function of the number of iterations n. Adopted parameters are presented in Table 5. The number of iterations N_{iter} were stored in line 12 inside Algorithm 1 throughout the MCS and rounded; m_{iter} represents the line search evaluations, which is an internal step required to solve the optimization problem with projected methods and causes a direct impact on the number of flops in the final complexity are also presented. Observe that N_{iter} presented in the Table is also depicted inside Fig. 4. In Fig. 4a, the first round of ε is presented for the scenario with different number of users; details about the MMSE performance for each scenario are also presented. For DSPG, PNNA and PG, the performance is similar to MMSE, however, the value $\varepsilon = 0.5$ causes a premature termination of the algorithm since their performance could be improved with more iterations.

This article has been accepted for publication in a future issue of this journal, but has not been fully edited. Content may change prior to final publication. Citation information: DOI 10.1109/ACCESS.2019.2902521, IEEE Access

TABLE 5: Tuned parameters for the simulations with different number of users. The order is [PN; DSPG; PNNA; PG].

Parameter	K=128	K=96	K=64	K=32
γ	[1; 0; 0; 0]	[0; 0; 0; 0]	[0; 0; 0; 0]	[0; 0; 0; 0]
β_{TM}	[0.5; 0.2; 0.4; 0.6]	[0.5; 0.4; 0.2; 0.2]	[0.5; 0.6; 0.3; 0.4]	[0.5; 0.3; 0.6; 0.3]
σ_{TM}	[0.3; 0.1; 0.1; 0.3]	[0.3; 0.4; 0.2; 0.1]	[0.3; 0.3; 0.1; 0.2]	[0.4; 0.2; 0.3; 0.1]
ε, round 1	[0.5; 0.5; 0.5; 0.5]	[0.5; 0.5; 0.5; 0.5]	[0.5; 0.5; 0.5; 0.5]	[0.5; 0.5; 0.5; 0.5]
ε, round 2	[0.5; 0.1; 0.1; 0.1]	[0.5; 0.1; 0.1; 0.1]	[0.1; 0.1; 0.1; 0.1]	[0.1; 0.1; 0.1; 0.1]
N_{iter}	[15; 29; 51; 37]	[6; 20; 23; 19]	[5; 15; 13; 12]	[3; 7; 6; 8]
m_{iter}	[6.49; 1.72; 4.01; 12.67]	[4.09; 2.11; 2.51; 4.63]	[2.89; 2.82; 2.40; 7.23]	[2.61; 1.70; 2.94; 5.64]

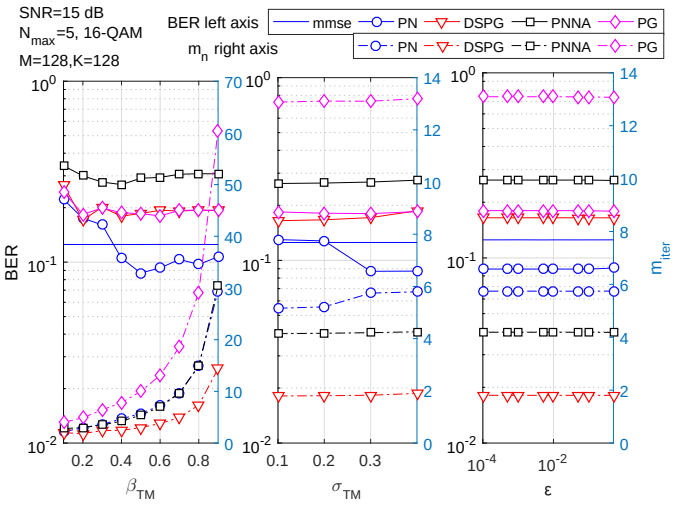

(a) Calibration with users $K = M = 128$.

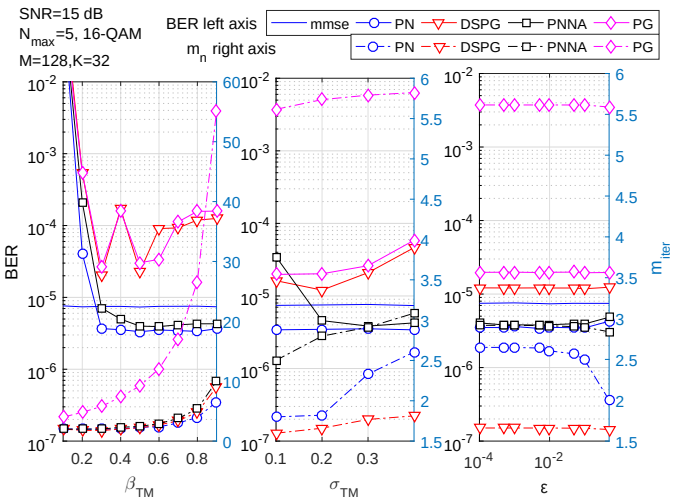

(b) Calibration with users $K = \frac{1}{4}M = 32$.

FIGURE 3: Performance varying the number of users in order to choose $\sigma_{\text{TM}}, \beta_{\text{TM}}$ and ε parameters.

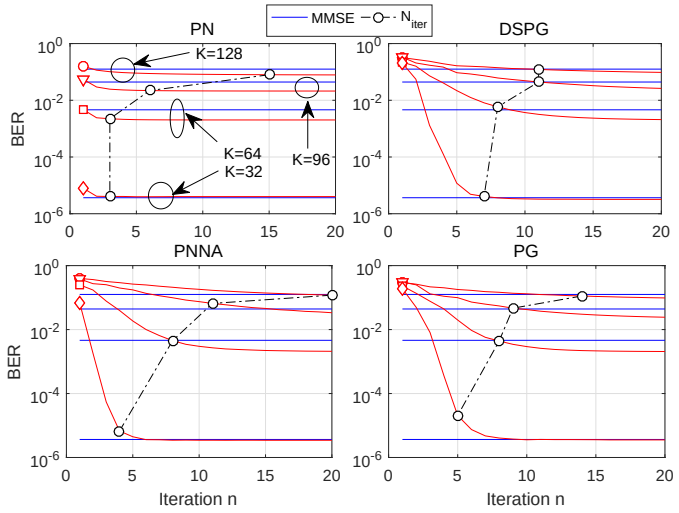

(a) Convergence considering values of ε for round 1.

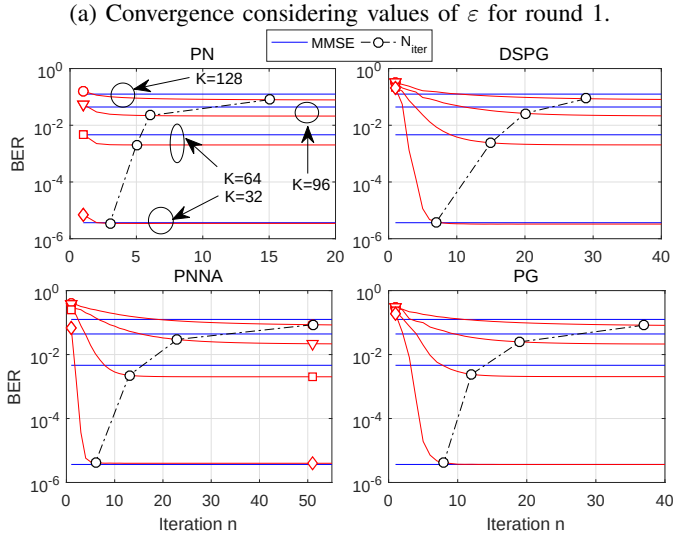

(b) Convergence considering values of ε for round 2.

FIGURE 4: Rate of convergence of projected algorithms applied to QP formulation with different number of users.

In Fig. 4b, the convergence of the algorithms are compared. Two extreme situations are analyzed; the other scenarios $K = \frac{3M}{4}$ and $K = \frac{M}{2}$ are interpolations between them. A deeper analysis of the computational complexity in terms of flops is presented in section VI, where the complexity is compared with MMSE.

- For $K = M = 128$, PN algorithm with ≈ 15 iterations can provide a better performance than MMSE with similar computational complexity order simply because it requires the calculation of the inverse of the Hessian. Neumann approximation for the inverse when $K \approx M$ is poor [6], and BER improvement of PNNA is slower than PG and DSPG. The PG and DSPG require a simpler $\mathbf{D}_n$ matrix (PG an identity, DSPG a diagonal matrix) and after around 30 iterations, they achieve a performance similar to PN.
- For $K = 32 = \frac{M}{4}$, the performance of QP-based

This article has been accepted for publication in a future issue of this journal, but has not been fully edited. Content may change prior to final publication. Citation information: DOI 10.1109/ACCESS.2019.2902521, IEEE Access

TABLE 6: Tuned parameters for the simulations with constant system loading. The order is [PN; DSPG; PNNA; PG].

Parameter	$M = 256, K = 64$
γ	[0; 0; 0; 0]
β_{TM}	[0,5; 0,5; 0,5; 0,5]
σ_{TM}	[0,3; 0,2; 0,2; 0,2]
ε	[0.1; 0.1; 0.1; 0.1]
N_{iter}	[4; 8; 6; 8]
m_{iter}	[2.29; 2.11; 2.50; 10.11]

detectors is almost the same achieved by the MMSE, as shown previously in Fig.1c; the number of iterations to achieve MMSE performance is reduced for all algorithms. For PN, around 4 iterations are required. Neumann approximation becomes more accurate with the reduction of $\frac{K}{M}$ [6]; in such low system loading scenario, the convergence of PNNA is substantially improved in comparison with $K = 128$, and less than 10 iterations are enough to provide MMSE-like BER; for PG and DSPG, less than 10 iterations are sufficient to achieve MMSE-like performance.

2) Constant System Loading

Here, simulations considering a constant system loading are presented in order to observe the behavior of the projected algorithms when the dimensionality of the problem increases (more users, more unknown variables in the QP problem), while keeping a constant (and low) system loading of $\frac{K}{M} = \frac{1}{4}$ aiming to maintain the characteristic of the channel hardening, i.e., a well-conditioned Hessian $\mathbf{H}^T\mathbf{H}$.

The convergence considering a constant system loading $\frac{K}{M} = \frac{1}{4}$ is presented in Fig.5. The procedure considered in the previous simulations are also deployed here. The input parameters $\sigma_{\text{TM}}, \beta_{\text{TM}}$ and ε are determined through numerical simulations as shown in Fig. 5a and condensed in Table 6, and the number of iterations N_{iter} and line search evaluations m_{iter} are obtained numerically; the N_{iter} is shown in Fig. 5b. A similar behavior is observed in the scenario 128×32 (from previous subsection) and 256×64; a reduced number of iterations (less than 10) are required for the projected algorithms and is an indicative that the method works in larger systems without great impacts on the number of iterations and, consequently, in complexity.

Considering the values of N_{iter} and m_{iter} obtained, the computational complexity is further characterized in the next section.

VI. COMPUTATIONAL COMPLEXITY

The computational complexity is analyzed in two parts. In the first, SDP, QP, LPℓ1 and LP$\ell\infty$ are compared in terms of complexity order; in the second part, the projected algorithms are evaluated in terms of flops and compared with the linear detector MMSE.

Initially, a complexity comparison considering SDP, QP, LPℓ1, LP$\ell\infty$ and linear detectors presented in subsection

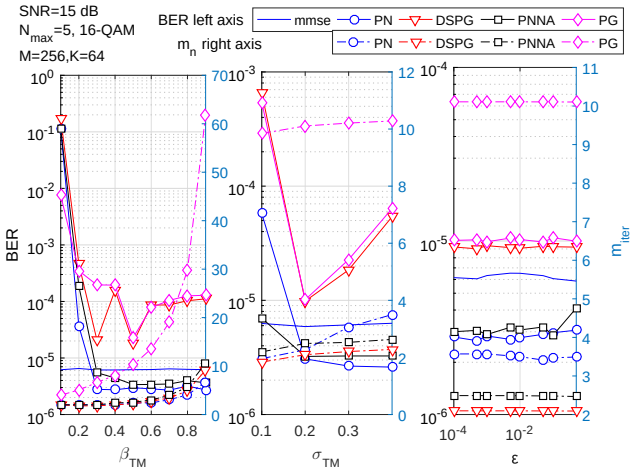

(a) Calibration of input parameters for constant system loading.

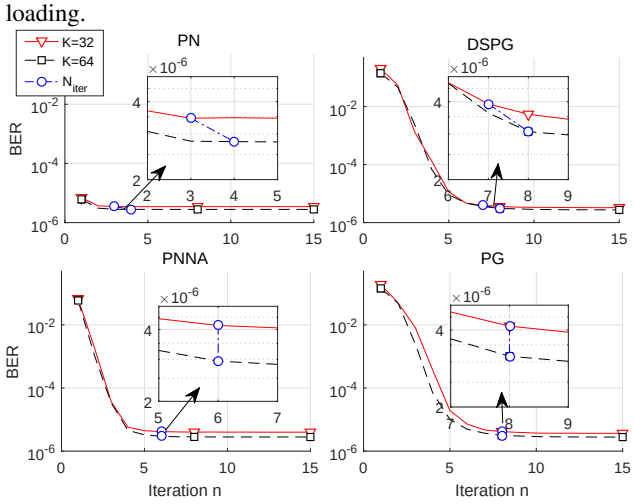

(b) Convergence for a constant system loading $\frac{1}{4}$, $M = 128$ and $M = 256$ with SNR= 15 dB.

FIGURE 5: Convergence and line search evaluations considering different number of BS and UE antennas, keeping the system loading $\frac{K}{M}$ constant.

V-A is considered using complexity metric given in terms of $\mathcal{O}$ (big-O) notation, as shown in Table 1. The complexity per iteration of SDP is the biggest, followed by LPℓ1; LP$\ell\infty$ and QP. The number of iterations for each detector evaluated numerically is presented in Table 7. Combining the information presented in those two tables, the SDP-based detector provides a good performance with a high complexity cost: each iteration costs more and N_{iter} is also greater than other detectors. LPℓ1 presents a cost per iteration higher, however costs $\approx$ 3 iterations less than LP$\ell\infty$. Regard QP, its complexity per iteration is lower and requires fewer N_{iter} than other detectors providing suitable trade-off among the performance of the studied M-MIMO detectors.

Regard the impact of the modulation order, for SDP, N_{iter} increased for higher orders, however this behavior was not observed for other detectors; only small fluctuations were observed. For QP, N_{iter} was around 8 to 9 iterations; for

This article has been accepted for publication in a future issue of this journal, but has not been fully edited. Content may change prior to final publication. Citation information: DOI 10.1109/ACCESS.2019.2902521, IEEE Access

TABLE 7: Number of iterations for different detectors under the condition SNR $= 15$ dB.

Detectors	4-QAM	16-QAM	64-QAM
LP$\ell 1$	15.35	14.11	13.25
LP$\ell\infty$	17.24	16.49	16.04
QP	7.88	9.55	9.02
SDP	16.72	21.74	23.62

LP$\ell\infty$ around 16 and 17 and for LP$\ell 1$, N_{iter} presented a small reduction around 2 iterations (from 15 to 13) as the modulation order increased.

In the second part, a more in-depth computational complexity analysis for the projected algorithms described in section V-B is developed considering the number of flops. Using expressions from Table 2 and substituting the respective number of iterations N_{iter} and line search evaluations m_{iter} obtained in subsection V-B, the plots presented in Fig. 6 are obtained.

From Fig. 6 i) with $K = 32$, MMSE provides the lowest number of flops. Although PG and DSPG have a diagonal $\mathbf{D}_n$ matrix and similar N_{iter}, the DSPG requires a lower m_{iter} than PG, hence, a lower number of flops. PN presented a low N_{iter} however it also requires a matrix inverse computation resulting in more complexity compared with MMSE. Finally, Neumann approximation is poor for large K and PNNA presented a slow convergence (high N_{iter}) resulting in higher complexity compared with PN approach.

In Fig. 6 ii), the number of flops considering a constant system loading is presented. Observing the flop-complexity expressions, the matrix-vector operations required for MMSE (Υ_{fixed}) are also required for the other algorithms, and the projected algorithms evaluates K^2 operations $N_{iter}m_{iter}$ times. So, the complexity order of MMSE and projected algorithms, now considering the $\mathcal{O}$ notation, is $\mathcal{O}(K^3)$ and $\mathcal{O}(N_{iter}m_{iter}K^2)$, respectively. Keeping the proportion $\frac{K}{M} = \frac{1}{4}$, the computational complexity order of DSPG would be lower than MMSE when $N_{iter}m_{iter} < K$. Indeed, we see that the number of iterations does not affect too much $N_{iter}m_{iter}$; hence, as K increases, the computational complexity approaches the MMSE complexity. Evaluating in terms of *flop*s, the computational complexity for DSPG was lower than MMSE for $M = 256$ and $K = 64$; in other words, DSPG provides good BER performance with low computational complexity in terms of *flop*s.

VII. CONCLUSIONS AND REMARKS

In the first part of this work, M-MIMO detectors using four promising optimization formulations, namely LPℓ_1, LPℓ_∞, QP and SDP are analyzed considering high-order modulation in realistic scenarios including spatial correlation, error in CSI, different system loading and modulation order. The SDP detector provided the best performance among the studied detectors in a variety of scenarios; the exception was the excessively high correlated scenario, $\rho = 0.9$, where

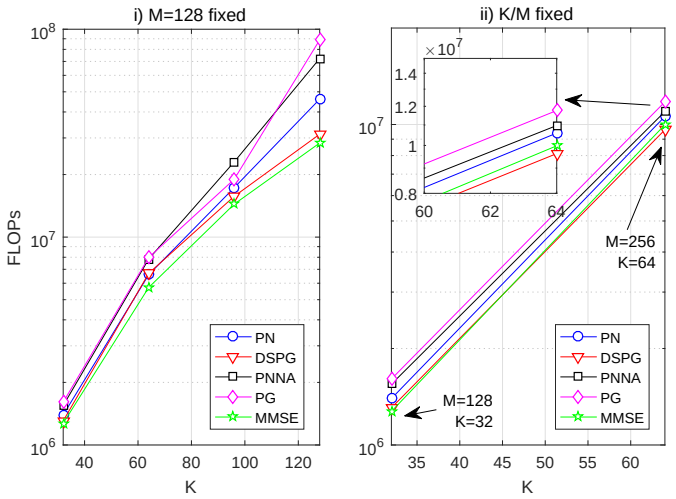

FIGURE 6: Number of FLOPs for the LS-MIMO detectors considering different system loading varying K users, and with a constant K/M, increasing both UE and BS antennas.

the performance of all detectors were severely degraded, and MMSE provided a slightly better performance. The LP$\ell\infty$ provided lower computational complexity per iteration compared with LP$\ell 1$ and a better performance under imperfect CSI and medium correlation $\rho = 0.5$; however, a worse performance for different system loading ($K = 64$ and $K = 32$), and similar performance for the low-order modulation 4-QAM. The QP detector showed the lowest complexity order per iteration and also better performance compared with both LP$\ell 1$ and LP$\ell\infty$.

In the second part, projected algorithms, which explore *simple* constraints of the formulated problem, were applied to find the transmitted symbols of a M-MIMO detector written as a QP problem. A methodology to determine the line search parameters was applied and, through numerical simulations, the improvements in the rate of convergence of the algorithms (reduction of N_{iter}) due to the well-conditioned Gram matrix (channel hardening) were evidenced; the convergence is slower for $K \approx M$ than for $K \ll M$. The computational complexity order of MMSE and projected algorithms are $\mathcal{O}(K^3)$ and $\mathcal{O}(N_{iter}m_{iter}K^2)$, respectively. The use of projected algorithms is suggested in scenarios where $N_{iter}m_{iter} < K$, noting that N_{iter} increases slowly as K increases while $\frac{K}{M} = \frac{1}{4}$, as observed during numerical simulations with $K = 32, M = 128$ and $K = 64, M = 256$. Hence, QP solved with DSPG provided better performance than MMSE in scenarios with $K \approx M$ and showed promising computational complexity for scenarios with increasing K and low system loading.

ACKNOWLEDGMENTS

This work has been partially supported by the National Council for Scientific and Technological Development (CNPq) of Brazil under Grant 304066/2015-0; by the State University of Londrina (UEL), and by the State Government

of Parana. All the agencies are gratefully acknowledged.

REFERENCES

[1] T. L. Marzetta, "Noncooperative cellular wireless with unlimited numbers of base station antennas," IEEE Trans. Wireless Commun., vol. 9, no. 11, pp. 3590–3600, November 2010.
[2] E. G. Larsson, O. Edfors, F. Tufvesson, and T. L. Marzetta, "Massive MIMO for next generation wireless systems," IEEE Commun. Mag., vol. 52, no. 2, pp. 186–195, February 2014.
[3] S. Yang and L. Hanzo, "Fifty years of MIMO detection: The road to large-scale MIMOs," Commun. Surveys Tuts., vol. 17, no. 4, pp. 1941–1988, Fourthquarter 2015.
[4] F. Rusek, D. Persson, B. K. Lau, E. G. Larsson, T. L. Marzetta, O. Edfors, and F. Tufvesson, "Scaling up MIMO: Opportunities and challenges with very large arrays," IEEE Signal Process. Mag., vol. 30, no. 1, pp. 40–60, Jan 2013.
[5] A. Chockalingam and B. S. Rajan, Large MIMO Systems. New York, NY, USA: Cambridge University Press, 2014.
[6] M. Wu, B. Yin, G. Wang, C. Dick, J. R. Cavallaro, and C. Studer, "Large-scale MIMO detection for 3GPP LTE: Algorithms and FPGA implementations," IEEE J. Sel. Topics Signal Process., vol. 8, no. 5, pp. 916–929, Oct 2014.
[7] L. Dai, X. Gao, X. Su, S. Han, C. I, and Z. Wang, "Low-complexity soft-output signal detection based on gauss-seidel method for uplink multiuser large-scale MIMO systems," IEEE Trans. Veh. Technol., vol. 64, no. 10, pp. 4839–4845, Oct 2015.
[8] C. Tang, C. Liu, L. Yuan, and Z. Xing, "High precision low complexity matrix inversion based on newton iteration for data detection in the massive MIMO," IEEE Commun. Lett., vol. 20, no. 3, pp. 490–493, March 2016.
[9] Y. Wang and H. Leib, "Sphere decoding for mimo systems with newton iterative matrix inversion," IEEE Commun. Lett., vol. 17, no. 2, pp. 389–392, February 2013.
[10] J. Minango and C. de Almeida, "Low complexity zero forcing detector based on newton-schultz iterative algorithm for massive mimo systems," IEEE Trans. Veh. Technol., pp. 1–1, 2018.
[11] M. Mandloi and V. Bhatia, "Low-complexity near-optimal iterative sequential detection for uplink massive MIMO systems," IEEE Commun. Lett., vol. 21, no. 3, pp. 568–571, March 2017.
[12] T. Cui, T. Ho, and C. Tellambura, "Linear programming detection and decoding for MIMO systems," in 2006 IEEE Int. Symp. on Inf. Theory, July 2006, pp. 1783–1787.
[13] Y. Hashimoto, K. Konishi, T. Takahashi, K. Uruma, and T. Furukawa, "L1 norm minimization approach to mimo detector," in 2014 8th International Conf. on Signal Proc. and Comm. Systems (ICSPCS), Dec 2014, pp. 1–4.
[14] A. Elghariani and M. Zoltowski, "Low complexity detection algorithms in large-scale MIMO systems," IEEE Trans. Wireless Commun., vol. 15, no. 3, pp. 1689–1702, March 2016.
[15] Y. H. Zhang, W. . Lu, and T. A. Gulliver, "Integer QP relaxation-based algorithms for intercarrier-interference reduction in OFDM systems," Canadian J. Elect. Comput. Eng., vol. 32, no. 4, pp. 199–205, Fall 2007.
[16] F. A. Bhatti, S. A. Khan, S. U. Rehman, and F. Rasool, "MIMO OFDM signal detection using quadratic programming," in 2011 IEEE 14th Int. Multitopic Conf., Dec 2011, pp. 323–328.
[17] N. D. Sidiropoulos and Z. Q. Luo, "A semidefinite relaxation approach to MIMO detection for high-order QAM constellations," IEEE Signal Process. Lett., vol. 13, no. 9, pp. 525–528, Sept 2006.
[18] Z. Q. Luo, W. K. Ma, A. M. C. So, Y. Ye, and S. Zhang, "Semidefinite relaxation of quadratic optimization problems," IEEE Signal Process. Mag., vol. 27, no. 3, pp. 20–34, May 2010.
[19] J. L. Negrão, A. M. Mussi, and T. Abrão, "Semidefinite relaxation for large scale MIMO detection," in XXXIV Simp. Br. Telecom. - SBrT2016, September 2016.
[20] W. Ma, C. Su, J. Jalden, T. Chang, and C. Chi, "The equivalence of semidefinite relaxation mimo detectors for higher-order qam," IEEE J. Sel. Topics Signal Process., vol. 3, no. 6, pp. 1038–1052, Dec 2009.
[21] S. Boyd and L. Vandenberghe, Convex Optimization. New York, NY, USA: Cambridge University Press, 2004.
[22] A. Antoniou and W.-S. Lu, Practical Optimization: Algorithms and Engineering Applications, 1st ed. New York, NY, USA: Springer, 2007.
[23] J. Nocedal and S. Wright, Numerical Optimization, ser. Springer Series in Operations Research and Financial Engineering. New York, NY, USA: Springer-Verlag New York, 2006.
[24] J. Gondzio, "Interior point methods 25 years later," Eur. J. Oper. Res., vol. 218, no. 3, pp. 587 – 601, 2012.
[25] D. P. Bertsekas, "Projected newton methods for optimization problems with simple constraints," in 1981 20th IEEE Conf. Decision Control including Symp. Adaptive Processes, Dec 1981, pp. 762–767.
[26] M. Schmidt, D. Kim, and S. Sra, Projected Newton-type methods in machine learning. Cambridge, MA, USA: MIT Press, Dec. 2011, pp. 305–330.
[27] D. Kim, S. Sra, and I. S. Dhillon, "Tackling Box-Constrained Optimization via a New Projected Quasi-Newton Approach," SIAM J. Sci. Comput., vol. 32, no. 6, pp. 3548–3563, 2010.
[28] Matlab. Lsqlin: Solve constrained linear least-squares problems. Accessed in 2018-11-18. [Online]. Available: https://www.mathworks.com/help/optim/ug/lsqlin.html
[29] ——. Quadratic programming algorithms. Accessed in 2018-11-18. [Online]. Available: https://www.mathworks.com/help/optim/ug/quadratic-programming-algorithms.html
[30] ——. Linprog: Solve linear programming problems. Accessed in 2018-11-18. [Online]. Available: https://www.mathworks.com/help/optim/ug/linprog.html
[31] R. H. Tütüncü, K. C. Toh, and M. J. Todd, "Solving semidefinite-quadratic-linear programs using SDPT3," Math. Program., vol. 95, no. 2, pp. 189–217, Feb 2003.
[32] W.-K. Ma, C.-C. Su, J. Jalden, and C.-Y. Chi, "Some results on 16-QAM MIMO detection using semidefinite relaxation," in 2008 IEEE International Conference on Acoustics, Speech and Signal Processing, March 2008, pp. 2673–2676.
[33] D. P. Bertsekas, Nonlinear Programming, 2nd ed. Belmont, Massachusetts, USA: Athena Scientific, 1999.
[34] J. Chen, "Gradient projection-based alternating minimization algorithm for designing hybrid beamforming in millimeter-wave MIMO systems," IEEE Commun. Lett., vol. 23, no. 1, pp. 112–115, Jan 2019.
[35] J. Chen, Z. Zhang, H. Lu, J. Hu, and G. E. Sobelman, "An intra-iterative interference cancellation detector for large-scale MIMO communications based on convex optimization," IEEE Trans. Circuits Syst. I, vol. 63, no. 11, pp. 2062–2072, Nov 2016.
[36] J. R. Hampton, Introduction to MIMO Communications. New York, NY, USA: Cambridge University Press, 2014.
[37] V. Zelst and J. Hammerschmidt, "A single coefficient spatial correlation model for multiple-input multiple-output (MIMO) radio channels," 27th General Assembly Int. Union of Radio Science (URSI), no. 1, pp. 2–5, 2002.
[38] R. Couillet and M. Debbah, Random Matrix Methods for Wireless Communications. Cambridge University Press, 2011.
[39] P. L. De Angelis, P. M. Pardalos, and G. Toraldo, Quadratic Programming with Box Constraints. Boston, MA: Springer US, 1997, pp. 73–93.
[40] R. A. Horn and C. R. Johnson, Matrix Analysis, 2nd ed. New York, NY, USA: Cambridge University Press, 2012.
[41] P. M. Pardalos and S. A. Vavasis, "Quadratic programming with one negative eigenvalue is NP-hard," J. Global Optim., vol. 1, no. 1, pp. 15–22, Mar 1991.
[42] M. Grant and S. Boyd, "CVX: Matlab software for disciplined convex programming, version 2.1," http://cvxr.com/cvx, Dec. 2014.
[43] ——, "Graph implementations for nonsmooth convex programs," in Recent Advances in Learning and Control, ser. Lecture Notes in Control and Information Sciences, V. Blondel, S. Boyd, and H. Kimura, Eds. Springer-Verlag Limited, 2008, pp. 95–110.
[44] M. S. K. Lau, S. P. Yue, K. V. Ling, and J. M. Maciejowski, "A comparison of interior point and active set methods for FPGA implementation of model predictive control," in 2009 European Control Conf. (ECC), Aug 2009, pp. 156–161.
[45] G. H. Golub and C. F. Van Loan, Matrix Computations, 4th ed. Baltimore, Maryland, EUA: Johns Hopkins University Press, 2013.
[46] J. C. M. Filho, R. N. de Souza, and T. Abrao, "Ant colony input parameters optimization for multiuser detection in DS/CDMA systems," Expert Syst. Appl., vol. 39, no. 17, pp. 12 876 – 12 884, 2012.